ARIEL

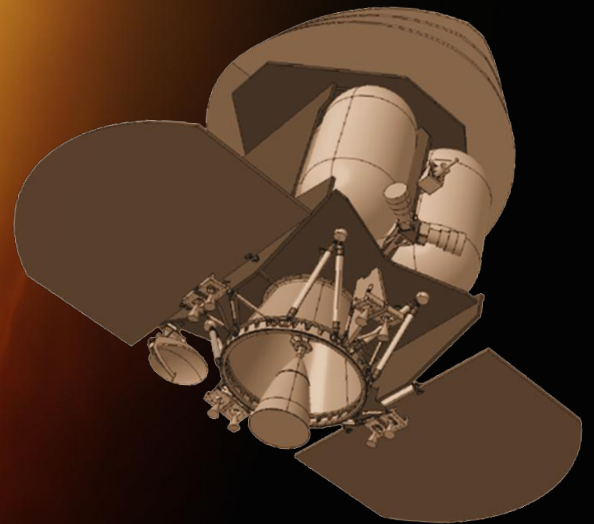## The Atmospheric Remote-Sensing Infrared Exoplanet Large-survey

Towards an H-R Diagram for Planets

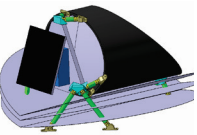A Candidate for the ESA M4 Mission

TABLE OF CONTENTS

1   EXECUTIVE SUMMARY

ESA's Cosmic Vision aims to investigate *what are the conditions for planet formation and the emergence of life?* For this, one must investigate and characterise extra-Solar planets. Thousands of exoplanets have now been discovered with a huge range of masses, sizes and orbits: from rocky Earth-like planets to large gas giants grazing the surface of their host star. However, the essential nature of these exoplanets remains largely mysterious: there is no known, discernible pattern linking the presence, size, or orbital parameters of a planet to the nature of its parent star. We have little idea whether the chemistry of a planet is linked to its formation environment, or whether the type of host star drives the physics and chemistry of the planet's birth, and evolution. Progress with these questions demands a large, unbiased survey of exoplanets. The proposed ARIEL mission will conduct such a survey and begin to explore the nature of exoplanet atmospheres and interiors and, through this, the key factors affecting the formation and evolution of planetary systems.

ARIEL will observe a large number (~500) of warm and hot transiting gas giants, Neptunes and super-Earths around a range of host star types using transit spectroscopy in the ~2-8 µm spectral range and broad-band photometry in the optical. We target planets hotter than 600K to take advantage of their well-mixed atmospheres which should show minimal condensation and sequestration of high-Z materials and thus reveal their bulk and elemental composition (especially C, O, N, S, Si). Observations of these hot exoplanets will allow the understanding of the early stages of planetary and atmospheric formation during the nebular phase and the following few millions years. ARIEL will thus provide a truly representative picture of the chemical nature of the exoplanets and relate this directly to the type and chemical environment of the host star. For this ambitious scientific programme, ARIEL is designed as a dedicated survey mission for transit and eclipse spectroscopy, capable of observing a large and well-defined planet sample within its 3.5-year mission lifetime. Transit and eclipse spectroscopy methods, whereby the signal from the star and planet are differentiated using knowledge of the planetary ephemerides, allow us to measure atmospheric signals from the planet at levels of at least 10^{-4} relative to the star and, given the bright nature of targets, also allows more sophisticated techniques, such as phase curve analysis and eclipse mapping, to give a deeper insight into the nature of the atmosphere. This requires a specifically designed, stable payload and satellite platform with broad, instantaneous wavelength coverage to detect many molecular species, probe the thermal structure, identify clouds and monitor the stellar activity. The wavelength range proposed covers all the expected major atmospheric gases from e.g. H_2O, CO_2, CH_4 NH_3, HCN, H_2S through to the more exotic metallic compounds, such as TiO, VO, and condensed species.

ARIEL's design is based on the successful study of the M3 EChO mission with simplifications and mass reductions to keep within the M4 programmatic constraints. ARIEL will carry a single, passively-cooled, highly capable and stable spectrometer covering $1.95 - 7.80$ µm with a resolving power of about 200 mounted on a single optical bench with the telescope and a Fine Guidance Sensor (FGS) that provides closed-loop feedback to the high stability pointing of the spacecraft. The FGS provides simultaneous information on the photometric stability of the target stars. The instrument design uses only technologies with a high degree of technical maturity. Transit spectroscopy means that no angular resolution is required and detailed performance studies show that a telescope collecting area of 0.64 m^2 is sufficient to achieve the necessary observations on all the ARIEL targets within the mission lifetime. The satellite is best placed into an L2 orbit to maximise the thermal stability and field of regard. ARIEL will be compatible with a launch into L2 orbit on a Vega-C launcher from Kourou using a propulsion module based on LISA Pathfinder. A payload consortium funded by national agencies will provide the full ARIEL payload (telescope and instrument) and ESA will provide the spacecraft. The ground segment responsibility and implementation will be split between ESA and the payload consortium. ARIEL is complementary to other international facilities (such as TESS, to be launched in 2017) and will build on the success of ESA exoplanet missions such as Cheops and PLATO, which will provide an optimised target list prior to launch.

Planetary science stands at the threshold of a revolution in our understanding of our place in the Universe: just how special are the Earth and our Solar System, and why? It is only by undertaking a comprehensive spectral survey of exoplanets, in a wide variety of environments, that we can hope to answer these fundamental questions. ARIEL represents a once in a generation opportunity to make a major impact on the knowledge of our place in the Cosmos – we intend to seize it.

ARIEL – Mission Summary	
Key Science Questions	• What are exoplanets made of? • How do planets and planetary systems form and evolve?
Science Objectives	• Detection of planetary atmospheres, their composition and structure • Determine vertical and horizontal temperature structure and their diurnal and seasonal variations • Identify chemical processes at work (thermochemistry, photochemistry, transport quenching) • Constrain planetary interiors (breaking the radius-mass degeneracy) • Quantify the energy budget (albedo, temperature) • Constrain formation and evolution models (evidence for migration) • Detect secondary atmospheres around terrestrial planets (evolution) • Investigate the impact of stellar and planetary environment on exoplanet properties
ARIEL Core Survey	• Survey of 500 transiting exoplanets from gas giants to super-Earths, in the very hot to warm zones of F to M type host stars • Target selection before launch based on ESA science team and community inputs • Delivery of a homogeneous catalogue of planetary spectra, yielding refined molecular abundances, chemical gradients and atmospheric structure; diurnal and seasonal variations; presence of clouds and measurement of albedo
ARIEL Observational Strategy	• Transit and eclipse spectroscopy with broad, instantaneous, uninterrupted spectra of all key molecules • High photometric stability on transit timescales • Required SNR obtained by summing a sufficient number of transits or eclipses • Large instantaneous sky coverage
Payload	• Afocal 3-mirror telescope, off-axis system, ~1.1 m x 0.7 m elliptical M1, unobstructed (effective area 0.64 m^2), diffraction-limited at 3 μm; • Highly-integrated broadband spectrometer instrument with modular architecture • Common optical train for all spectrometers and the fine guidance system optical module • Continuous wavelength coverage from $1.95 - 7.8$ μm in baseline design, with resolving power of $\lambda/\Delta\lambda \sim 200$ • Two photometric bands in VIS-NIR ($0.55 - 0.7$ μm and $0.8 - 1.0$ μm) provided by FGS. • Passively cooled MCT detectors at ~40K spectrometer and ~60-70K for FGS
Spacecraft	• S/C Dry mass ~780 kg including 20% system margin plus ~1150 kg propellant for internal propulsion system for transfer to L2. • Dimensions: Ø 2.2 m x 3.3 m when stowed, 3.8 x 2.2 x 3.3 m when solar array wings deployed. • Pointing requirements: coarse APE of 20 arcsec (3σ) for target acquisition by FGS; PRE of 100 milli-arcsecond rms for 10 seconds to ~hours. • Attitude control system: reaction wheels only complemented by a Fine-Guidance System operating in the visible within the AOCS control loop. • Thermal Control System: Passive cooling of telescope via 3 V-grooves to ≤ 70 K; dedicated radiator for spectrometer detector to cool to approximately $35 - 40$ K. No Active Cooling. • Telecommand, Telemetry and Communication: X-band, ~80 Gbit of science data per week transmitted with a High Gain Antenna to a 35 m ESTRACK station
Launcher, Orbit, Mission Phases and Operations	• Launch from Kourou on a Vega-C into LEO (250 x 3000 km orbit) the transfer to Halo orbit at L2 using integrated propulsion module (LISA Pathfinder based). Launch in 2025. • Nominal mission duration 3.5 years plus 6 months transit, cooldown and commissioning. • MOC at ESOC, SOC at ESAC, Instrument Operations and Science Data Centre distributed across consortium members states • 2x3 hours ground contact sessions per week for tele-command uplink and science downlink.
Data Policy	• Short proprietary period after nominal SNR is reached, shrinking from 6 to 1 month after 3 years.

2 SCIENCE CASE

2.1 THE ARIEL MISSION AS PART OF COSMIC VISION

2.1.1 Background: highlights & limits of current knowledge of planets

Since their discovery in the early 1990's, planets have been found around every type of star, including pulsars and binaries. As they are the leftover of the stellar formation process, planets appear to be rather ubiquitous. Current statistical estimates indicate that, on average, every star in our Galaxy hosts at least one planetary companion (Cassan et al., *Nature*, 2012; Batalha, 2015) and therefore $\sim 10^{11}$ planets should exist just in our Milky Way.

The first major theme of ESA's Cosmic Vision program poses the questions of how do planets form and what are the conditions that might make them (or their moons) habitable. Even within the limits of our current observational capabilities, extrasolar planets have given a unique contribution in improving our understanding of these subjects and provided us a clearer view of the place the Solar System and the Earth occupy in the galactic context. As a result, a great deal of effort has been, and is being, spent to increase the number of known extrasolar planets (~ 2000) and overcome the limits imposed by the incomplete sample currently available (Figure 2-1).
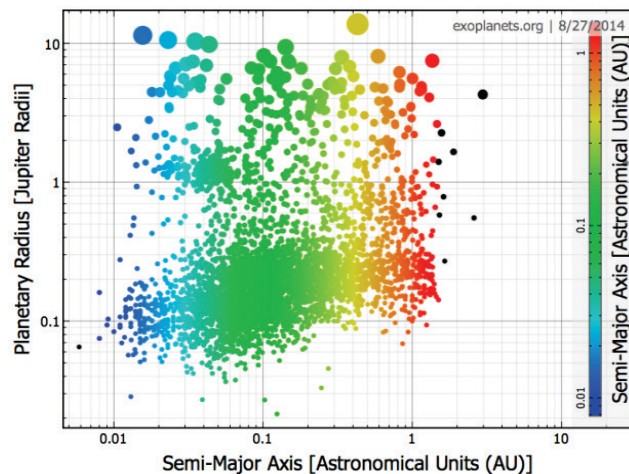
Figure 2-1: Currently known exoplanets, plotted as a function of distance to the star and planetary radii (courtesy of exoplanets.org). The graph suggests a continuous distribution of planetary sizes − from sub-Earths to super-Jupiters − and planetary temperatures than span two orders of magnitude.

While the number of planets discovered is still far from the hundreds of billions mentioned above, the European Space Agency GAIA mission will discover tens of thousands new planets (Perryman et al., 2014; Sozzetti et al., 2010, 2014). In addition to the ongoing release of results from Kepler (Batalha, 2015), ground-based surveys and the continuing K2 mission will add to the current ground and space based efforts (see Table 1). In the future we can look forward to many, many more discoveries from the Cheops (ESA), TESS (NASA) and PLATO (ESA) missions (Broeg et al., 2013; Ricker et al., 2014; Rauer et al., 2014).

The information provided by the presently planned efforts, however, mainly deals with the orbital data and the basic physical parameters (e.g. mass, size) of the discovered planets. Therefore, in the next decade, emphasis in the field of exo-planetary science must shift from "discovery" to "understanding". By which we mean understanding the nature of the exo-planetary bodies and their formation and evolutionary history. In all scientific disciplines, taxonomy is often the first step toward understanding, yet to date we do not have even a simple taxonomy of planets and planetary systems.

In comparison, astrophysics faced a similar situation with the classification of stars in the late 19th and early 20th century. Here it was the systematic observations of stellar luminosity and colours of large numbers of stars that led to the breakthrough in our understanding and the definition of the classification schemes that we are so familiar with today. The striking observational phenomenon that stellar brightness correlates with their perceived colours was first noted by Russell (1910) and Hertzsprung (1912) and allowed a link between observation and a theoretical understanding of their interior structure and their nuclear power sources (Eddington, 1924; Bethe, 1939). Thus, the observation of a few basic observables in a large enough sample allowed scientists to predict both the physical and chemical parameters and subsequent evolution of virtually all stars. This has proved to be an immensely powerful tool, not only in studying "local" stellar evolution, but also in tracing the chemical history of the universe and even large scale cosmology. We seek now similar tools to understand the formation and evolution of planets.

Unfortunately, planets do not appear to be as well behaved as stars: hence it is a 21st century problem! To date very little empirical correlation is apparent among their observable parameters. For instance, knowledge of the <u>mass</u> provides only very basic information about a planet's nature, namely whether it is a gas giant, an icy giant or a rocky one, and sometimes the last two categories cannot be

distinguished from each other. For planets transiting in front of their parent stars – of which some 1100 are known today– the simplest observables are the planetary radius and, when combined with radial velocity, the mass. Mass and radius allow the estimation of the planetary density. From Figure 2-2 it is evident that even gas giants can exist with a broad range of interior structures and core composition, as shown from the different densities observed (e.g. Guillot et al., 2005; Fortney et al., 2007).
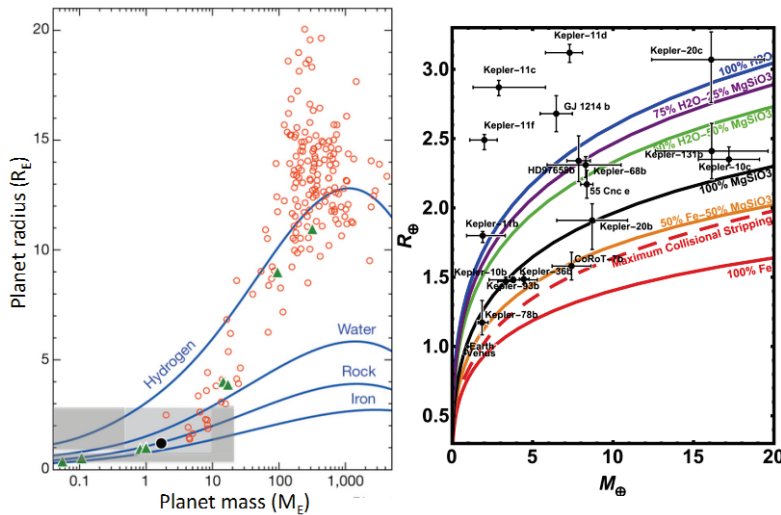
Figure 2-2: Left: Masses and radii of transiting exoplanets (Howard et al, 2013). Coloured lines show mass-radius relations for a variety of internal compositions: the models cannot fully capture the variety of cases and break the degeneracies in the interpretation of the bulk composition. Right: zoom into the lower mass regime indicated as a grey rectangle on the left (Zeng & Sasselov, 2013). Planets discussed in the text are labelled.

While the mass-radius observations have stimulated very interesting theoretical work, the implications on planetary formation and evolution mechanisms are still unclear. Most likely, the different bulk densities reflect the different nature and size of the planet's core, which in turn will depend on both the formation mechanism and the "birth distance" from the parent star. Objects lighter than ten Earth masses (super-Earths, Figure 2-2 right-hand panel) are even more enigmatic, we cannot derive their properties based on mass and radius alone (Valencia et al., 2013; Adams et al., 2008; Grasset et al., 2009). Currently, we can only guess that the extraordinarily hot and rocky planets CoRoT-7b, Kepler-10b, Kepler-78b and 55 Cnc-e sport silicate compounds in the gaseous and liquid phases (Léger et al., 2011). The "mega-Earth", Kepler-10c (Dumusque et al., 2014), is twice the Earth's size but is ~ 17 times heavier, making it among the densest planets currently known. The 5 inner planets orbiting Kepler-11 (Lissauer et al., 2011) are showing an extraordinary diversity, while being dynamically packed in orbits less than 0.45 AU.

Their masses are spanning from ~2 to ~13 Earth masses and a factor 6 in densities. Kepler 11b and c are possibly super-Earths with H_2O and/or H/He envelopes. Kepler 11d, e, f resemble mini-Neptunes. It is clear that the characterisation of the atmospheres of those and other planets is essential to disentangle the degeneracies in the mass-radius relationship.

2.1.2 The way forward: the chemical composition of a large sample of planets

A breakthrough in our understanding of the planet formation and evolution mechanisms – and therefore of the origin of their diversity – will only happen through the observation of the planetary bulk and atmospheric composition of a statistically large sample of planets. Knowing what exoplanets made of is essential to clarify, e.g. whether a planet was born in the orbit it is observed in or whether it has migrated over a large distance. Knowledge of the chemical makeup of a large sample of planets will also allow us to determine the key mechanisms that govern planetary evolution at different time scales. Obviously we do not have direct access to the internal composition of an exoplanet (or indeed of Solar System planets) to study these effects, but we do have access to their atmospheric composition. For the atmospheres to be our window into to their bulk composition, however, we need to study planets in different conditions compared to those in our Solar System. The Sun's planets are relatively cold and, as a result, their atmospheric composition is significantly altered by condensation and sinking of different chemical species, both volatile and refractory (see e.g. Figure 2-3). By contrast, hot exoplanets represent a natural laboratory for chemistry and formation studies. This is because their higher atmospheric temperatures limit the effects of condensation and sinking of the volatile species, thus making the atmospheric composition more representative of the bulk one. Hot planets also allow us to investigate exotic chemical regimes (Si-rich and metal-rich atmospheres) that are impossible to observe in the Solar System and offer us hints of the composition of the high-Z materials present in the interior of colder planets (see §2.5).

2.1.3 Current observations of exo-atmospheres: strengths & pitfalls

In the past decade, pioneering results have been obtained using transit spectroscopy with Hubble,

Spitzer and ground-based facilities, enabling the detection of a few of the most abundant ionic, atomic and molecular species and to constrain the planet's thermal structure (e.g. Charbonneau et al., 2002; Vidal-Madjiar et al., 2003; Knutson et al., 2007; Swain et al., 2008; Linsky et al., 2010; Snellen et al., 2010, 2014; Majeau et al., 2012). The infrared (IR) range, in particular, offers the possibility of probing the neutral atmospheres of exoplanets. In the IR the molecular bands are more intense and broader than in the visible (Tinetti et al., 2007a) and less perturbed by small particle clouds, hence easier to detect. On a large scale, the IR transit and eclipse spectra of hot-Jupiters seem to be dominated by the signature of water vapour (e.g. Barman 2007, Beaulieu et al. 2010; Birkby et al., 2013; Burrows et al. 2007, Charbonneau et al. 2008; Crouzet et al. 2012, 2014; Danielski et al. 2014; Deming et al. 2013; Grillmair et al. 2008; Kreidberg et al., 2014b, McCullough et al. 2014; Swain et al. 2008, 2009; Tinetti et al. 2007b, 2010, Todorov et al., 2014). Similarly, the atmosphere of hot-Neptune HAT-P-11b appears to be water-rich (Fraine et al., 2014). The data available for other warm Neptunes, such as GJ 436b, GJ 3470b are suggestive of cloudy atmospheres and do not always allow a conclusive identification of their composition (Stevenson et al. 2010; Beaulieu et al. 2011; Knutson et al. 2011; Morello et al., 2014b; Fukui et al. 2013; Ehrenreich et al, 2014). The analysis of the transit spectra for the transiting 6.5 M_{Earth} super-Earth GJ 1214b has oscillated between a metal-rich or a cloudy atmosphere (e.g. Bean et al. 2010; Berta et al., 2012; Kreidberg et al., 2014, Stevenson et al., 2014).

Despite these early successes, current data are very sparse, i.e. there is not enough wavelength coverage and most of the time the observations were not recorded simultaneously. Notice that an absolute calibration at the level of 10^{-4} is not guaranteed by current instruments, and therefore caution is needed

when one combines multiple datasets at different wavelengths which were not recorded simultaneously. The degeneracy of solutions embedded in the current transit observations (Swain et al., 2009; Madhusudhan and Seager, 2009; Lee et al., 2012; Line et al., 2013; Waldmann et al., 2014) inhibits any serious attempt to estimate the elemental abundances or any meaningful classification of the planets analysed. New and better data of uniform quality are needed for this purpose.

2.1.4 The way forward: ARIEL

The way forward is, therefore, through the direct measurement of the atmospheric composition and structure of hundreds of exoplanets. A statistically significant number of planets need to be observed in order to fully test models and understand which physical parameters are most relevant. This requires observations of a large sample of objects (hundreds), generally repeatedly or on long timescales, which can only be done with a dedicated instrument from space, rather than with multi-purpose telescopes (e.g. JWST & E-ELT) which will be able to observe a few tens of planets (see §2.3 for further details).

In order to fulfil this ambitious scientific program, ARIEL has been conceived as a dedicated survey mission for transit, eclipse & phase-curve spectroscopy capable of observing a large, diverse and well-defined planet sample. The transit and eclipse spectroscopy method, whereby the signal from the star and planet are differentiated using knowledge of the planetary ephemerides, allows us to measure atmospheric signals from the planet at levels of at least 10^{-4} relative to the star. This can only be achieved in conjunction with a carefully designed stable payload and satellite platform. It is necessary to provide broad instantaneous wavelength coverage to detect as many molecular species as possible, to probe the thermal structure and albedo of the planetary atmospheres and to correct for contaminating effects of the stellar photosphere (see §3.4 for details).
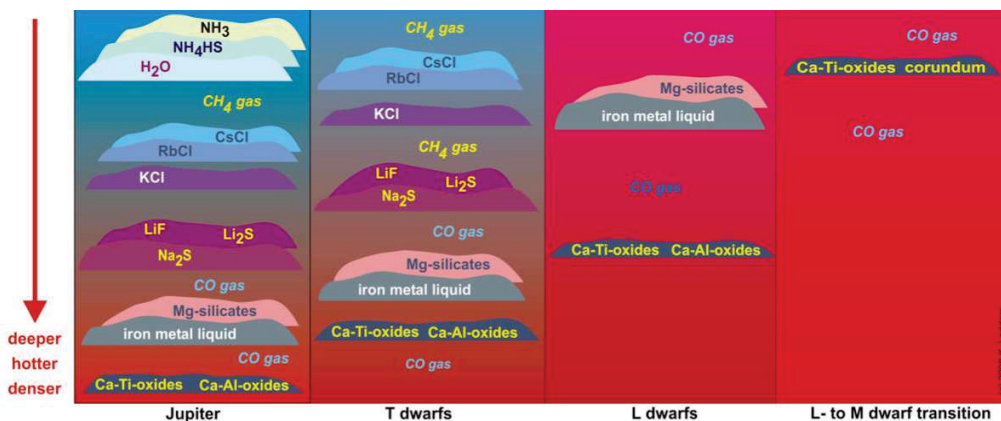

Figure 2-3: Cloud layers in atmospheres ranging from our Jupiter to the hottest brown dwarfs (Lodders & Fegley, 2006). Condensate clouds of various species form at specific points in the temperature - pressure profile. As atmospheres cool, these clouds sink deeper, falling below the observable gaseous layer.

2.2 KEY SCIENCE QUESTIONS ADDRESSED BY ARIEL

ARIEL will address the fundamental questions:

- – *What are exoplanets made of?*
- – *How do planets form and evolve?*

through the direct measurement of the atmospheric and bulk chemical composition. ARIEL will focus on planets hotter than 600 K, for which the atmospheric composition is more representative of the bulk one.
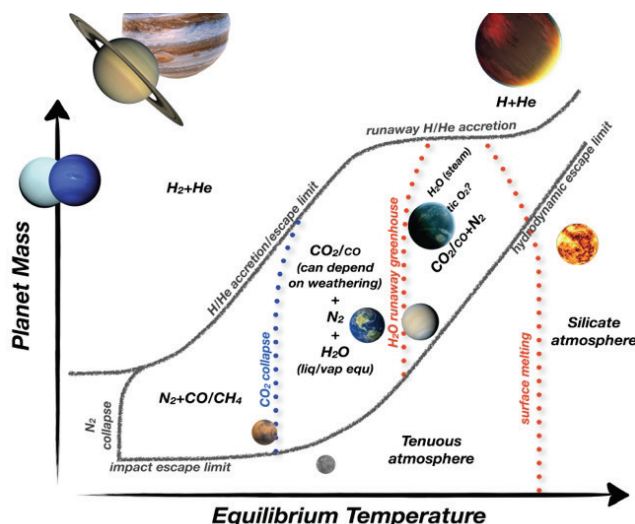
Figure 2-4: Schematic summary of the various classes of atmospheres as predicted by Leconte et al. (2014). Only the expected dominant species are indicated, other (trace) gases will be present. Each line represents a transition from one regime to another, but these "transitions" need tight calibrations from observations. The axes do not have numerical values as they are unknown. Solar System planets are indicated, together with a lava planet, an Ocean planet and a hot Jupiter. ARIEL will observe planets hotter than ~ 600K and heavier than ~ a few Earth-masses: many atmospheric regime transitions are expected to occur in this domain (see §2.5).

ARIEL will observe super-Earths, Neptune-like and Jupiter-like exoplanets around stars of various masses. These broad classes of planets are all expected to have very different formation, migration and evolution histories that will be imprinted on their atmospheric and bulk chemical signatures. Many theoretical studies have tried to understand and model the various processes controlling the formation and evolution of planetary atmospheres, with some success for the Solar System. However, such atmospheric evolution models need confirmation and tight calibrations from observations.

In Figure 2-4 we show the predicted bulk atmospheric compositions as a function of planetary temperature and mass (Leconte et al., 2014; Forget

& Leconte, 2014). ARIEL will focus on the upper right part of the diagram, providing the observational constraints for a large population of planets (hundreds) hotter than~ 600K and heavier than ~ a few Earth-masses. The statistical approach provided by ARIEL is *conditio sine qua non* to confirm or identify new transitions between different regimes, and explain the physical processes behind them. Notice that gas giants and Neptunes, are notably mainly made of hydrogen and helium. For these planets, therefore, the relevant questions and transitions concern all the molecules and atoms other than hydrogen and helium (see §2.5).

2.3 KEY Q&A ABOUT ARIEL

1. *Why do we need another exoplanet mission? [after K2, TESS, Cheops , PLATO]*

NASA Kepler, K2, TESS and ESA Cheops & PLATO are all missions performing photometric observations in the visible wavelengths to detect new transiting exoplanets or measure the radii of the planets discovered through radial velocity. Thanks to those missions, thousands of transiting exoplanets will be discovered in the next decade, especially the ones orbiting bright stars. The next logical step to take is IR spectroscopy to reveal the composition of those planets (see ESA-EPRAT report, MS1 [1]).

None of the above mentioned missions will do spectroscopic characterization of exoplanets in the IR, like ARIEL. ARIEL will be the first dedicated mission, worldwide, to measure the chemical composition and thermal structures of hundreds of exoplanets, enabling planetary science beyond the boundaries of the Solar System.

2. *Why do we need to observe hundreds of planets? [as opposed to a few tens with general purpose instruments]*

Work in exoplanet spectroscopy, has thus far been undertaken piecemeal with one or perhaps a few spectra over a narrow wavelength range being studied at any one time. This approach is inadequate to provide answers to the key questions of exoplanetary science spelled out in the previous sections. A statistically significant number of planets (approximately an order of magnitude larger than the sample observed with future general purpose facilities) needs to be observed in order to fully test models and understand which are the relevant physical parameters. This requires observations of a

---

[1] *http://sci.esa.int/jump.cfm?oid=47855*

large sample of objects, generally on long timescales, which can only be done with a dedicated instrument like ARIEL, rather than with multi-purpose telescopes. ARIEL will enable a paradigm shift: by identifying the main constituents of hundreds of exoplanets in various mass/temperature regimes, we would be looking no longer at individual cases but at populations. Such a universal view is critical to understand the processes of planet formation and evolution and how they behave in various environments.

3. Why space? [as opposed to ground facilities]

Broad, instantaneous wavelength coverage is necessary to detect as many molecular species as possible, to probe the thermal structure of the planetary atmospheres and to correct for the contaminating effects of the stellar photosphere. Since the ARIEL investigation includes planets with temperatures hotter than 600K, this requires a continuous wavelength coverage ~ 2 to 8 μm in the IR and a simultaneous monitoring of the stellar activity through a visible channel. From the ground, the possibility to access the 2 to 8 μm spectral region is seriously hampered by the telluric contamination. Also, at hot temperature the molecular bands are broadened, requiring only modest spectral resolving power to be detected, easily obtainable by a relatively small telescope in space (see Figure 3-2 in §3.1).

Finally, to observe hundreds of planets an agile, highly stable platform from space is required. For an ARIEL-like mission, the complete sky is accessible within a year, with a source at the ecliptic observable for ~30% of the mission lifetime (see §5.3.2). This is not achievable from the ground.

4. Is a 1–m class telescope too small for exoplanet spectroscopy? [as opposed to 6.5 m telescope in space or 30 m on the ground?]

No. If we assume the observations to be dominated by the stellar photon noise, the planetary SNR goes linearly with telescope diameter (D). For instance, if we observed with a 6.5m telescope a target star with Mag K = 11, we would obtain the same planetary SNR with a 1m telescope by observing a target star which is ~2 Mag brighter. By focusing on targets which are brighter than K ~ 9.5, we can obtain excellent SNR with a reasonable integration time. Some of these bright sources will be observed previously by MIRI, therefore providing a way to observe wavelengths longer than 8 micron. By contrast, JWST -NIRSPEC Prism (partially

overlapping to ARIEL wavelength range), being extremely sensitive, can observe only targets fainter than Mag J = 11 to avoid saturation [2]. While spectroscopic characterisation of exoplanetary atmospheres with ARIEL is perforce restricted to targets bright enough to permit acquisition of the necessary high signal-to-noise data, among the current crop of transiting exoplanets some ~60 targets are brighter than Mag K=9.5, yet the surface of this vast treasure trove has been barely scratched. By 2025, this number is expected to be at least 10-20 times higher thanks to K2, TESS (launching 2017), Cheops (launching 2017), PLATO (launching 2024) etc. (see§2.4.2).

Notice also that a large structure from space, might represent an encumbrance when trying to reach the pointing stability required by transit observations and certainly might limit the ability to move and repoint agilely from one target to another in the sky.
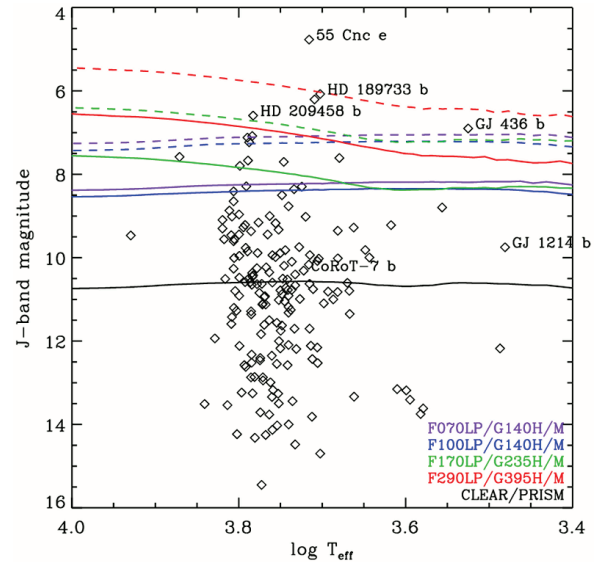
Figure 2-5: J-band limiting magnitudes for the different NIRSpec modes as a function of host star temperature[2]. The colored dashed lines are for the high resolution gratings, the coloured solid lines for the medium resolution gratings, and the solid black line for the prism. Sources below the lines can be observed in the full wavelength range of the given mode as specified in the table above. Labeled planets are known optimal targets for ARIEL.

A 1m class telescope from space would trade a lower spectral resolution over a broad, simultaneous wavelength coverage with extremely high spectral resolution over a narrow spectral range obtainable with a ~30m from the ground. The higher SNR from the ground would be hampered by the telluric contamination. The two configurations are highly complementary: to get the big picture we need a

dedicated telescope from space, to address very focused questions for a more limited number of planets, a large telescope from the ground is optimal.

5. Why a dedicated mission? [in an epoch of JWST & ELT]

Future general purpose facilities with large collecting areas (James Webb Space Telescope, ESO-Extremely Large Telescope, etc.) will allow the acquisition of better exoplanet spectra, compared to the currently available, especially from fainter targets. A few tens of planets will be observed with JWST and E-ELT in great detail, but to address the questions of formation and evolution of exoplanets we need to be able to observe a sample that is an order of magnitude larger (see response to question 2).

Having a large collective area, i.e. more photons, is certainly positive, but the lesson learnt from Spitzer and Hubble is that other aspects may be as critical, e.g. the instrument stability and the knowledge of the instrument systematics. Kepler has been an incontestable success because it was built from start to achieve the 10^{-4} to 10^{-5} photometric precision needed to discover Earth-size planets. Another critical point is the stellar activity (see §3.4.2), which often interferes with the possibility of combining measurements at different wavelengths, if recorded at different times. Moreover, instruments are most of the time not calibrated at the level needed to combine multiple observations. The ability to observe simultaneously a broad wavelength range permits to solve these issues.

6. Why will ARIEL target warm & hot planets? [as opposed to focusing e.g. on habitable zone]

Hot planets offer the unique opportunity to have access to the bulk and elemental composition, as there is no cold trap in their atmospheres for species such as H_2O, NH_3, CH_4, SiO, CO_2, CO and, depending on the temperature, metallic compounds e.g. TiO, VO, CrH. The knowledge of hot planets is therefore imperative to understand the big-picture before we focus on colder regimes. Additionally, a large fraction of the currently available/expected to be discovered planets will orbit very close to their star and therefore will be hot. Having a short annual period, these are the best targets for transit and eclipse spectroscopy measurements.

A long term scientific objective is to characterize the whole range of exoplanets, including, of course, potentially habitable ones. ARIEL would act as a

pathfinder for future, even more ambitious campaigns.

7. Why also gaseous planets are important? [not just terrestrial]

While the search for habitable planets naturally focuses on terrestrial bodies, in the struggle to understand how planetary systems form and under which conditions they can produce habitable environments giant planets occupy a special place. From the study of the Solar System we know that the delivery of water and all the elements necessary for pre-biotic chemistry and the appearance of life on Earth, be it primordial or late, is associated to the formation and dynamical evolution of the giant planets. Contrary to what the present orderly nature of the Solar System would suggest, some scenarios actually link the formation of the terrestrial planets and their initial water budget to extensive migration events of the giant planets at the very beginning of the life of the Solar System. Understanding how and where giant planets form and when and why they migrate is therefore the key to unveiling what set of conditions and processes resulted in the Earth and us.

8. Why transit method? [as opposed to direct imaging]

In parallel with transit studies, in the next decade, direct imaging is expected to provide insight into hot, young planets at large separations from their parent star, i.e. gaseous planets newly formed in the outer regions of their planetary disc and not (yet?) migrated in. The first spectra of hot, young super-Jupiters at large separation from their host stars, were observed in the past years (e.g. Bonnefoy et al., 2013; Konopacky et al., 2013). Spectroscopy in the wavelength range of YJHK-band will start soon with dedicated instruments on VLT (SPHERE), Gemini (GPI), Subaru (SCExAO). The comparison of the chemical composition of these young gaseous objects to the composition of their migrated siblings probed through transit, will be of great help to understand the role played by migration and by extreme irradiation on gaseous planets.

Scientifically, the advantage of transiting planets is that the planetary size and the mass are known. Direct imaging observations suffer from the lack of knowledge of the planetary radius and often the mass. When the mass and the radius are not known, model estimates need to be invoked, increasing the source of degeneracy. Observationally, the transit and eclipse spectroscopy methods allow us to measure atmospheric signals from the planet at levels

of at least 10^{-4} relative to the star. No angular resolution is needed, as the signals from the star and from the planet are differentiated using knowledge of the planetary ephemerides.

Finally, a space mission for direct imaging would be technically more challenging than a transit one and certainly more expensive: the telescope cannot be a light bucket, to start with. The said mission, though, would open up the spectroscopic exploration of planets at larger separation from the stars, a domain that is impracticable with transits.

9. Isn't stellar activity a critical hurdle for exoplanet spectroscopy?

Not if we can monitor VIS and IR wavelength simultaneously. See §3.4.2 for further discussion.

10. Can clouds prevent the detection of molecules? What if all planets are cloudy?

Clouds modify the albedo, contribute to the green-house effect, and sequester the chemical species which condense out. Clouds therefore have a critical impact on the atmospheric energy budget and compositional balance. If present, clouds will be revealed by ARIEL through transit and eclipse spectroscopy and photometry. Clouds show, in fact, distinctive spectroscopic signatures depending on their particle size, shape and distribution (see Figure 3-3). Current observations in the VIS and NIR with Hubble and MOST have suggested their presence in some of the atmospheres analysed (e.g. Rowe et al., 2008; Sing et al., 2011; Demory et al., 2013; Kreidberg et al., 2014; Knutson et al, 2014). We do not know, though, how they are spatially distributed and whether they are a transient phenomenon or not. Further observations over a broad spectral window and through time are needed to start answering these questions (see e.g. most recent work done for brown dwarfs by Apai et al., 2013). This is an additional reason to justify a dedicated mission, as repeated observations through time and phase-curves for a large number of planets can be done only thorough a dedicated telescope from space. ARIEL's broad wavelength range and sensitivity enables the identification of different molecular species and types of clouds, if present. Concerning the cloud composition, the only way to tackle this question remotely and not in situ is in a statistical way. Planets at similar temperatures should exhibit similar condensates in their atmospheres (Figure 2-3).

11. What are the differences between EChO & ARIEL?

ARIEL will focus on warm and hot planets, whereas EChO was also targeting temperate ones. Because of this choice, ARIEL wavelength range is narrower ($1.95 - 7.8$ μm + 2 visible / NIR bands on ARIEL as opposed to 0.5-16 μm on EChO), allowing a much simpler payload: i.e. no active cooling, one instrument module as opposed to 3 modules, telescope diffraction limit at 3 μm. Being launched after TESS, Cheops & PLATO, a large number of bright targets will be available for ARIEL. A combination of bright sources and increased throughput (because of the simpler payload), will permit to reduce the ARIEL telescope diameter, making it cheaper & simpler.

12. Why are ESA and Europe well positioned to build an ARIEL mission?

Europe has invested serious resources to be at the forefront of exoplanet detection (RV & transit surveys from the ground, Corot, Cheops and PLATO). The next obvious step to be taken in the European exoplanet roadmap, is a dedicated mission for IR spectroscopy of the planets detected through the space and ground facilities (see ESA EPRAT report[1]). This will continue to keep Europe as the world-leader in exoplanet science.

Our proposal will build upon the leading role of the scientists and institutes who are part of this consortium in building PI instruments for ESA's previous very successful IR and sub-millimetre astronomical missions: the LWS for the Infrared Space Observatory (ISO), SPIRE for the Herschel Space Observatory, MIRI for the forthcoming JWST and the Planck thermal system, as well as Solar System space instruments on Venus Express, Mars Express, JUICE, Cassini, Rosetta etc.

ARIEL will provide a large number of spectra to be analysed and interpreted. Many teams in our consortium, are building the necessary model infrastructure to interpret exoplanet spectra, predict atmospheric dynamics, chemistry, formation and structure of the interior (e.g. ERC-funded programs: E3ARTHS (chemistry of exoplanets); ExoMol (molecular database for exoplanets), MoltenEarths (interior of super-Earths), ExoLights (data analysis & retrieval of exoplanet spectra)). Therefore we are in an excellent position to lead the characterisation of the variety of exoplanets observed by ARIEL.

2.4 ASSUMPTIONS NEEDED TO ACHIEVE THE SCIENCE OBJECTIVES

2.4.1 How do we observe exo-atmospheres?

For transiting planets, we have <u>five complementary methods to sound their atmospheric composition and thermal structure</u>, we describe them briefly in the following paragraphs. ARIEL will use them all.
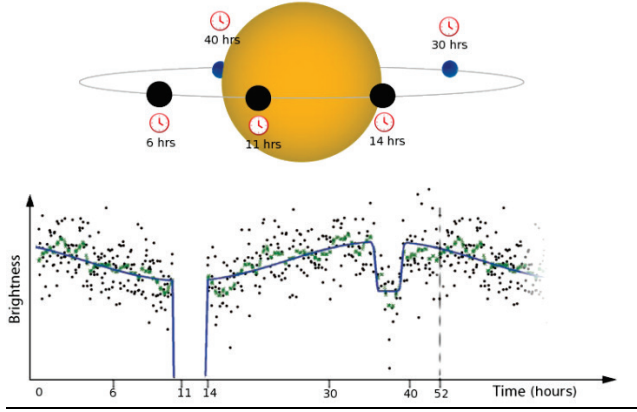
Figure 2-6: Methods adopted by ARIEL to probe the exoplanet composition and structure: orbital lightcurve of the transiting exoplanet HAT-P-7b as observed by Kepler (Borucki et al., 2009). The transit and eclipse are visible.

1. When a planet passes in front of its host star (**transit**), the star flux is reduced by a few percent, corresponding to the planet/star projected area ratio (transit depth, Figure 2-6). The planetary radius can be inferred from this measurement. If atomic or molecular species are present in the exoplanet's atmosphere, the inferred radius is larger at some specific wavelengths (absorption) corresponding to the spectral signatures of these species (Seager and Sasselov, 2000; Brown, 2001, Tinetti et al., 2007b). The transit depth $\Delta F(\lambda)$ as a function of wavelength (λ) is given by:

$$\Delta F(\lambda) = \frac{2 \int_0^{z_{max}} (R_p + z)(1 - e^{-\tau(z,\lambda)}) dz}{R_*^2} \quad (1)$$

where z is the altitude above R_p and τ the optical depth. Eq. (1) has a unique solution provided we know R_p accurately. R_p is the planetary radius at which the planet becomes opaque at all λ. For a terrestrial planet, R_p usually coincides with the radius at the surface. For a gaseous planet, R_p may correspond to a pressure $p_0 \sim 1$-10 bar.

2. A direct measurement of the planet's emission/reflection can be obtained through the observation of the **planetary eclipse**, by recording the difference between the combined star+planet signal, measured just before and after the eclipse, and the stellar flux alone, measured during the eclipse, Figure 2-6. Observations provide measurements of the flux emitted/reflected by the planet in units of the stellar flux (Charbonneau et al., 2005; Deming et al., 2005). The planet/star flux ratio is defined as:

$$\phi(\lambda) = (R_p/R_*)^2 \ F_p(\lambda)/F_*(\lambda) \quad (2)$$

3. In addition to transit and eclipse observations, monitoring the flux of the star+planet system over the orbital period (**phase curve**) allows the retrieval of information on the planet emission at different phase angles (Figure 2-6). Such observations have to be performed from space, as they typically span over a time interval of more than a day (e.g. Knutson et al., 2007; Borucki et al. 2009, Snellen et al., 2010).

The combination of the three prime observational techniques utilized by ARIEL provides us with information from different parts of the planet atmosphere; from the terminator region via transit spectroscopy, from the day-side hemisphere via eclipse spectroscopy, and from the unilluminated night-side hemisphere using phase variations.
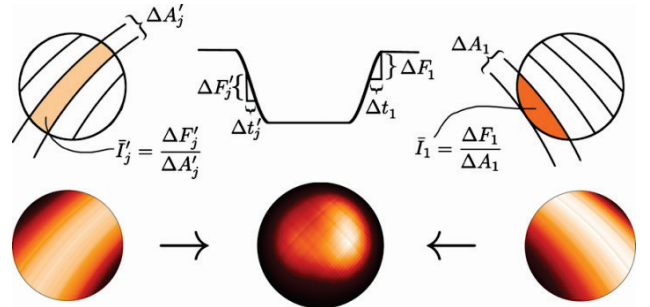
Figure 2-7: Methods adopted by ARIEL to probe the exoplanet composition & structure. <u>Top</u>: slice mapping with ingress and egress maps as well as a combined map of HD189733b at 8 μm. These were achieved with Spitzer (Majeau et al., 2012, De Witt et al., 2012). <u>Right</u>: time series of brown-dwarf narrowband light curves observed with HST-WFC3 (Apai et al, 2013). The spectral bands have been selected to probe specific atmospheric depths and inhomogeneities in the cloud decks.
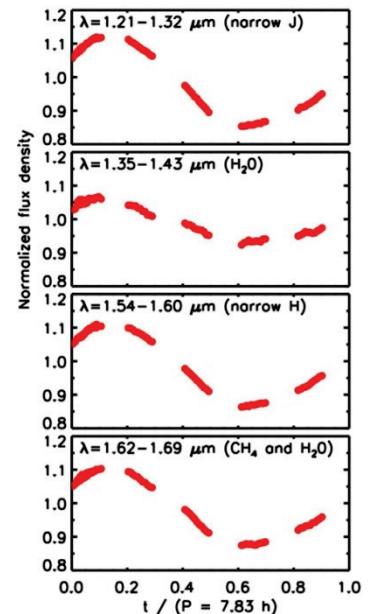
4. In addition, eclipses can be used to spatially resolve the day-side hemisphere (**eclipse mapping**). During ingress and egress, the partial occultation effectively maps the photospheric emission region of the planet (Rauscher et al., 2007). Figure 2-7 illustrates eclipse mapping observations (Majeau et al., 2012).

5. Finally, an important aspect of ARIEL is the repeated observations of a number of key planets in both transit and eclipse mode (**time series of narrow spectral bands**). This will allow the monitoring of global meteorological variations in the planetary atmospheres, and to probe cloud distribution and patchiness (see e.g. Apai et al.,

2013 for similar work on brown dwarfs, Figure 2-7).

2.4.2 Targets available for ARIEL

ARIEL will study a large population of hot and warm planets, already discovered by other facilities. In particular it will focus on hundreds of gaseous objects (Jupiters, Saturns, Neptunes) and tens of super-Earths/sub-Neptunes around bright stars of all types. Several surveys both from ground and from space will provide targets with the necessary characteristics to meet the objectives of the mission. Table 2-1 and Figure 2-8 summarise the most important surveys from which we expect a significant contribution to the final core sample. The list is not exhaustive.

Survey/Mission	Key characteristics	Stellar types	Planets relevant to ARIEL	Notes
WASP/SuperWASP (Pollacco et al., 2006)	• Ground photometric survey • All sky, ongoing	G-early K	100 *J* Few *N*	P_{orb} < 10 days; > 70 *J* already discovered
K2 (Beichman et al., 2014)	• Space survey • Survey in the ecliptic plane • Ongoing	All	~ 500 *J* ~500 *SE, N*	P_{orb} < 5 days
HATNet/HATSouth (Bakos et al., 2002)	• Ground photometric survey • All sky, ongoing	G/K	100 *J* Few *N*	P_{orb} < 10 days; > 50 *J* already discovered
HARPS, HARPS-N, Keck, ESPRESSO, CARMENES, SPiROU	• Ground RV surveys VIS/IR • All sky, bright stars • Ongoing/being built	G/K/M	See below	Discovered the brightest targets in each category. Transit search through photometric follow-up
CHEOPS (Broeg et al., 2013)	• Space photometric follow-up • 2017-2021 (3.5yr) • Monitoring of RV-detected planets	G/K/M	10 *N* 5 *SE*	Also used to refine parameters of planets detected by ground-based transit surveys
NGTS (Chazelas et al., 2012)	• Ground photometric survey • -50 < dec < -30 • 2014 − 2019	G/K/M	100 *J* 20 *N* 20 *SE*	P_{orb} < 16 days
APACHE (Sozzetti et al, 2013)	• Ground photometric survey • Monitoring of 3,000 M	M	5 *SN/SE*	P_{orb} < 10 days
GAIA (Lindegren, 2010)	• Space astrometric survey • All sky • 2014-2019	All	10-15 *J*	Around M stars 0.5-3 AU
MEarth (Nutzman et al., 2008)	• Ground photometric Survey • Ongoing	Late-M	5 *SN/SE*	P_{orb} < 10 days; GJ 1214b
TESS (Ricker et al., 2014)	• Space photometric survey • 45,000 square degree • Launch 2017	G/K/M	650 *J* 1000 *N* 700 *SN*; 300 *SE*	P_{orb} < 50 days
PLATO (Rauer et al., 2014)	• Space photometric survey • 2250 square degrees • Launch 2024	All	~1000 *J* 1200 *N* 700 *SN*; 600 *SE*	The hot and large planets should be detected sooner.

Table 2-1: Summary of the main surveys/projects that will provide targets for ARIEL in the next ten years. The columns on stars and expected planets refer specifically to the observations relevant for ARIEL. J=Jupiters, N=Neptunes, SN=sub-Neptunes, SE= Super-Earths.

PLATO expected numbers of planets

$m_V \leq 11$ (with stellar activity)
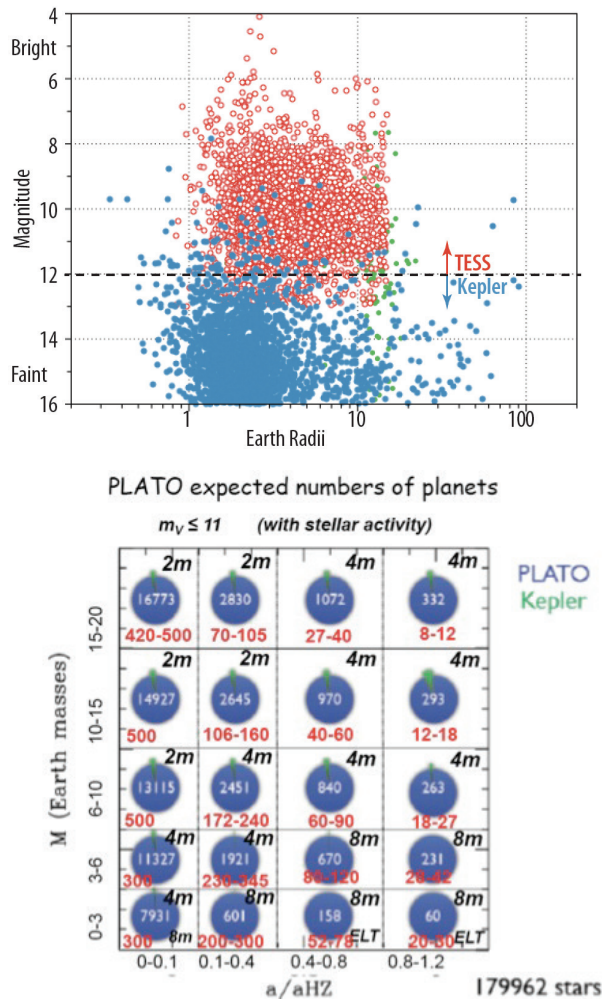
Figure 2-8: <u>*Top*</u>*: The planets detected by TESS (red) will typically be 3-5 magnitudes brighter than those found by Kepler (blue) thus making them excellent targets for ARIEL (Ricker et al. 2014).* <u>*Bottom*</u>*: Expected planet yield from the PLATO mission (red numbers) as a function of separation from the star (in units of habitable zone distance) and mass (see Rauer et al., 2014 for details). ARIEL will observe spectroscopically in the IR planets in the 2 columns on the left, with the exception of the bottom row.*

2.5 EXPECTED SCIENTIFIC RESULTS

2.5.1 Tens of molecules, hundreds of planets, thousands of spectra…

ARIEL will observe spectroscopically hundreds of warm and hot transiting planets at different temperatures around a variety of stellar types to establish what these planets are made of. illustrates the capabilities of AREIL of recording good quality spectra for a range of planetary types. Note that the simulated spectra were generated assuming the current knowledge about these planets, which is in many cases negligible or none when it comes to atmospheric composition.

The diversity in compositions is expected to be linked to different formation, evolution scenarios (see §2.5.2 and §2.5.3). In particular ARIEL will:

- Classify the variety of planets at different temperatures, nominally from ~600K to 3000K.

- Measure both albedo and thermal emission to determine the planetary energy budget, through broadband eclipse measurements in the visible (VIS) and infrared (IR).

- Identify the variety of chemical components present in warm & hot exoplanets' atmospheres. ARIEL will enable the detection of all the molecular species expected to play a key role in the physics and chemistry of planetary atmospheres. More specifically, molecular species such as H_2O, CH_4, CO_2, CO, NH_3, HCN, C_2H_2 are key to understand the C-N-O chemistry of exoplanets (Venot et al., 2012; Moses et al., 2012). In addition to these candidate absorbers, molecular species such as SiO, H_2S, PH_3, and H_3^+ are also pivotal to trace the formation history and evolution of giant and terrestrial exoplanets. For hot gaseous planets, TiO, VO and metal hydrides (TiH, CrH, FeH etc.) are also expected by analogy to brown dwarfs (Sharp & Burrows, 2007).

- Enable an optimal retrieval of the chemical abundances and thermal profiles (see §3.2).

- Detect the presence of clouds, constrain their spatial distribution and temporal variability (see §2.4.1) and potential composition (through the non-detection of the corresponding volatile species, albedo & transmission properties).

2.5.2 Chemical composition & evolution of gaseous planets

Gaseous planets (giants & Neptunes) are mostly made of hydrogen and helium and are expected to be always in gaseous form, so that the relevant questions concern the amounts of all elements other than hydrogen and helium, i.e. the heavy elements, that are present. The atmospheres of hot Jupiters and Neptunes present a critical advantage compared to the planets of the Solar System: their high temperature. Unlike Jupiter, Saturn, Uranus and Neptune, there is no cold trap in their atmosphere for species such as H_2O, CH_4, NH_3, CO_2 etc., which condense at much colder temperatures. Observations of hot gaseous exoplanets can therefore provide a unique access to their elementary composition (especially C, O, N, S) and enable the understanding of the early stage of planetary and atmospheric formation during the nebular phase and the following few millions years (see §2.5.3).
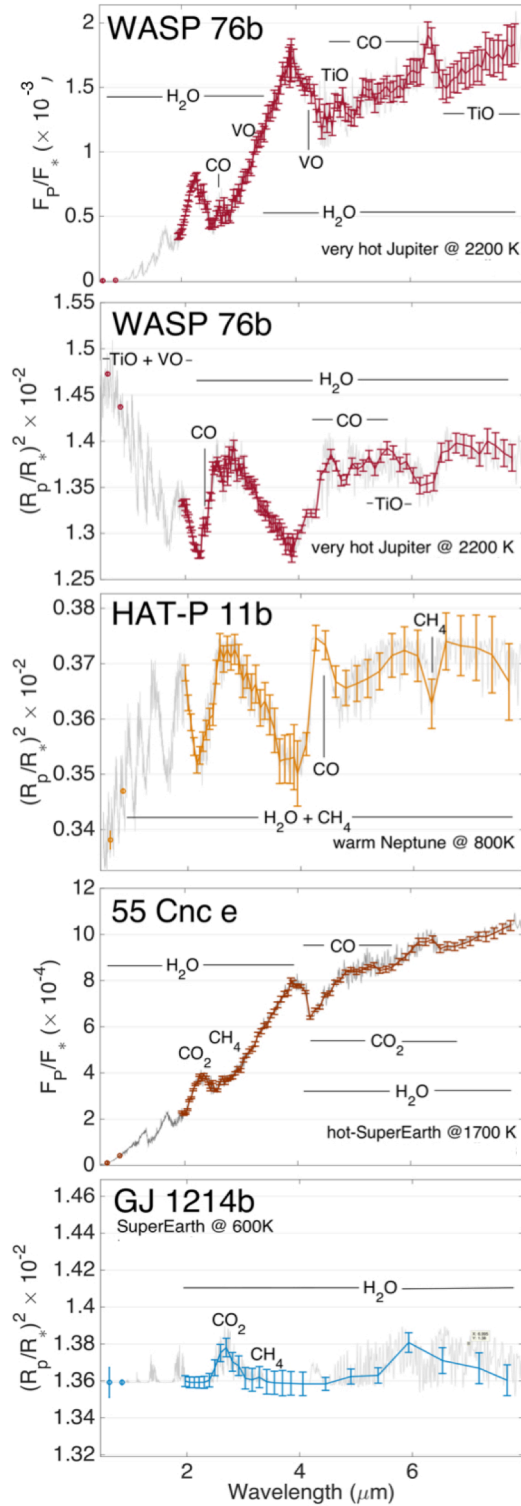
Figure 2-8: *Simulated spectra of 5 existing planets with different sizes and temperatures as observed by ARIEL. The simulations were obtained with our instrument end-to-end simulator, ARIEL-Sim (Pascale et al., 2014) validated against the ESA radiometric model by Puig et al. (2014). Top & second row: hot-Jupiter WASP-76b at 2200K around a F-type star, mag. K = 8.5, both transit & eclipse spesctra are shown. The TiO and VO signatures are easy detectable despite the very low abundances assumed. Third row: transit spectrum of warm Neptune HAT-P-11b at 800K around a K-type star, mag. K= 7. Fourth row: eclipse spectrum of hot super-Earth 55-Cnc-e around a G-type star, Mag K =4. Bottom: transit spectrum of warm super-Earth GJ1214b at 600 K around a M star, Mag K=9. The planet is assumed entirely covered by clouds as hypothesized by the latest studies (Kreidberg et al., 2014).*

To derive the elementary composition, we need to extract the relative abundances of the molecular species present in the atmosphere in great detail. This can be done through spectral retrieval models (see §3.2) applied to the spectra observed by ARIEL. This information is also critical to test the effectiveness of the physical and chemical processes directly responsible for planetary diversity and evolution (e.g. photochemistry, cloud formation, atmospheric dynamics, escape processes etc.). In particular, out-of-equilibrium processes (mixing and photodissociations) influence the relative abundances of the trace gases present in the atmosphere, so the observed spectra may or may not correspond to a chemical equilibrium composition. The influence of mixing and photolysis, though, does not have the same impact on the composition depending of the temperature of the atmosphere and on the intensity of these processes. Venot et al. (2015) have studied how it should vary the equilibrium/disequilibrium limit with vertical mixing, assumed to range from 10^3 to 10^{12} cm^2/s. Figure 2-9 represents the equilibrium/disequilibrium lines as a function of pressure and temperature, for different vertical mixing intensities. The atmospheric pressure sounded by the ARIEL observations would range from approximately 1 to 10^3 mbar. Exoplanets with a temperature higher than 1500 K in this pressure range are likely to be at chemical equilibrium.
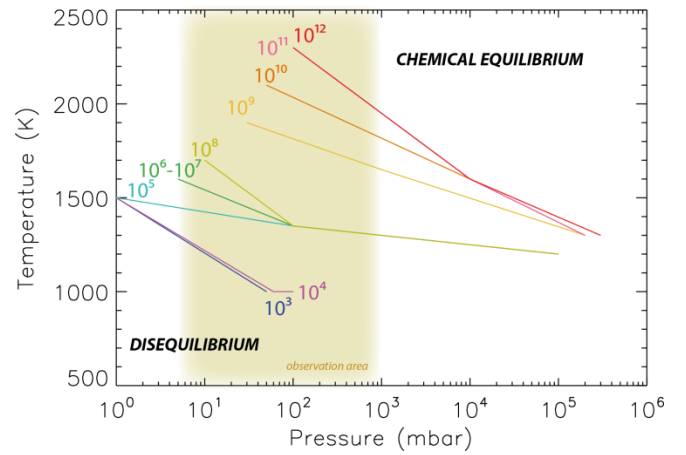
Figure 2-9: *P-T chemical equilibrium/disequilibrum transition lines (cm^2 s^{-1}) calculated for different vertical mixing intensities. They are represented by different colours. For instance, an atmospheric layer at 1500K and 10^2 mbar is at chemical equilibrium if the vertical mixing is lower than 10^9 cm^{2}s^{-1} (Venot et al., 2015). The observation area is shown yellow shaded.*

Planets with a lower temperature, are likely to be partially or entirely out of equilibrium. This evaluation depends on the value of the vertical mixing in the atmosphere, which is very uncertain, hence requires observational constraints.

Nevertheless, eddy mixing coefficients of about 10^8 cm^{2}s^{-1} are commonly used in the community of exoplanets. Two different C/O ratios have been tested (C/O solar and C/O=1.1) but this parameter has no impact on the equilibrium/disequilibrium lines (Venot et al., 2015).

Temp	Day-side	Night-side	Dynamics/Chemistry	Cloud type	Observables by ARIEL
VERY HOT > 1500K	Equilibrium chemistry Bulk composition is observable through atmosphere	Equilibrium chemistry Bulk composition is observable through atmosphere	2D/3D models represents well chemistry & dynamics	Ca/Ti/V oxides Corundum	- Trace gases relative abundances (especially H$_2$O, TO, VO, CO..) - Vertical & horizontal thermal structure through transits, eclipses & phase curves - Cloud detection through albedo and blue/red filters transit observations. - Cloud composition: detection TiO, VO, TiH.. gases - Inhomogeneities in the cloud decks through time-series
HOT ~800-1500K	Equilibrium chemistry Bulk composition is observable through atmosphere	Non-equilibrium chemistry Bulk composition is partially observable through atmosphere	Equilibrium transition CO/CH$_4$	Mg-silicates Fe Na$_2$S LiCl SiO$_2$	- Trace gases relative abundances (especially CH$_4$, HCN, NH$_3$) - Vertical & horizontal thermal structure through transits, eclipses & phase curves - Cloud detection through albedo and blue/red filters transit observations. - Cloud composition: detection FeH, SiO gases. Detection of alkali metals (Na, Li, K) from ground. - Inhomogeneities in the cloud decks through time-series
WARM ~400-800 K	- Non-equilibrium chem. - Negligible difference between day/night - Information on bulk composition at ~ T > 600K		1-D models represents well chemistry & dynamics Equilibrium transition N$_2$/NH$_3$	KCl	- Trace gases relative abundances (especially CH$_4$, HCN, NH$_3$) - Vertical thermal structure eclipses - Cloud detection through albedo and blue/red filters transit obs. - Inhomogeneities in the cloud decks through time-series
TEMPERATE & COLD <300K	- Non-equilibrium chemistry - No information on bulk composition - Negligible difference between day/night - More species are condensed out in clouds & interior			H$_2$O, CO$_2$ NH$_3$, H$_2$S CH$_4$, C$_2$H$_6$	Solar System planets, No ARIEL observations

Table 2-2: Expected classes of gaseous planets according to chemistry and dynamical models (Venot et al., 2015; Lodders & Fegley, 2006; Agundez et al., 2012). The predicted transitions need to be confirmed or confuted by ARIEL observations.

Table 2-2 summarises how ARIEL will test the validity of current theoretical predictions, which hypothesize classes of gaseous planets according to chemical and dynamical properties.

2.5.3   Formation of gaseous planets

As the study of the formation and evolution of the Solar System and its different planetary bodies taught us, orbital parameters and mass and size are not enough to solve the puzzle of the origin of a planetary system and to constrain its past evolution. The orbital evolution of planets is randomly affected by planetary encounters and can be drastically altered by migration. Migration, in turn, can act either very early, due to the interaction between a planet and the circumstellar disk in which it is embedded in (e.g D'Angelo et al. 2011; Kley & Nelson 2012), or at a later time, as a result of planet-planet scattering in unstable multiplanet configurations (Weidenschilling & Marzari 1996; Chatterjee et al. 2008). Finally, the onset of the dynamical instability that will result in the planet-planet scattering event is affected by unknown or poorly constrained parameters, like the mass present in the form of solid bodies in the early life of the planetary system, and is therefore difficult to pinpoint in time (Tsiganis et al. 2005; Levison et al. 2011).

The experience derived from the study of the Solar System tells us that the additional information needed to solve the puzzle posed by the history of a planetary system and of its planets is compositional in nature (see e.g. Raymond et al. 2006; Turrini & Svetsov 2014). Migration and, more generally, the formation and dynamical history of a giant planet, affect the composition in different ways (Guillot & Gladman 2000; Matter et al. 2009; Turrini et al., 2014). Firstly it affects the bulk elemental composition of the gaseous envelope by making it capture gas and solids from different regions of the circumstellar disk (therefore with different ratios between the condensate and gaseous phases for the most abundant elements like C and O, see Figure 2-10, top panel, and Turrini et al., 2014). Additionally, it affects the efficiency with which the long-range gravitational pull of the giant planets is able to accrete solid material from far away regions of the protoplanetary disk, enhancing the abundance of refractory elements and metals in the gaseous envelope (see Figure 2-10, bottom panel, and Turrini et al., 2014).

ARIEL will be able to investigate the presence of high-Z materials in the atmospheres of hot planets, which are impossible to observe in the Solar System

giant planets, as they have condensed out/sunk into their interior.
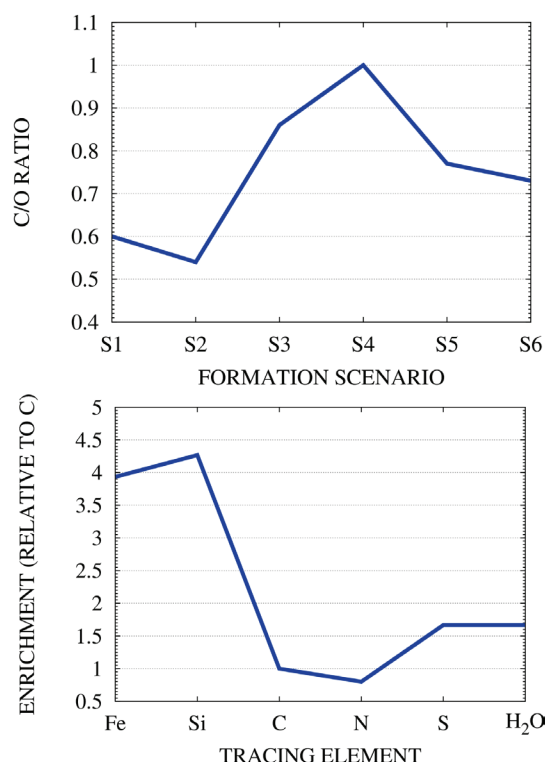
Figure 2-10: Effects of the formation and migration history of a giant planet on its atmospheric composition from the simulations of Turrini, et al. (2014). <u>Top</u>: atmospheric C/O ratio for a giant planet accreting only gas from inside the H_2O ice line (scenario 1), gas and solids from inside the H_2O ice line (scenario 2), only gas from outside the H_2O ice line but inside the CO_2 ice line (scenario 3), only gas from beyond the CO_2 ice line (scenario 4), only gas from inside and outside the H_2O ice line and from beyond the CO_2 ice line (scenario 5), gas and solids from inside and outside the H_2O ice line and from beyond the CO_2 ice line (scenario 6). <u>Bottom</u>: atmospheric enrichment of a giant planet (relative to the C enrichment) for water and different tracing elements as a result of the post-formation accretion of solids due to the long-range action of its gravitational perturbation. As can be seen, elements like Fe and Si are significantly more enriched than C but they would sink at depth in the case of a cold giant planet like Jupiter (see Taylor et al. 2004 on the transient detection of metals and silicates in the Jovian atmosphere after the impact of comet Shoemaker-Levy 9).

2.5.4   Formation & evolution of terrestrial-type planets

Several scenarios may occur for the formation and evolution of terrestrial-type planets – i.e. predominantly solid planets (Figure 2-4). To start with, these objects could have formed *in situ*, or have moved from their original location because of dynamical interaction with other bodies, or they could be remnant cores of more gaseous objects which have migrated in. Having a lower mass, their atmospheres could have evolved quite dramatically from the initial composition, with lighter molecules, such as hydrogen, escaping more easily. Impacts with

other bodies, such as asteroids or comets, or volcanic activity might also alter significantly the composition of the primordial atmosphere. ARIEL can confirm the presence or absence of a substantial atmosphere enveloping hot terrestrial planets. On top of this, ARIEL can detect the composition of their atmospheres (CO_2, SiO, H_2O etc.), so we can test the validity of current theoretical predictions (Figure 2-4). In particular:

(i) A very thick atmosphere (several Earth masses) of heavy gas, such as carbon dioxide, ammonia, water vapour or nitrogen, is not realistic because it requires amounts of nitrogen, carbon, and oxygen with respect to silicon much higher than all the stellar ratios detected so far. If ARIEL detects an atmosphere which is not made of hydrogen and helium, the planet is almost certainly from the terrestrial family, which means that the thickness of the atmosphere is negligible with respect to the planetary radius. In that case, theoretical works provided by many authors in the last decade (Léger et al., 2004; Valencia et al., 2006, 2007; Adams & Seager, 2008; Grasset et al., 2009) can be fully exploited to characterise the inner structure of the planet.

(ii) If an object exhibits a radius that is bigger than that of a pure water world (water being the least dense, most abundant material except for H/He) of the same mass, this tells us that at least a few % of the total mass of the planet is made of low density species, most likely H_2 and He. The fact that many objects less massive than Neptune are in this regime shows that it is possible to accrete a large fraction of gas down to 2-3 M_{Earth}, the mass of Kepler-11 f. ARIEL can test this

hypothesis by probing the presence of H_2, He and H_2O through primary transit spectroscopy.

(iii) Among the most extreme examples in Figure 2-4, "lava planets", such as 55 Cnc e, are so close to their host star that the temperatures reached on the dayside are sufficient to melt the surface itself. As a result some elements, usually referred to as "refractory", become more volatile and can form a thin silicate atmosphere (Léger et al., 2011). Depending on the composition of the crust, the most abundant species should be, Na, K, O_2, O and SiO. In addition, silicate clouds could form. ARIEL will test this hypothesis by observing the atmospheres of planets like 55 Cnc e (Figure 2-8).

(iv) In current formation models, if the planet is formed close to the snow line, the water content of the planetesimals could be significantly large and tens to thousands of Earth oceans of water could be accreted (Elkins-Tanton, 2011). This suggests the existence of a vast population of planets with deep oceans (aqua-planets) or whose bulk composition is dominated by water (Ocean planets (Léger et al., 2004). ARIEL will test this scenario through transit and eclipse spectroscopy of candidate Ocean planets such as GJ1214b.

(v) A major motivation for exoplanet characterisation is to understand the probability of occurrence of habitable worlds, i.e. suitable for surface liquid water. While ARIEL will not study habitable planets, its major contribution to this topic results from its capability to detect the presence of atmospheres on many terrestrial planets outside the habitable zone and, in many cases, characterise them.

3 SCIENTIFIC REQUIREMENTS

ARIEL will study exoplanets both as a population & as individual objects. We describe in the following sections how ARIEL would achieve its objectives.

3.1 WAVELENGTH COVERAGE & SPECTRAL RESOLVING POWER

To maximise the scientific impact achievable by ARIEL, we need to access all the molecular species expected to play a key role in the physics and chemistry of planetary atmospheres. It is also essential that we can observe warm and hot planets at different temperatures (nominally from ~600 K to 3000 K, Figure 3-1) to probe the differences in

composition potentially linked to formation and evolution scenarios.

Broad, simultaneous wavelength coverage is therefore required to:

- Measure both albedo and thermal emission to determine the planetary energy budget (Figure 3-1).
- Classify the variety of planets at different temperatures.
- Detect the variety of chemical components present in warm & hot exoplanet atmospheres
- Guarantee redundancy (i.e. molecules detected in multiple bands of the spectrum) to secure the

reliability of the detection – especially when multiple chemical species overlap in a particular spectral range (Figure 3-2).

- Enable an optimal retrieval of the chemical abundances and thermal profile (§3.2).
- Detect clouds and constrain their spatial distribution and temporal variability (Figure 3-3).
- Correct for stellar variability (see §3.4.2)

This means covering the largest wavelength range feasible given the temperature limits (~600-3000 K). Table 3-1 summarises the choices made for ARIEL to maximise the scientific return.

(i) For hot and warm planets, the wavelength coverage $1.95 - 7.8$ µm is critical for ARIEL, as it guarantees that ALL the key chemical species (H_2O, CH_4, CO, CO_2, NH_3) and all other species (VO, TiO, H_2S, SiO, H_3^+, C_2H_2, C_2H_4, C_2H_6, PH_3, HCN, TiH, CrH etc.) can be detected, if present, in all the exoplanet types observed by ARIEL (see Figure 3-2).

(ii) Redundancy (i.e. molecules detected in multiple bands of the spectrum) significantly improves the reliability of the detection, especially when multiple chemical species overlap in a particular spectral range. The ARIEL wavelength coverage

Wavelength range	Resolving power	Scientific motivation
Blue filter – $0.55 - 0.75$ µm	Integrated band	- Correction stellar activity (optimised early stars) - Measurement of planetary albedo - Detection of clouds
Red filter – $0.75 - 1.0$ µm	Integrated band	- Correction stellar activity (optimised late stars) - Measurement of planetary albedo - Detection of clouds
IR spectrograph – $1.95 - 7.8$ µm	100-200	- Detection of atmospheric chemical components - Measurement of planet temperature (optimised warm-hot) - Retrieval of molecular abundances - Retrieval of vertical and horizontal thermal structure - Detection temporal variability (weather/cloud distribution)

Table 3-1: summary of the ARIEL spectral coverage (left column) and resolving power (central column). The key scientific motivations are listed in the right column
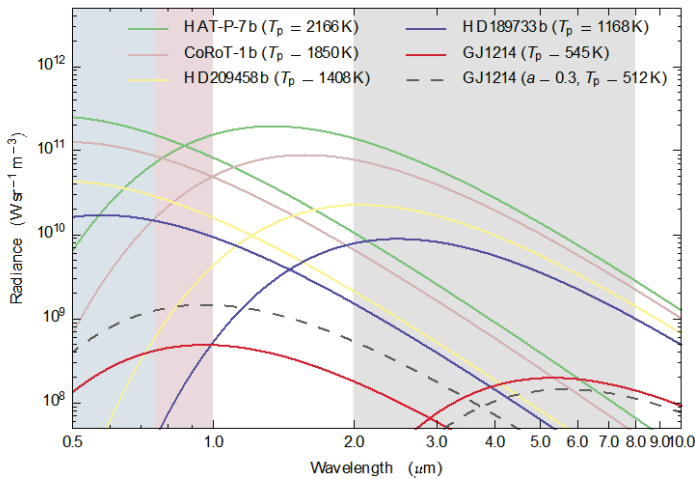
Figure 3-1: Reflected and thermal components for very hot (HAT-P-7b and CoRoT-1b), hot (HD209458b and HD189733b) and warm objects (GJ 436b and GJ 1214b). Calculations are made for a very low value of the albedo a = 0.1, and for a=0.3 in the case of GJ1214b. The grey area indicates the spectral window covered by the ARIEL spectrograph, the blue and red bands the 2 ARIEL photometric bands in the visible to monitor stellar activities, detect clouds and measure the planetary albedo.

Some spectral regions are more critical than others, as it is explained in the following paragraphs (Tinetti, Encrenaz, Coustenis, 2013; Encrenaz et al., 2014).

guarantees that the key species can be detected in multiple spectral bands.

(iii) Redundancy in molecular detection is also necessary to allow the retrieval of the vertical thermal structure and molecular abundances. The wavelength range $1.95 - 7.8$ µm guarantees the retrieval of molecular abundances and thermal profiles, especially for gaseous planets, with an increasing difficulty in retrieving said information for colder atmospheres (see §3.2 and Barstow et al., 2014).

(iv) A spectral resolving power of R = 100-200 will permit the detection of most molecules at warm and hot temperature. For smaller and more challenging planets, R = 50 is also an adequate solution, given the spectral broadening due to the high temperature (Tinetti, Encrenaz, Coustenis, 2013).

(v) In the visible, 2 bands are sufficient to measure the planetary albedo (see Figure 3-1), differentiate the detection of Rayleigh scattering as opposed to clouds (see Figure 3-3), to

measure the planetary albedo and to correct for stellar variability (see §3.4.2).
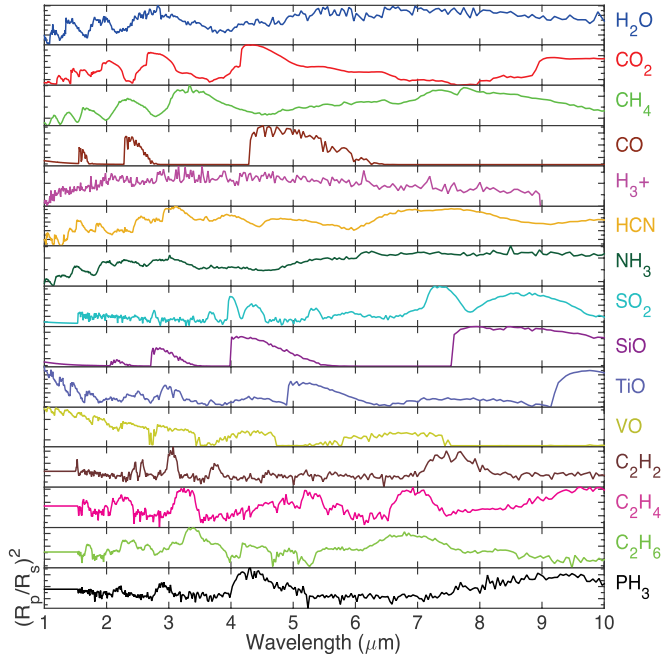
Figure 3-2: Molecular signatures in the 1-10 μm range at the required spectral resolving power proposed for ARIEL (R=100).
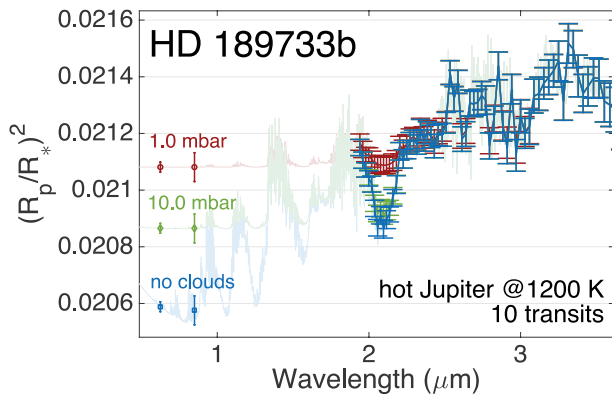
Figure 3-3: Cloud signature in the 0.5-3 μm range: ARIEL will measure simultaneously the relative contribution of the "blue" and "red" bands in the visible, and the spectral contribution in the 1.95-7.8 μm range (simulations obtained with the ARIEL instrument simulator, see §4.8). Through these measurements ARIEL will detect the presence of clouds/hazes, and constrain cloud parameters such as altitude, thickness, particle-size.

3.2 OPTIMISED RETRIEVAL OF MOLECULAR SPECIES & THERMAL PROFILES

To optimise the wavelength range, spectral resolution (R) & Signal-to-Noise Ratio (SNR) needed to achieve the science requirements and goals, we have used a suite of direct and inverse radiative transfer models developed by different teams part of the ARIEL collaboration and run in parallel. In particular we show here the results obtained with two retrieval models: NEMESIS & TauREx.

The Non-linear optimal Estimator for MultivariateE spectral analysis (NEMESIS) (Irwin et al. 2008) uses a combination of the correlated-k forward model with an optimal estimation retrieval scheme (Rodgers 2000). It has been used to successfully investigate planetary atmospheres in our own Solar System and beyond (Lee et al., 2012; Barstow et al., 2014a,b). Here simulated spectra are generated using an input atmospheric model, and random noise of the appropriate magnitude added. These are then used as inputs for the NEMESIS optimal estimation retrieval scheme and the retrieved atmospheric state compared with the input.".

Tau-REx (Tau Retrieval for Exoplanets), as developed by Waldmann et al. (2014), is a line-by-line radiative transfer fully Bayesian retrieval framework. It contains 1) the optimised use of molecular line-lists from the ExoMol project (Yurchenko and Tennyson, 2014); 2) an unbiased atmospheric composition prior selection, through custom built pattern recognition software; 3) the use of two independent algorithms to fully sample the Bayesian likelihood space: nested sampling as well as a more classical Markov Chain Monte Carlo approach; 4) iterative Bayesian parameter and model selection using the full Bayesian Evidence as well as the Savage-Dickey Ratio for nested models.

3.2.1 Transit spectra

We used TauREx to investigate the impact of SNR and spectral resolution on the retrievability of individual model parameters from transit spectra as observed by ARIEL. Model parameters include the planetary temperature, molecular abundances and cloud parameters. We report in Figure 3-4 and Figure 3-5 the results obtained in the case of a hot Jupiter and warm-Neptune respectively. Spectral retrieval of gas abundances for a hot-Jupiter and warm Neptune from transit spectra using NEMESIS gave similar results. These simulations confirm that an SNR ~ 10 and R ~ 100 would allow a good retrieval of the chemical species, while an SNR ~ 20 and a R ~ 200 would provide very accurate results. For the majority of the targets observed by ARIEL, these performances can be reached between 1 and a few tens of transits.

We have also run some blind tests, where forward models of cloudy planets generated by TauRex were combined to a noise model generated by the ARIEL instrument simulator (§4.8) and then they were analysed with NEMESIS. NEMESIS could retrieve the presence of clouds and of the correct atmospheric constituents (Figure 3-6 and Figure 3-7). In the case of GJ1214b: H_2O (5×10^{-2}), CO_2 (10^{-4}), CH_4 (5×10^{-4}),

all the gasses in the simulation, are well retrieved. In the case of WASP54b, H_2O (10^{-5}), CO (10^{-5}), CH_4 (10^{-5}) are well retrieved but CO_2 (10^{-5}) falls short.
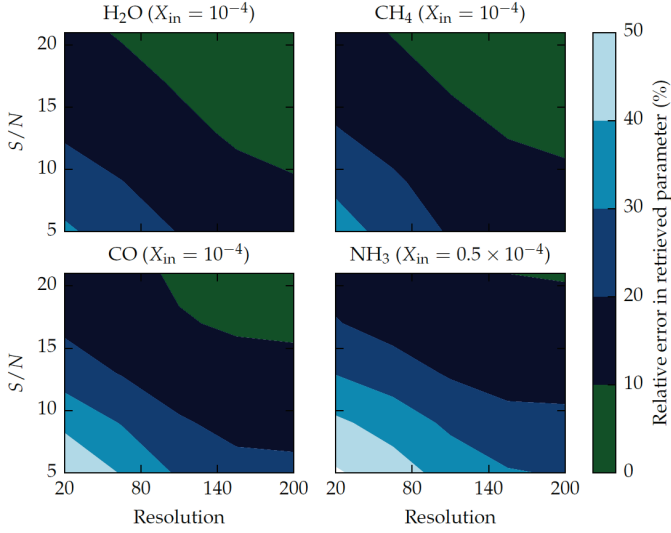
Figure 3-4: Spectral retrieval of cloud-free hot-Jupiter atmospheres observed with transit spectroscopy. The error in the estimation of the molecular abundances is provided as a function of the spectral resolution & SNR obtainable with ARIEL.
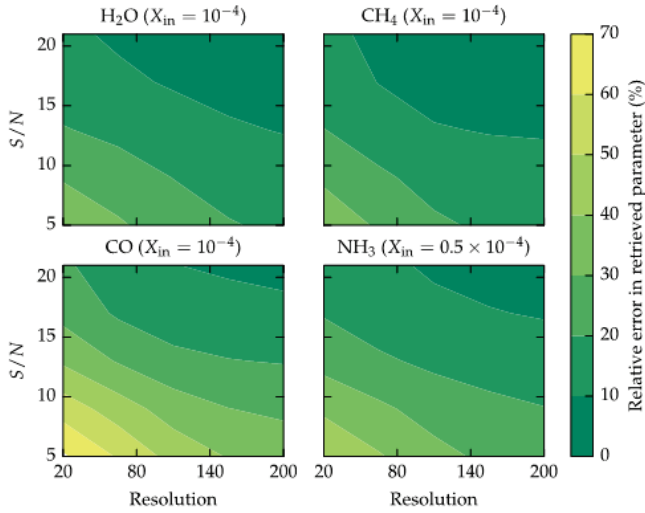
Figure 3-5: Spectral retrieval of cloud-free warm Neptune atmospheres observed with transit spectroscopy. The error in the estimation of the molecular abundances is provided as a function of the spectral resolution & SNR.

3.2.2 Eclipse spectra

To assess the performances of ARIEL in doing eclipse spectroscopy, we performed the retrieval of the vertical thermal structure and gas abundances for a hot-Jupiter and warm Neptune from eclipse spectra using NEMESIS. Simulated spectra were generated using an input atmospheric model, and random noise of the appropriate magnitude added. These were then used as inputs for the NEMESIS optimal estimation retrieval scheme and the retrieved atmospheric state compared with the input. We show in Figure 3-8 the

results of the retrieval of the vertical thermal profiles and molecular abundances.
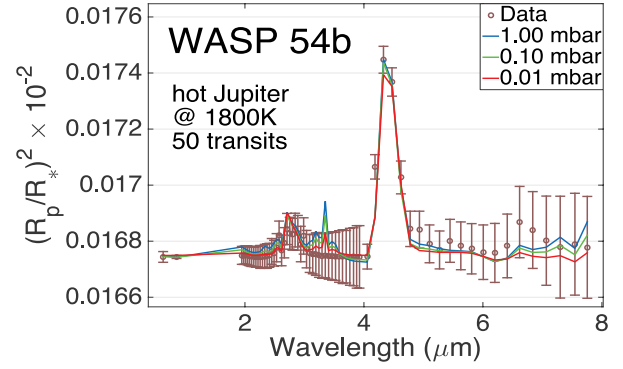
Figure 3-6: NEMESIS retrieval results for the transit spectrum of WASP54b assumed to be completely covered by clouds. The input model to ARIELSim was generated by the TauRex code whereas the retrieval was performed by the independent NEMESIS code. Continuous coloured lines show retrieval results for various cloud top layer pressures for a reducing atmosphere. The spectrum could not be fit with a cloud-free model.
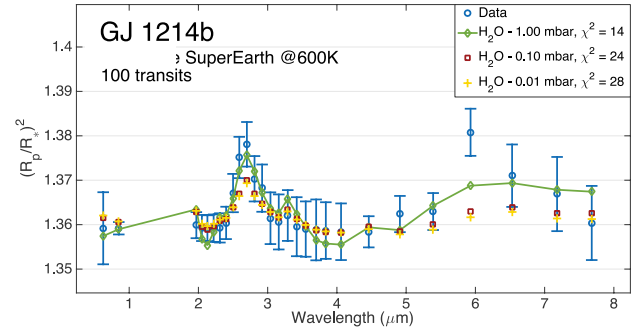
Figure 3-7: NEMESIS retrieval results for the transit spectrum of GJ1214b assumed to be completely covered by clouds. The input model to ARIELSim was generated by the TauRex code whereas the retrieval was performed by the independent NEMESIS code. Continuous coloured lines show retrieval results for various cloud top layer pressures for a water dominated atmospheric composition.
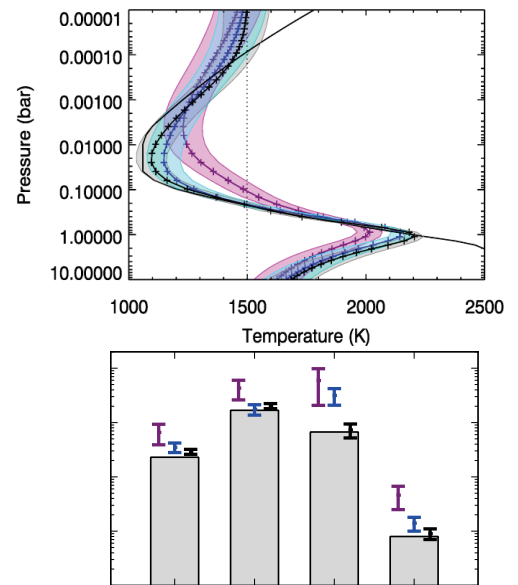
Figure 3-8: Retrieval of T-P profile and gas abundances performed with NEMESIS for a range of SNRs: 5 (purple),10

(blue) and 20 (black) at 5 µm. The bars show the input values, the three error bars show the retrieved values for each molecule (purple SNR 5, blue SNR 10, black SNR 20, as in the TP plots). <u>Top:</u> hot-Jupiter; <u>Bottom:</u> warm Neptune. In both cases, there is noticeable improvements in temperature retrieval from SNR 5-10, but increasing to 20 it does not add as much. Gas retrievals improve as the SNR increases.
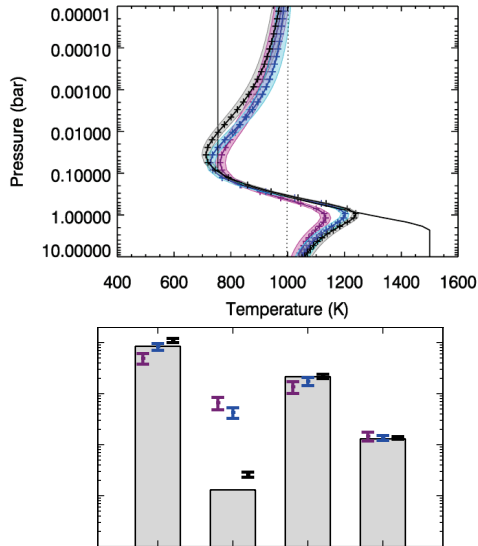
3.2.3 Observing strategy

ARIEL will visit a large and well-defined set of targets (a few hundreds, see §3.3). Repeated visits may be required to build up the SNR of individual target spectra. The maximum duration of a visit to a target system will be less than 10 hours, i.e. the time of the transit itself, plus half that time before and then after the transit. The time between successive transit observations will depend on the orbital period and scheduling, and could be as little as a fraction of a day, to as long as a few days (with the exception of high eccentric orbit planets). In principle, the targets may be in any part of the sky, and as such the satellite needs a large field of regard, with minimal constraints (due to Earth/Sun) on the direction in which it can be pointed. Most of the targets will require between one and a few tens of transits/eclipses depending on the brightness and spectral type of the host star, and planetary radius and temperature (see). The most challenging targets for ARIEL will be warm super-Earths such as GJ1214b, which is a relatively small and cold planet, orbiting an M dwarf whose brightness is close to the limit required by ARIEL (mag K~9). Up to ~100 repeated observations with ARIEL will be needed to obtain a good SNR and resolution for GJ1214b, but ~850 transits of this target will be available during the duration of the mission. The complete sky shall be accessible within a year, with a source at the

ecliptic observable for ~30% of the mission lifetime (see §5.3.2).

The ability to fulfil the scientific program during the mission lifetime strongly depends on the optimization of the observations. Because the planetary transits and eclipses happen at specific epochs (given by ephemerides), the observation program, the data transfer sequences and the on-board calibration phases have to be well-defined and are time critical. The final performance evaluation of ARIEL also needs to take into account the way the observation and calibration/data transfer phases are optimized.

We have simulated an observing programme with an assumed target reference sample using scheduling simulation tools (Garcia-Piquer et al., 2014; Morales et al., 2014). These tools aim to check the feasibility and efficiency of the observation program. They include optimisation routines that allow the scheduling assuming knowledge of the visibility of the objects, the transit/occultation ephemerides, the expected spacecraft performance and some assumed calibration and data transfer phases. The net result of the overall process is that using a target list as defined in §3.3 the ARIEL mission would meet its scientific objectives.

3.3 THE ARIEL TARGET SAMPLE

ARIEL will study a large population of hot and warm planets, already discovered by other facilities (see §2.3.2). In particular it will focus on hundreds of gaseous objects (Jupiters, Saturns, Neptunes) around stars brighter than mag K=9.5 and tens of super-Earths/sub-Neptunes around stars brighter than mag K =9. There are ~ 60 currently known planets complying with these requirements.

To generate a core mission sample to be observed by ARIEL in 3.5 years, we have created a list of targets with different stellar types (F, G, K, M, brighter than K=9.5) and planetary parameters (size: Jupiters, Neptunes, super-Earths, sub-Neptunes; temperature: from 600K to 2200K; main molecular component: H_2, N_2, H_2O). For each of the target, we have calculated the required number of transits/eclipses to achieve the SNR/R needed to perform an accurate retrieval of the gas abundances and thermal properties. We found that ~ 500 planets can be observed during the mission lifetime with the required SNR/R

To calculate the number of transit/occultation revisits necessary to achieve a specified SNR/R and

the possible revisits during a given mission lifetime, we have used two complementary approaches:

1. The first approach taken is based on a static radiometric model that takes the required performance figures for the payload to 'size' the mission (Puig et al., 2014).

2. The second approach is to use a model that simulates the actual performance of the mission as realistically as possible (ARIEL-Sim, see §4.8). This end-to-end simulation is fully dynamic and accounts for the major systematic influences on the performance such as pointing jitter, internal thermal radiation sources, detector dark current and noise etc. (Pascale et al., 2014; Waldmann and Pascale, 2014). The ETLOS module (Varley et al., 2014) was used to run ARIEL-Sim for the entire core sample.

Both models have been used to calculate the observation duration needed for the targets in the ARIEL sample. The use of separate performance models with similar results gives confidence that the mission can be undertaken as planned and can deliver the science described in this proposal. We find that a nominal mission lifetime of 3.5 years is sufficient to fulfill the science requirements for ~ 500 planets, including hundreds of warm and hot Jupiters and Neptunes and tens of warm and hot super-Earths and sub-Neptunes.

This number of planets, is in agreement with current estimates of planet population in the solar neighbourhood (Ribas & Lovis, 2014) and with the predicted results of current surveys and future missions (Cheops, TESS, PLATO).

3.4 DEALING WITH SYSTEMATIC & ASTROPHYSICAL NOISE

3.4.1 ARIEL performances requirements

ARIEL's top-level requirement is that the photometric stability over the frequency band of interest shall not add significantly to the photometric noise from the astrophysical scene (star, planet and zodiacal light). The frequency band over which the requirement applies is between 2.8×10^{-5} Hz and 3.7 mHz, or ~5 minutes to 10 hours (Puig et al., 2014; Eccleston et al., 2104; Pascale et al., 2014; Waldmann and Pascale, 2014). This implies having the capability to remove any residual systematics and to co-add the elementary observations from many repeat visits to a given target. The photometric stability budget is described in §4.8 using the tools

described by Pascale et al. (2014), Waldmann and Pascale (2014) and Puig et al. (2014). To achieve the required performance, particular attention is required to:

- the design of the instrument
- the calibration strategy to characterise all possible systematic variations in performance
- the data processing pipeline(s).

3.4.2 Correcting for stellar activity

The differential spectroscopy measurement strategy of ARIEL (before/during/after the transit) is affected by changes in the host star spectrum on the timescale of the transit. Changes in the host star spectrum are caused by magnetic activity (flares, co-rotating active regions and spots) and convective turbulence (granulation, pulsations).

Results from the Kepler mission (Basri et al. 2013) indicate that most G dwarfs have photometric dispersions less than 50 ppm over a period of 6 hours, while most late-K and M dwarfs vary at a level of some 500 ppm. Note that Kepler operates in the visible where stellar photometric variability is few times higher than in the "sweet spot" of ARIEL – the NIR and MIR – because of the contrast between surface inhomogeneities and the stellar photosphere.

The ARIEL mission has been designed to be self-sufficient in its ability to correct for the effects of stellar activity. This is possible thanks to the instantaneous, broad-wavelength coverage and the strong chromatic dependence of light modulations caused by stellar variations.

The impact of stellar variations on the ARIEL data has been carefully evaluated by many teams working on ARIEL. We have explored several possible approaches to evaluate the effect of oscillations and stellar activity and developed methodologies to prove the performance of ARIEL data in reaching the required precision (Herrero et al., 2014; Micela, 2014; Danielski et al., 2015; Scandariato et al., 2014). We describe here the methodologies to prove the performance of ARIEL data in reaching the required precision.

3.4.2.1 Oscillations and granulation

The turbulent layer of the host star's interior causes two processes that change the star's luminosity: granulation and acoustic pressure wave oscillations. Both granulation and oscillations are visible as stochastic luminosity variations. In most cases, the

radius and gravity amplitudes are negligible, and thus the luminosity amplitude is almost entirely due to changes in temperature. This allows use of the ARIEL optical channel photometry to correct the IR spectra via spectral energy distributions calculated from model atmospheres for different host star temperatures. The large ARIEL bandpass allows to accurately calculate the relative spectral change of the star spectrum in the infrared.

For oscillations, we calculated the timescales and amplitudes of optical and infrared variability based on our simulations using the BiSON solar data from Broomhall et al. (2009) where amplitudes and frequencies were rescaled using the scaling relations from Kjeldsen and Bedding (2011).

Spectral type	Time scale (min)	Var 0.5um	Var 1.9um	Var 3.9um	Var 7.8um
F2V	5.4-20	188ppm	48ppm	27ppm	12ppm
Sun	3.6-12	101ppm	27ppm	11ppm	6ppm
K2V	3.6-13	74ppm	19ppm	11ppm	5ppm
M2V	2.68.7	37ppm	8ppm	4ppm	2ppm

Table 3-2: Amplitude and time scale for host star variability due to oscillations.

The peak-to-peak variation due to oscillations was computed on a 10 hour basis. The Marcs model atmosphere parameters for the different spectral types were chosen following Habets & Heintze (1981) and Pickles (1998).

Spectral type	Time scale	Var 0.5um	Var 1.95um	Var 3.9um	Var 7.8um
Sun	1min	100ppm	25 ppm	12ppm	6ppm
	10 h	200ppm	50 ppm	25ppm	12ppm

Table 3-3: Amplitude and time scale for host star variability due to granulation.
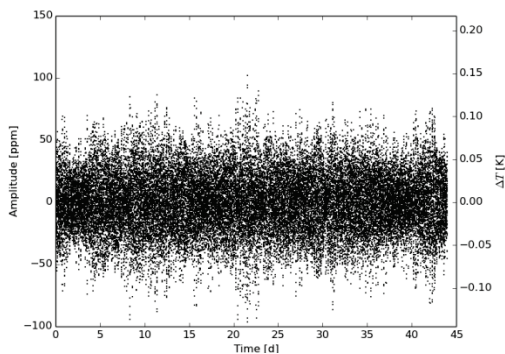
Figure 3-9: Simulation of stochastic luminosity variations due to oscillations (F2 dwarf) at 0.5 μm.

For granulation, the variability for solar type stars was simulated using different red noise components due to active regions and background granulation

(Palle et al., 1995). The scaling from the optical to the infrared was done using SEDs from Marcs models (Gustafsson et al., 2008).

3.4.2.2 Active Regions

The effects of stellar activity on ARIEL's observations will vary for transit and eclipse observations. Alterations in the spot distribution across the stellar surface can modify the transit depth (because of the changing ratio of photosphere and spotted areas on the face of the star) when multiple transit observations are combined, potentially giving rise to spurious planetary radius variations. The situation is simpler for occultations, where the planetary emission follows directly from the depth measurement. In this case, only activity-induced variations on the timescale of the duration of the occultation need to be corrected for to ensure that the proper stellar flux baseline is used. We have developed two different methods based on models to correct for effects occurring during transits.
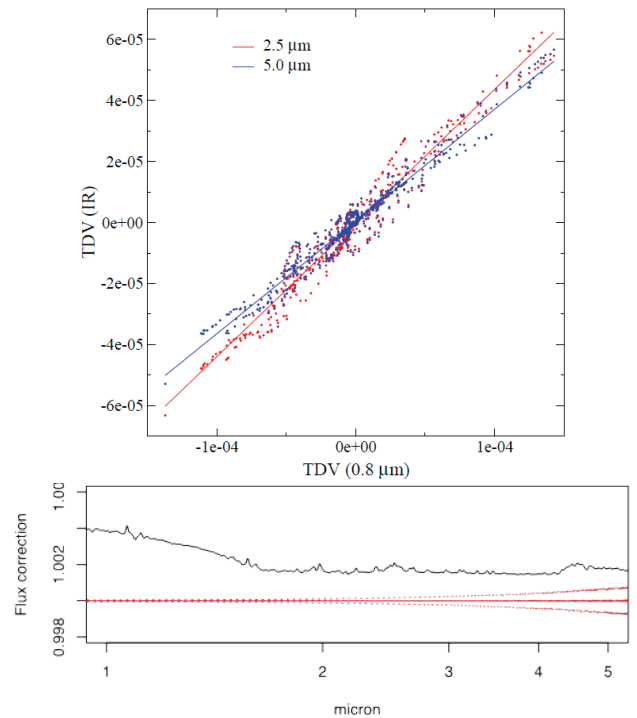
Figure 3-10: Top (method 1): Correlation of activity-induced transit depth variations (TDV) in the visible (0.8 μm) and the IR (2.5 and 5.0 μm). Bottom (method 2): Spectrum distortion without corrections (solid black line), residual distortion after correction (median and 25 -75% percentiles of simulations).

Method 1 – A realistic stellar simulator has been developed that produces time series data with the same properties as the measurements from ARIEL. The simulator considers surface inhomogeneities in the form of (dark) starspots and (bright) faculae, takes into account limb darkening (or brightening in the case of faculae), and includes time-variable effects

such as differential rotation and active region evolution. We have generated series of transits at wavelengths 0.8, 2.5, and 5.0 µm, measured the transit depths and calculated the variations of those depths with time. There is a well-defined correlation between activity-induced transit depth variations in the visible (0.8 µm) and the IR (2.5 and 5.0 µm). An illustration of the correlation between visible and IR transit depth variations (TDV) can be seen in Figure 3-10 (top). In practice, the correction of ARIEL data for stellar activity using, for example, a series of measurements in the visible and an IR band can be done using the following expression:

$$d_{IR}^{corr} = d_{IR} + a_0 + a_1 \cdot (d_{VIS} - \langle d_{VIS} \rangle),$$

where d stands for the transit depth, and a_0 and a_1 are the coefficients of a linear fit that can be determined from simulations.

A number of combinations of stellar photospheres and active region parameters (size and location of spots, temperature contrast) were considered to obtain a statistical view of the method (Herrero et al. 2014). In all the explored cases, the procedure provides a correction of the transit data to a few times 10^{-5}, and thus is fully compliant with ARIEL noise requirements.

Method 2 – A complementary method has been developed to reconstruct the spectral energy distribution of the target stars in the IR using the visible spectrum (0.55-1 µm) as an instantaneous calibrator. Having a sufficient number of spectra of a given stars observed at different levels of activity, it is possible to calibrate the method for each star. The approach, based on Principal Component Analysis, has been developed on a grid (in spot temperature and filling factor) of models of active stars and has been tested through simulations taking into account the photon noise. In all the explored cases the first two components are retained: the first component is related to the slope of the spectrum while higher order components are related to features of the spectrum. The method has been validated through extensive simulations with a variety of star-spot combinations. Figure 3-10 shows e.g. the stellar spectrum distortion, with and without correction, for a T_{eff}=5200 K star, and a stellar SNR=500. Also in this case the correction is entirely compliant with ARIEL requirements (Micela 2014).

3.4.2.3 Empirical Correction

A further approach has focused on statistical methods to de-correlate astrophysical noise from the desired science signal. Given single time series on an active star with various modes of pulsation obtained by the Kepler space telescope, Waldmann (2012) showed that a randomly chosen pulsation mode of the star could be isolated and the remaining auto-correlative noise of the star suppressed, resulting in a strong reduction of the stellar noise component. Similar concepts apply to periodic exoplanetary light-curves observed over multiple transits and/or wavelengths. The results were repeated for a sample of Kepler stellar light curves, spanning from M to G types. In all cases a correction of the order of 10^{-5} to $5 \cdot 10^{-4}$ depending on the frequency of the sampling (i.e. 10 hours continuous observations every day or 10 hours once a week), was obtained (Danielski et al., 2015).

3.4.2.4 Validations: Observational Check

Finally we started an observational program aimed to simultaneously monitor active stars in visible and infrared with very precise instruments (Danielski et al., in prep.). An example of simultaneous observations can be seen in Figure 3-11 that reports the CoRoT (black line) and Spitzer (4.5 µm, red line) light curves of an early K field star moderately active obtained during the simultaneous campaign CoRoT − Spitzer on NGC 2264 (Cody et al. 2014). Each curve is normalized to the unit. It is evident that the variations of the two light curves are well correlated and that the amplitude in CoRoT is about twice of that observe with Spitzer, in agreement with the expectation for a system star-spot(s) (e.g. Ballerini et al. 2012), supporting the hypotheses adopted in the model-based methods above.
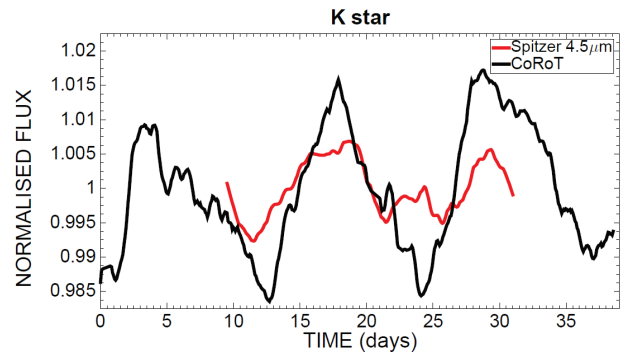
Figure 3-11: CoRoT (black line) and Spitzer (4.5 mu, red line) light curves of an early K field stars moderately active observed during the simultaneous campaign CoRoT − Spitzer on NGC 2264 (Cody et al. 2014). Each curve is normalized to the unit.

4 PROPOSED SCIENCE PAYLOAD

4.1 PAYLOAD MODULE ARCHITECTURE

The ARIEL payload module (PLM) consists of an integrated suite of telescope, spectrometer and FGS / photometer along with the necessary supporting hardware and services (such as optical bench, harnesses, radiators etc). The mission carries a single dedicated payload for its primary mission objectives; this payload will be developed and delivered by the ARIEL payload consortium. A block diagram of the payload architecture is shown in Figure 4-1.

The PLM will interface to the service module via a set of thermally isolating support struts or bi-pods, and will be radiatively shielded from the Service Module (SVM) and the solar input loads by a set of 3 V-Grooves. The isolating supports and V-Grooves are proposed to fall under the responsibility of the spacecraft prime contractor, all hardware fully in the cold zone of the spacecraft will be provided by the consortium. This enables a completely aligned and verified payload to be delivered to spacecraft level, thereby minimising the complexity (and risks) associated with the full spacecraft AIV program and allowing the best possible calibration of the payload without the complexity associated with a full S/C test.

4.1.1 Deliverable Units Definition

4.1.1.1 Cold Payload Units:

The ARIEL cold units are optically coupled via a common optics module and all referenced to the common optical bench. The units are thermally isolated by the S/C provided v-groove shields and the detectors are cooled by a dedicated radiator.

- **Telescope unit (ATU - ARIEL Telescope Unit)** – mirrors and M2 mechanism assembled and aligned onto telescope structure and baffle – mounts onto payload optical bench.
- **Optical bench (OB)** – mounting and alignment structure for telescope and instrument units. Mounts from S/C provided struts with quasi-kinematic mounting. Passively cooled.
- **Common optics (COM)** – mirrors and dichroics linking telescope and instrument – directly mounted on optical bench. Thermally controlled via the optical bench.
- **IR Spectrometer (AIRS – ARIEL IR Spectrometer)** – primary science payload. Optical module with optical interface to common optics – mechanically mounts on optical bench. Thermally controlled via the optical bench for the structure and optics and via cold strap to the payload radiator for the detector.
- **Fine Guidance Sensor (FGS)** – Optical module with optical interface to common optics – mounts on optical bench. Thermally controlled via the optical bench for the structure and optics and via cold strap to the payload radiator for the detector.
- **Thermal hardware** (ATH - ARIEL Thermal Hardware) – dedicated radiator for detectors and optical module cooling plus thermal straps to provide detector interfaces. Mounts off OB.

4.1.1.2 Warm Payload Units:

The ARIEL payload electronics consist of three boxes that act as Remote Terminal Units (RTUs) via Spacewire to the S/C CDMS. All high level commanding, operational sequencing and data storage is within the S/C CDMS, there is no assumed intelligence within the unts.

- **Instrument Control Unit (ICU)** – drives for spectrometer detectors, calibration source, thermistors (including any mounted on OB) etc. Command & data handling, compression & processing (if needed), formatting. I/O to CDMS.
- **FGS Electronics (FGE)** – drives for FGS detectors, thermistors etc. Command handling. Data handling, compression (if needed), processing (if needed) and formatting. FGS data processing. I/O to CDMS via Spacewire
- **Telescope Control Unit (TCU)** – Drives for M2 actuators, heaters, thermistors etc. Command handling. Data formatting. I/O to CDMS via Spacewire
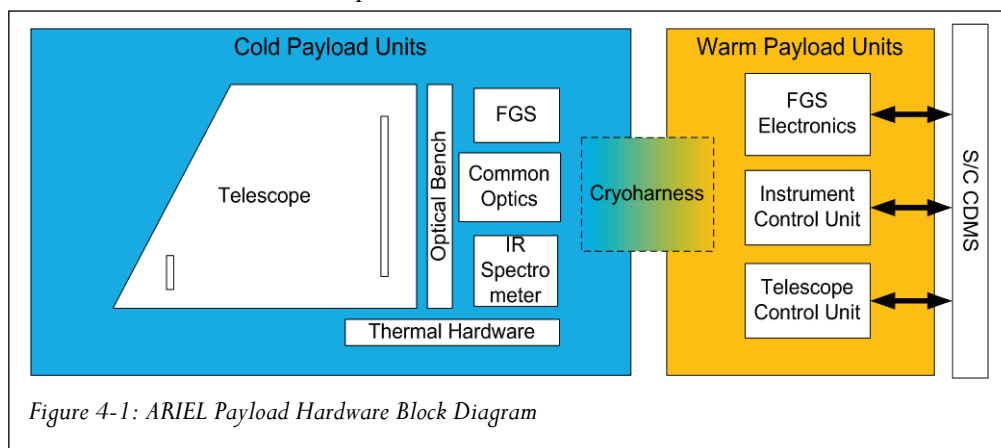
Figure 4-1: ARIEL Payload Hardware Block Diagram

- **Cryoharness: –** harness connecting warm and cold payload units including internal harnessing

between units on optical bench.

4.1.2 Payload Module Layout
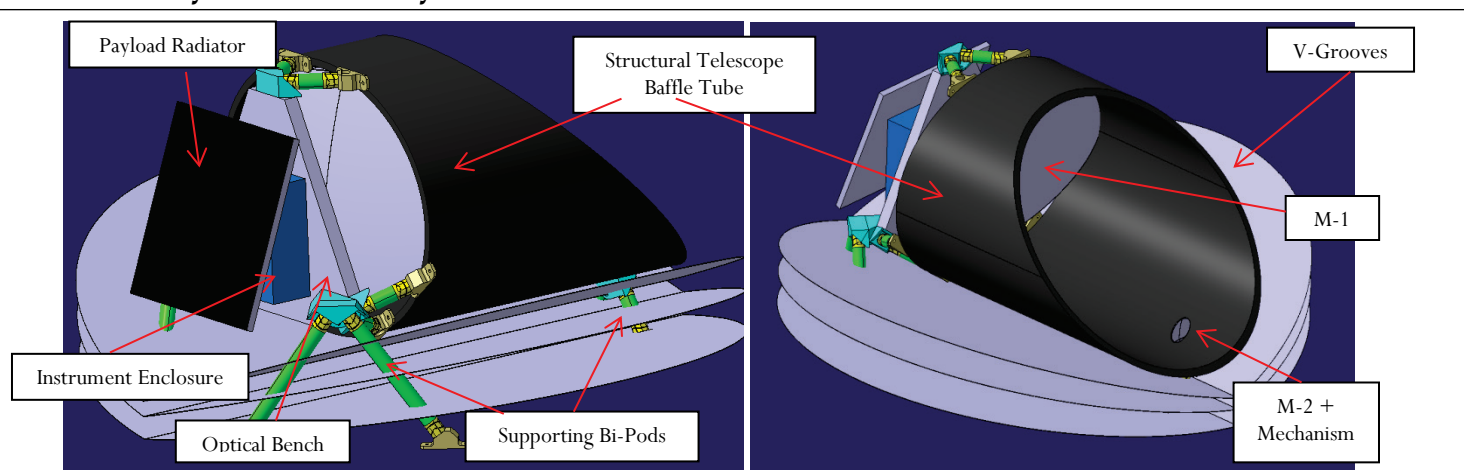
Figure 4-2: Overall Layout of ARIEL Payload Module

The ARIEL payload module is based upon a horizontal telescope configuration. The M1 and M2 are supported on a structural telescope baffle. The rear of the telescope assembly is supported from a combined payload optical bench. The instrument volume supported on this bench is enclosed by a housing structure to prevent stray light entering the detector chain. From the optical bench the Payload Radiator is supported via 3 pairs of bi-pod struts. The entire structure is supported through V groove thermal shields by the spacecraft via thermally isolating kinematic mounts (provided by the S/C prime). Provisionally the payload optical bench will be constructed from carbon fibre to closely match the proposed SiC M1/M2/Telescope structure. The mounting regime for the telescope will be investigated fully within the A1 phase where a detailed material trade-off can be carried out. Detailed mechanical analysis of the telescope mounting and support will also need to be carried out as the entire payload structure (apart from the bi-pod mounts that interface to the spacecraft) will be supplied by the consortium.

4.1.3 Payload Optical Bench Design

The instrument enclosure contains the FGS / NIR-Phot unit and a two band spectrometer, AIRS. The FGS input is split away from the incoming beam first via a Dichroic D1. The spectrometer channel light
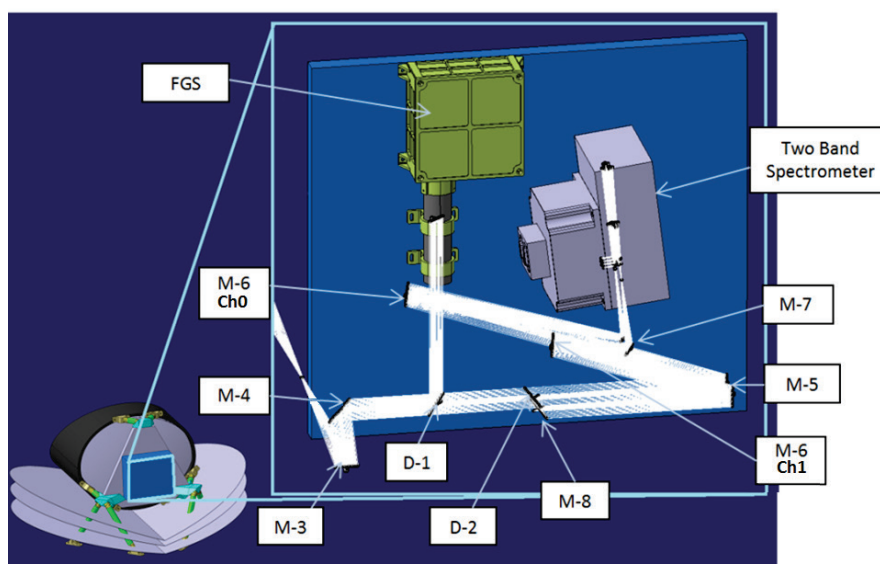
Figure 4-3: Instrument Bench Layout on Rear of ARIEL Primary Mirror

path is split into two sub-channels via a second dichroic, D2.

The current instrument layout is based upon an all-aluminium construction that was originally envisaged for the project. The design of the mounting of the detectors and optics will have to be studied in detail within phase A1 in order to accommodate the proposed carbon fibre payload optical bench structure.

4.1.4 Payload Module Thermal Architecture

The ARIEL payload thermal architecture is based on a purely passive design (Figure 4-4, left panel): a three V-Groove radiators configuration that, in the L2 environment, can provide stable temperature stages down to the 40-50K range with loads up to 1 W. The

PLM thermal design is based upon the main requirements, summarized in the following table together with the present evaluation of the loads on cold stages:

ARIEL payload thermal requirements table: The values in this table are estimated by preliminary thermal analyses and downscaling of the EChO mission study results			Thermal Interface (TIF) temperature and expected load[1] [mW]				
			VG1 (TIF1)	VG2 (TIF2)	VG3 (TIF3)	TOB/IOB (TIF 4)	Instrument Radiator (TIF5)
			T_Op [K]	T_Op [K]	T_Op [K]	T_Op [K]	T_Op [K]
Payload Unit	**T_Op [K]**	**dT[2] [K]**	≤150	≤100	≤55	≤55	≤40
Telescope	< 70	± 1	-	-	-	-	-
FGS Optics	≤50	± 0.5	-	-	-	-	-
FGS detectors + Temperature Control	≤50	± 0.05	-	-	-	-	10 + 5
FGS FEE	≤55	± 2	-	-	-	65	-
Spectrometer Optics	≤50	± 0.5	-	-	-	-	-
Spectro detectors + Temperature Control	≤42	± 0.05	-	-	-	-	10 + 5
Spectrometer FEE	≤55	± 2	-	-	-	20	-
Parasitic leaks[1] (struts + harness + radiation)	NA	NA	250	200	150	25	15
Total load[1] (w/ 50% margin) [mW]			250	200	150	110	45[3]

Notes: [1] Based on preliminary thermal modelling (Figure 4-4 right panel) and EChO mission proposal results (Eccleston et al, 2014)

   [2] Peak to peak value over a typical observation time (10 hours)

   [3] ARIEL PLM thermal design ensures that a ≤ 0.65 m[2] radiator is sufficient to achieve required performance

Table 4-1: Main thermal requirements and expected loads for the ARIEL payload

The operating temperatures of the Telescope Assembly (mirrors, baffle and payload optical bench) are achieved with a high emissivity baffle that, working as a large surface radiator, improves mirrors cooling, stability and optical performances. The FGS and Spectrometer detectors are cooled, via their temperature control stages (TCS), by a dedicated radiator (area ≤ 0.65 m[2]), mounted on the Payload Optical Bench, that will benefit of the cold radiative environment set by the last V-Groove and the Telescope Assembly.

The FGS and Spectrometer optical units and the cold Front End Electronics (FEE) are mounted on, and thermally coupled to, the Optical Bench to allow an efficient heat rejection to space. The Instrument radiative thermal control is achieved by proper shielding of the instrument cavity and each unit. The warm electronics is located in the SVM. All harness from SVM to the instrument units is thermally linked to each passive stage (VG1, VG2, VG3 and OB) for maximum parasitic interception.

Figure 4-4: Left: ARIEL thermal scheme with the main Thermal Interfaces (TIF); Right: preliminary GMM / TMM
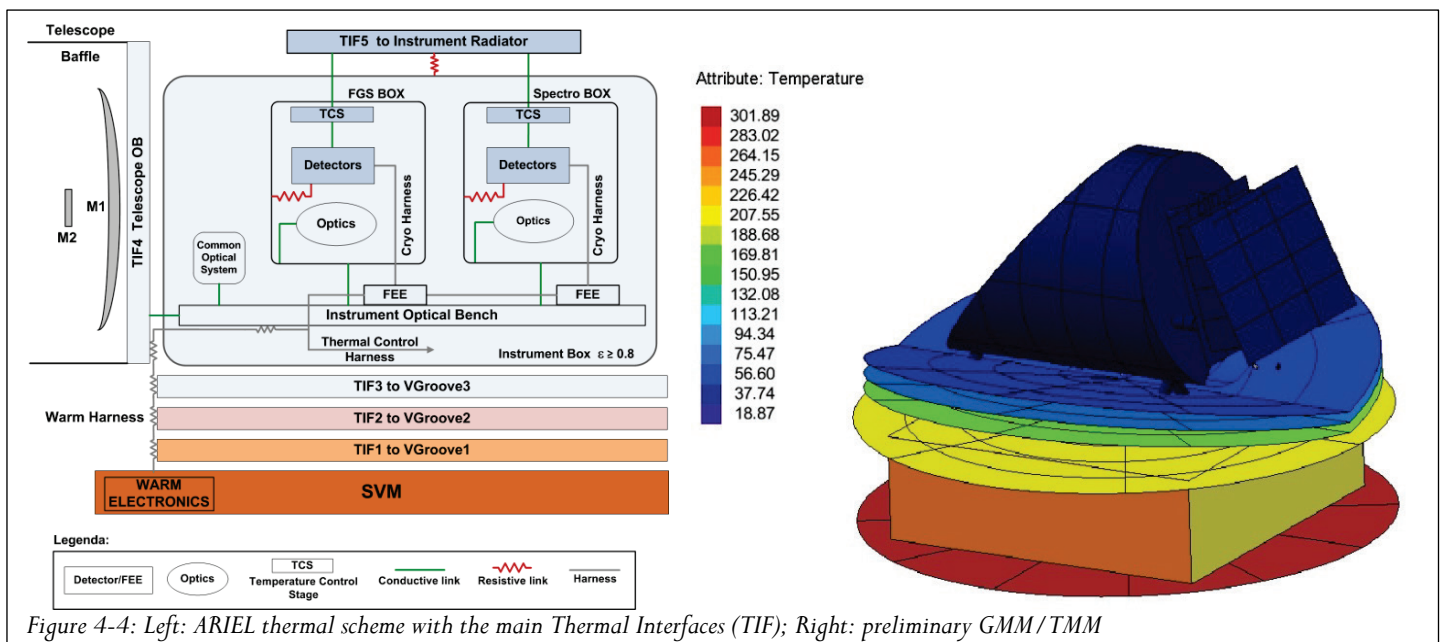
4.2 TELESCOPE DESIGN

4.2.1 Optical Design

Figure 4-5 shows the layout of the telescope and its local optical co-ordinate system. Two mirrors, M1 and M2, form an unobscured Cassegrain telescope with a prime focus below M1. The telescope optical axis is along z. The entrance aperture is at the primary mirror, M1. After prime focus, mirror M3, an off-axis parabola (OAP), produces a collimated beam. This beam is reflected along the +x axis by plane mirror M4. Dichroic D1 reflects the FGS wavelengths along +y to the FGS. D1 transmits the spectrometer wavelengths and the transmitted beam passes to a second dichroic, D2, which reflects the channel 0 (CH0) wavelengths along the +z axis while transmitting channel 1 (CH1). The CH0 beam is reflected by plane mirror M8 to generate parallel CH0 and CH1 beams, both travelling along the +x axis, separated by about 30 mm. Both beams are folded through 20 degrees by a single plane mirror, M5. A separate OAP in each channel, M6, focusses each beam and a separate mirror, M7, directs each focus to the spectrometer input. The focal points have identical x and y co-ordinates and are separated in z by the 30 mm separation generated by D2. The chief rays in each channel at the spectrometer input are almost parallel and their directions are set by M7 to match the entrance pupils of the two channels of the spectrometer. The focal length of the CH1 OAP is half that of CH0, giving a factor of two between the focal ratios of the beams delivered to the spectrometer focus. The f-ratios are chosen to control pixel sampling in the spectrometer. The as-built image quality will be diffraction limited at 3 um over a field of view (full angle) of 30 arcsec (equating to an RMS WFE of approximately 220nm). Table 4-2 summarises the telescope properties and Table 4-3 gives a draft specification for the dichroics.

The expected optical throughput of the whole system (telescope, common optics, FGS & spectrometer) for all channels is shown in Figure 4-5 lower right panel.

4.2.2 Manufacturing Plan

The Consortium telescope team led by France (with important contributions from Belgium (cryogenic testing) & Spain (control electronics)) will manage the telescope design and development. France will organize its contribution combining the resources of the three space laboratories from Paris area (LESIA, CEA, IAS) and IAP in an integrated way. LESIA will be in charge of the design architecture of the telescope optical systems. A team led by CEA, with contributions from LESIA and IAS will be responsible for the thermal and mechanical design and will oversee the development of the SiC structure. Under the responsibility of the telescope team, SiC mirrors, carbon fibre structure, baffle and telescope assembly will be subcontracted. The telescope team will be responsible of the optical, mechanical and thermal design and architecture in close collaboration with the subcontractor (this possibility has been discussed with Airbus Fr). The assembled telescope will be aligned and tested at ambient temperature in France at CEA or IAS (TBD), with an integrated team built from the different institutes using existing facilities. The cryogenic verification and alignment tests will be done at CSL by Belgium.

While the telescope baseline is SiC mirrors mounted on a carbon fibre structure, it is planned to study during phase A the possibility to use lightened tailored cryogenic Zerodur© mirrors. It is shown that Zerodur© CTE matches almost perfectly the carbon fibre reinforced polymer allowing a very stable telescope, practically insensitive to temperature variations and without any significant mass increase. This may provide a more stable and lower cost solution for the ARIEL telescope.

4.2.3 Alignment and Verification

Alignment will be based on initial positioning of components using accurate machining and metrology followed by iterative measurement of the wavefront aberration and adjustment of selected degrees of freedom. Mirrors M1 and M2 form an unobscured Cassegrain telescope and they can be tested as a system with an interferometric check of image quality at the prime focus below M1. The remaining powered components consist of off-axis parabolas and can be aligned and tested in a similar manner. Critical aspects of the whole telescope to be tested include the wavefront error and boresight stability, and an interferometric measurement can be made on the whole assembly, both at ambient temperature and cryogenically with suitable adaptions to the test equipment and vacuum chamber (such as windows for beam injection). Given the size of the entrance pupil, consideration will be given to use of sub-aperture tests; this will be studied as part of phase A.
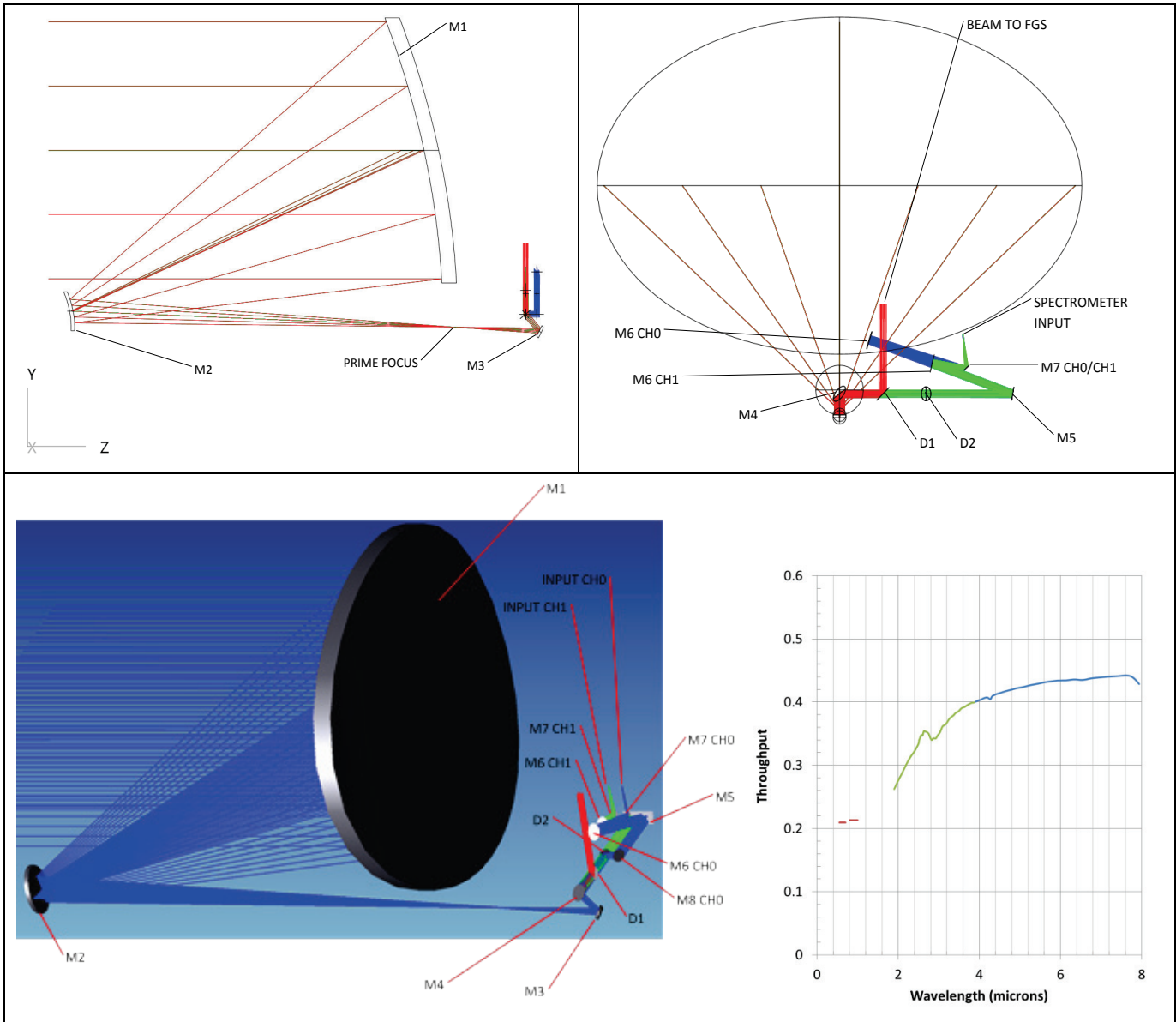
Figure 4-5: Telescope layout: Side view (top left-hand figure). Top view (top right-hand figure). Isometric view (bottom left figure). The co-ordinate system is shown in the top left-hand figure. Complete end to end throughput is shown in the bottom right figure for the FGS channels (red), Spectrometer Ch0 (Green) and Spectrometer Ch1 (Blue).

Parameter	Ch0 (1.95–3.9m)	Ch1(3.9-7.8um)
Telescope f/number	f/13.4 (for 0.9 diameter circular aperture)	
Entrance pupil diameter	Elliptical, 1.1 m x 0.7 m (equivalent to 0.9 m circular)	
Plate scale at prime focus	58 um / arc sec	
Collimated beam diameter after M3	Elliptical, 22.2 mm x 14.5 mm	
f/no at spectrometer input	20.5	10.3
Space envelope (optics only)	1400 mm (z) x 950 mm (y) x 1200 mm (x)	

Table 4-2: Telescope properties

Dichroic	Use	Reflectance Specification		Transmission Specifications	
		R_{min}	R_{max}	T_{min}	T_{max}
D1	Separation of FGS beam from Spectrometer	<0.55 μm	1.0 μm	1.95 μm	>7.8 μm
D2	Sub-separation of Spectrometer channels	<1.95 μm	3.9 μm	3.9 μm	>7.8 μm
D3	Sub-separation of FGS / NIR-Phot channels	<0.55 μm	0.7 μm	0.8 μm	>1.0 μm

Table 4-3: ARIEL Dichroic Wavelength Draft Specifications

4.2.4 Structure & Baffles

The structural design of the telescope support is based on the ThalesAlenia Space (TAS) design proposed for EChO during the M3 phase A study (Puig et al, 2014). A trade off made by the TAS team during the study showed that the mass is lower and the space available is most efficiently used by adopting the baffle as a structural element. In the TAS concept M1 and the baffle were to be supported directly, and separately, from a CFRP optical bench with M2 supported in turn from the baffle. A full FEM and thermal analysis of this concept was carried out showing it met all the interface requirements for EChO which was to be launched on a Soyuz. We have slightly adapted the concept (as shown in Figure 4-2) such that the baffle now holds both M1 and M2 as a single structure and is then interfaced to a CFRP optical bench which also supports the (rather smaller) instrument. In this way the telescope assembly, consisting of M1 and M2 integrated, aligned and tested with the baffle structure, can be delivered as a single item to the payload AIV centre. The payload optical bench and the instrument are also delivered to the payload AIV centre and the whole is integrated and tested as a unit before delivery to system level. The support structure for the payload is via three bipods mounted onto the SVM central cone and interfacing to a combination of the payload optical bench and the structural baffle (see Figure 4-2) in a similar manner as in the TAS EChO study. The difference we are proposing here is to have a separate set of bipods which mount the structural baffle (including M1 and M2) to the payload optical bench. The detailed design and analysis of the telescope assembly structure and its interfaces will be undertaken as part of the phase A study for ARIEL.

4.2.5 Telescope Thermal Management

The telescope will be passively cooled to ≤70K. The telescope baffle provides a large radiator area with a good view to deep space; this provides sufficient radiative cooling to dump the parasitic loads from the PLM support struts, cryo-harnesses and radiative load from the final V-Groove.

The telescope will also incorporate contamination control heaters on the M1 & M2 mirrors pus on the Payload module optical bench. These heaters will be active during the early orbit operations to ensure that the sensitive optical surfaces remain warmer than the support structure through the critical parts of cooldown. A temperature delta of ~40K will be maintained between the baffle (which will act as a contamination getter for water and other contaminants being off-gassed by the PLM) and the optical surfaces. An initial calculation of the power required to maintain this temperature gradient shows that approximately 100W of heater power is required during this phase. This would hold the sensitive surfaces at 200K while the baffle cools below 160K where the H_2O will freeze out. The telescope thermal monitoring and control will be conducted by the Telescope Control Unit (TCU), see §4.5.5.

4.3 SPECTROMETER DESIGN

The prime science payload for ARIEL is a broadband, low resolution NIR spectrometer operating between 1.95 μm and 7.8 μm. This is a single module that incorporates two channels covering the 1.95-3.9 μm and 3.9-7.8 μm ranges, respectively. Wavelength splitting between the two channels is achieved by the D2 dichroic filter, as shown in Figure 4-6. This spectrometer is mounted on an Optical Bench hosting also the FGS and the interface to the telescope, amongst which the field of view is shared between different wavelength ranges.

4.3.1 Optical Design

A preliminary design of the proposed payload has been done. It consists mainly of separate optics and grating for each of the wavelength channels integrating the full wavelength range onto a single detector. The optical design is kept simple with the minimal number of components and without any mechanisms, thus providing many advantages in terms of compact and lightweight instrument architecture.

The spectrometer layout is shown in Figure 4-6. The simple optical layout of each channel is based on a single spherical mirror receiving the incident light beam as well as the dispersed beams from a flat grating in a Littrow configuration improving the aberration performance. The resulting image quality is diffraction limited over the whole ARIEL spectral range. The input light beam has F#=10.3 for the longer-wavelength channel and F#=20.5 for the shorter-wavelength channel, in order to get the same 2 pixel sampling (36 um on the detector plane) at the shortest wavelength of each channel.

This spectrometer design provides a flat resolving power R ~ 200 throughout the spectral range; it

allows tuning of the design resolving power by simply varying the grating angle.

The focal plane with the detector module is folded through 90° by a flat mirror to give clearance for the input beams and the grating mount. The 512x512 pixel detector receives the dispersed light from both the channels; the two spectra are separated along the spatial direction by about 5.0 mm.

The spectrometer design specifications and performance are reported in Table 4.3.
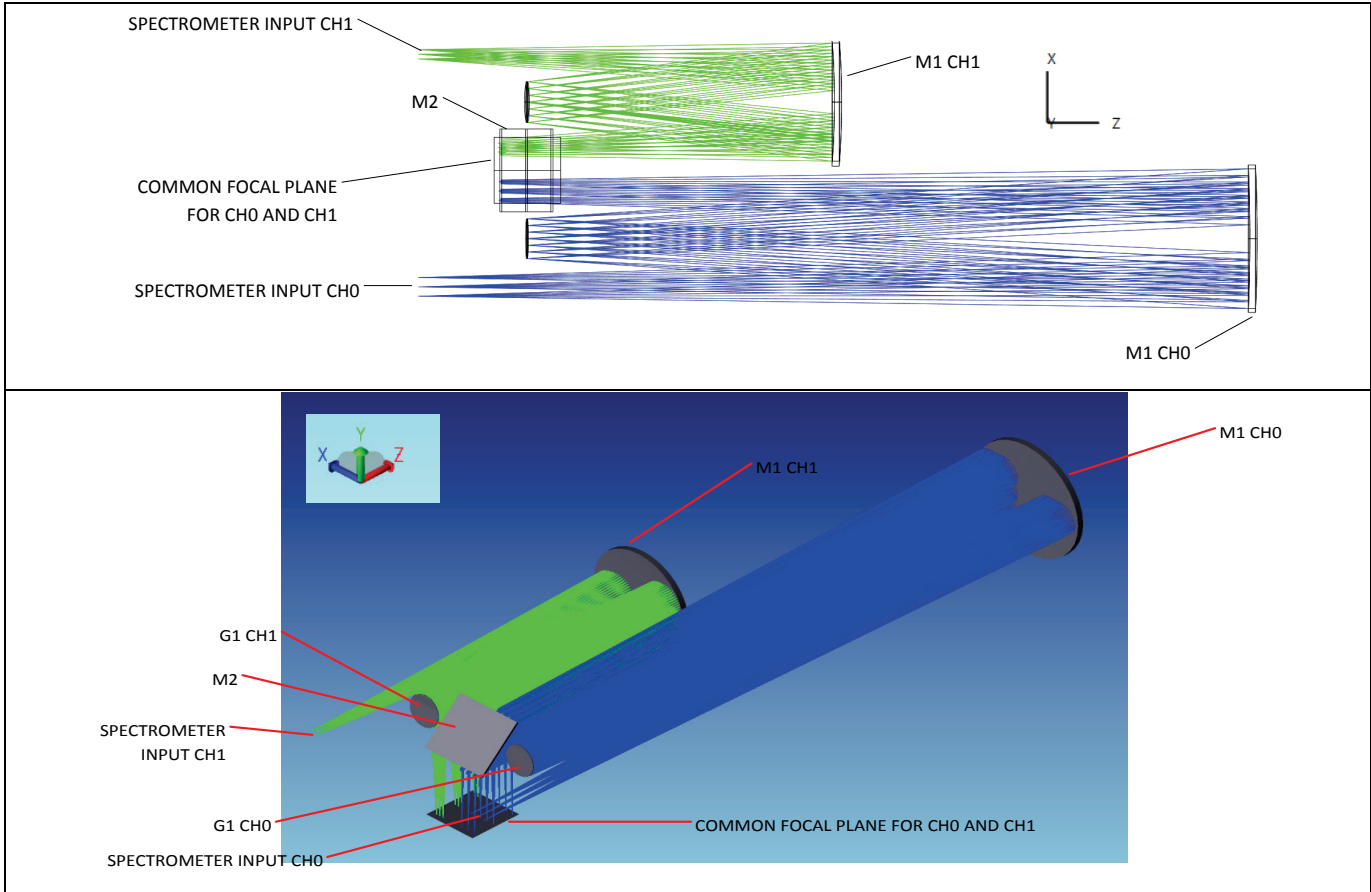
Figure 4-6: Spectrometer Layout: View in XZ plane (top figure). Isometric view (bottom figure)

Parameter	Ch0 (1.95-3.9m)	Ch1(3.9-7.8um)
Input slit FOV on sky (full angle)	2.2 x 13 arc sec	4.4 x 26 arc sec
Input size physical size	0.19 mm x 1.2 mm	
Grating width (W)	5.5 mm	5.5 mm
Diffraction order	-1	-1
Ruling density	36 lines / mm	
Grating incidence angle (θ_i)	3.0 deg	6.0 deg
Resolving power, R=λ/dλ (dλ = Rayleigh criterion)	197 (all λ)	
FWHM of a spectral line	2 pixels (min λ) 3 pixels (centre λ) 4 pixels (max λ)	
Spot size perpendicular to dispersion direction (FWHM)	2.2 pixels (min λ) 3.3 pixels (centre λ) 4.4 pixels (max λ)	
Length of spectrum on detector	8.0 mm	
Separation of spectra on detector (centre to centre of slit)	5.0 mm	
Plate scale at the detector	0.2 arc sec / pixel	0.4 arc sec / pixel
Dispersion	4.4 nm / pixel (all λ)	8.9 nm / pixel (all λ)
Space envelope (optics only)	120 mm (z) x 50 mm (x) x 50 mm (y)	

Table 4-4: Spectrometer properties

4.3.2   MIR-Spec Detector Selection

The baseline detector for the ARIEL science spectrometer is the Teledyne MCT array developed for NEOCam. A detailed summary of this device's performance is provided by McMurtry et al. (Optical Engineering, 52, 9, 2013). Currently tested devices have an 18μm pixel pitch and a cut-off wavelength between 9.3 and 10.6 μm. When operated at a temperature of 42K (see Figure 4-8), the devices has an operability of 94%, a dark current of 16 e⁻ s⁻¹ for 90% of detector pixels (200 e⁻s⁻¹ for 95% of detector pixels), a read noise distribution with mode of 20 e⁻ (Fowler-1), and a well depth in excess of 40ke⁻. The Quantum Efficiency without AR coating is measured in excess of 60%. We plan to temperature-control the detector array and stabilise it to a few mK-rms, which results in a negligible variation in the device performance. In §4.8 and Figure 4-13, we show that this detector achieves photon-noise limited performance. The device technology readiness is currently estimated to be at level 4 to 5, while the control-electronics, SIDECAR ASIC, and ROIC being at a much higher level, as these are effectively the same technology used on NIRSpec on JWST.

The MCT array will be fine-tuned for ARIEL. The MCT material will have a lower cut-off wavelength, and the array will have two AR coating applied on the
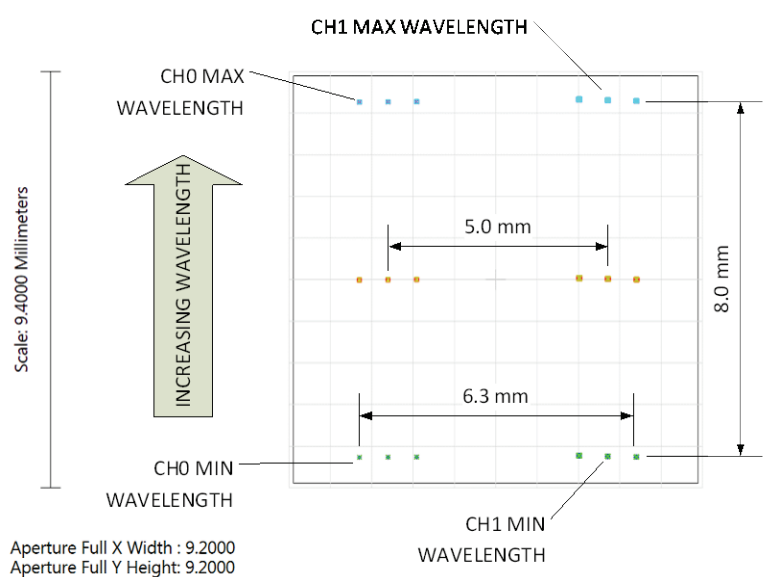
Figure 4-7: Layout of the spectra from both channels on a single 512 x 512 pixel detector. The dispersion direction is vertical in the figure and three wavelengths (min, centre and max) are plotted for each channel. The slit direction is horizontal in the figure and three positions are plotted (centre and edges of the slit).

same device, each optimised for one particular spectrometer channel. This will increase QE and operability, while decreasing dark current.

Alternative solutions from European manufacturers are also considered. Selex-ES, AIM and CEA/LETI all have ongoing development programmes for low dark current MWIR, LWIR detectors, funded by a combination of private, national and European resources, including ESA contracts. Although still in development phase, this effort can result in an all European solution for the ARIEL focal plane.
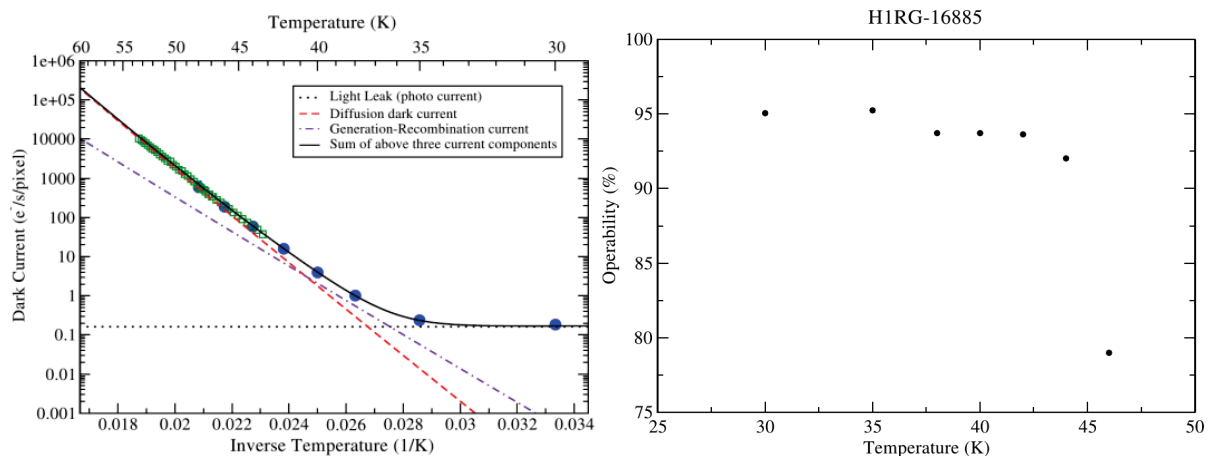
Figure 4-8: Dark current (above right) and operability (above right) for the Teledyne MCT focal plane array in the baseline design for the ARIEL science spectrograph. From McMurtry et al., Optical Engineering, 52, 9, 2013. A picture of the NEOCam detector is shown to the lower right.
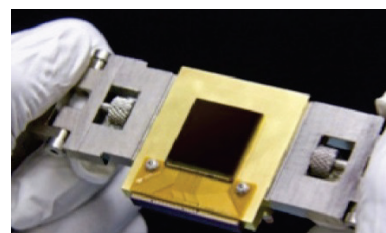
4.4 FINE GUIDANCE SYSTEM / NIR PHOTOMETER DESIGN

4.4.1 Design Concept

4.4.1.1 Objectives and concept

The Fine Guidance System's (FGS) main task is to ensure the centering, focusing and guiding of the satellite, but it will also provide high precision photometry of the target for science. In particular, the data from the FGS will be used for de-trending and data analysis on ground. The sensor uses star light coming through the optical path of the telescope to determine the changes in the line of sight of the ARIEL instrument. The attitude measurement is then fused with the rate information form Star Tracker, a high performance gyro and used as input for the control loop stabilising the spacecraft. To realise a guiding and a photometry targets two spectral bands are defined: NIR-Phot1: $0.55 - 0.7\mu m$ and NIR-Phot2: $0.8 - 1.0\mu m$. The information from both cannels is used as a stellar monitor and to provide photometric information to constrain the VIS/NIR portion of the exoplanet spectra. We will use the information from the NIR-Phot2 channel as the nominal FGS information to feed into the AOCS. In case of failure in the system then the information from the other channel can be used instead. The spectral bands are selected from the incoming light using a dichroic filter.

The system is composed of an optics box at the instrument optical bench (see Figure 4-9) containing cryogenic optics with two detector modules at 45K. At an intermediate stage temperature stage of 55K , the cold front-end electronics (CFEE) are located. In the service module the FGS WFEE and FGS control Electronics (FGE) are accommodated in temperature 270 K - 300 K. They control and read the detectors and carry out the data processing. FGS systems are independent from the spectrometer instrument, thus have their own power and data interfaces with spacecraft. The FGS is also involved in the focusing of the main telescope. This will be done using images from the two detector arrays, which have different focus offset. The procedure will be done on ground.
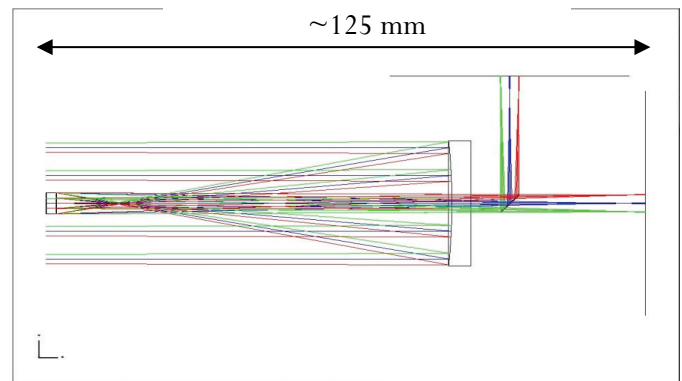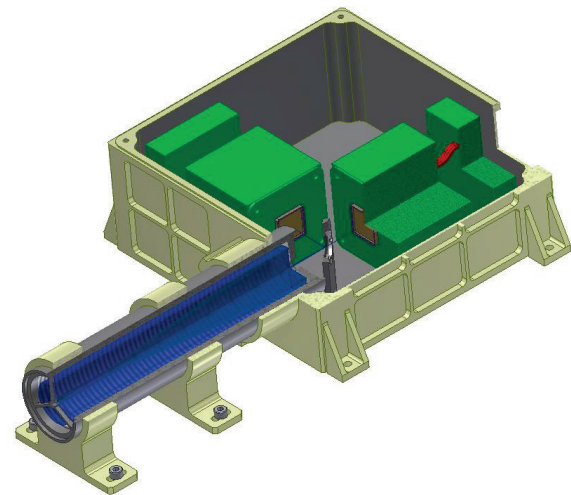
Figure 4-9: Mechanical and Optical Design of proposed FGS / NIR-Phot module

4.4.1.2 FGS Opto-mechanical Module Design

The FGS optical module has been designed for following basic assumptions:

- On-sky FoV: >20"x20"
- Detector: MCT FPA with array and pixel size minimum (15um for MCT) and ~256x256,
- Minimum bin/star image spread FWHM: 2x2 or 3x3 pixels
- WFE: better than the telescope diff-limit @ 3 μm

Having above assumptions, the telescope in Gregorian configuration is proposed with Focal length: 667mm, F-number of 25.8 using a parabolic primary and spherical secondary mirror giving ~3% central obscuration. A flat dichroic then splits the two sub-bands $(0,55 - 0.7\ \mu m : 0,8 - 1.0\ \mu m)$ of the FGS / NIR-Phot to the two detectors.

Base on the optical design, mechanical dimensions of the dichroic beam splitter mirror and the MCT detector with accompany electronics, the design of the unit is done and presented in Figure 4-9

4.4.1.3 FGS / NIR-Phot Detector

The FGS and the spectrometer are mounted on the same optics bench, and hence to avoid additional heat leak into the cold payload the two FGS detectors need to be operated at approximately 50K. MCT focal plane arrays are used in the design, and are operated as imagers. The expected signal at the focal plane is from a few ke-/s/pix for the faintest targets to hundreds of ke-/s/pix, and issues related to dark current and read noise are hence much less critical than for the spectrometer. Devices operating in the optical/NIR up to the required 1 μm are available from a number or European (Selex-ES, AIM, Sofradir, Xenics and VIGO) and US (Teledyne, Raytheon) manufacturers, with different TRL levels. The US devices have currently higher TRL compared to European devices, but European manufacturers are undertaking vigorous programs to enhance the TRL of their devices, also with funding from ESA.

The proposed FGS design is baselined around a Selex-ES device with pixel pitch of 15 μm. It is based on existing design such as NIR LFA CMT detectors, with sub e-/s/pix dark currents. Technology readiness is expected to be currently at a level 4. Ongoing ROIC development is planned which will improve the TRL to 5 during the study phase. Alternative European solutions are available, at a comparable TRLs. As a backup, US FPAs from either Raytheon or Teledyne have TRL>5 (e.g. H1RG devices with Sidecar electronics).

4.4.2 Use of FGS as WFE Sensor

Since the prime science instrument (spectrometer) has no field of view and the telescope is effectively a light-bucket, variations in the telescope WFE over timescales substantially different to the transits can be ignored. At timescales of the durations of the transits (minutes to hours) the FGS / NIR-Phot module is designed such that it can provide basic information about the telescope Wave Front Error while in-flight in order to allow decorrelation of the science data for any thermo-elastically caused fluctuations in the PSF output from the telescope.

This will be done by the setting of the two detectors for the separate channels slightly out of focus in opposite directions, then using the system as a Shack-Hartmann wave-front sensor. Image data (from a windowed region of approximately 50 x 50 pixels around the target star) from both detectors will be captured and stored with the science and guidance

data at a rate of approximately 0.1Hz. This image data will be processed on ground and small changes in the telescope WFE in range of a few minutes and levels of approximately 40nm can be detected.

This system may also be used during the commissioning of the payload to iterate and optimise the telescope focus and spherical aberrations by an iterative loop (with ground control) feeding into the M2 mirror mechanism.

4.4.3 FGS Control Electronics & Software

4.4.3.1 FGS Control Electronics

The FGS has its own control electronics in the SVM to carry out all necessary communication, control and data processing tasks. It will drive and read the FGS detector electronics, establish a control loop with the spacecraft and deliver scientific data products. The FGS shall start and stop the relative attitude measurement on command from ICU. The attitude at the time of the command shall be used as the initial attitude for the relative attitude measurement The FGS shall deliver photometric measurements with $2 - 10$ Hz rate. This will be an encircled energy measurement within a defined regions from the centroid of the source. The FGS shall deliver new relative attitude measurements with $2 - 10$ Hz update rate to the AOCS control system. This data will be centroid and FWHM information to $1/10^{th}$ of a pixel precision. The FGS shall dump the complete (or windowed) detector images on command. This enables the use of the FGS to monitor telescope WFE as described in §4.4.2. These data products will also be sent as science data products to ground.

The precise overall telemetry contribution of the FGS depends on the parameter configuration, which is at this point TBD, but our current estimation is 10 kbit/s.

The FGS control electronics in the service module are independent from the spectrometer channels and the spectrometer ICU.

4.4.3.2 FGS Algorithms and Software Design

The FCE unit will have to carry out and support a number of different tasks. There will be functions to control the FGS subsystems, process the detector data, communicate with the spacecraft, all according to the current mode of operation. The FGS shall permit in-orbit reprogramming of its software.

The FGS will also be during ground test and commissioning for focusing the main telescope. This is limiting the amount of intentional defocus. The PSF will be spread over 50-60 total pixels, with a FWHM of 3 x 3 pixels. The main requirement is a 10 milliarcsecond centroiding performance at 10 Hz for the faint targets.

In the warm FGS control electronics the data will be processed in real-time. Output data products are calibrated, cropped and reformatted images, centroid coordinates, dimensions and errors in both axes, photometry, glitch count and housekeeping. On-board compression will be used to reduce the telemetry. Additional data processing capabilities include frame stacking for PSF measurements.

4.5 INSTRUMENT ELECTRONICS

4.5.1 Electrical Architecture

The ARIEL payload overall electrical architecture (Figure 4-10) can be basically subdivided in two sections: detector with its ROIC (Read Out Integrated Circuit) and cold front-end electronics (cFEE) on one side and warm electronics on the other side. The cold instrument cavity is kept at ~45 K in order to meet the strict operative thermal requirements and is connected to the cFEEs and to the warm electronics by means of very low thermal conductance cryo-harnessing.

The Instrument Control Unit (ICU) is structured in three main sub-units:

- Data Processing Unit (DPU): a digital sub-unit with processing capabilities to implement the scientific digital data on-board processing, the data storage and packetisation, the telemetry and telecommand packets handling and the clock/synchronization needed;

- Housekeeping and Calibration source Unit (HCU): a sub-unit designed to provide instrument/channel thermal control, calibration source and HKs management.

- Power Supply Unit (PSU): it will distribute the secondary voltages to the instrument
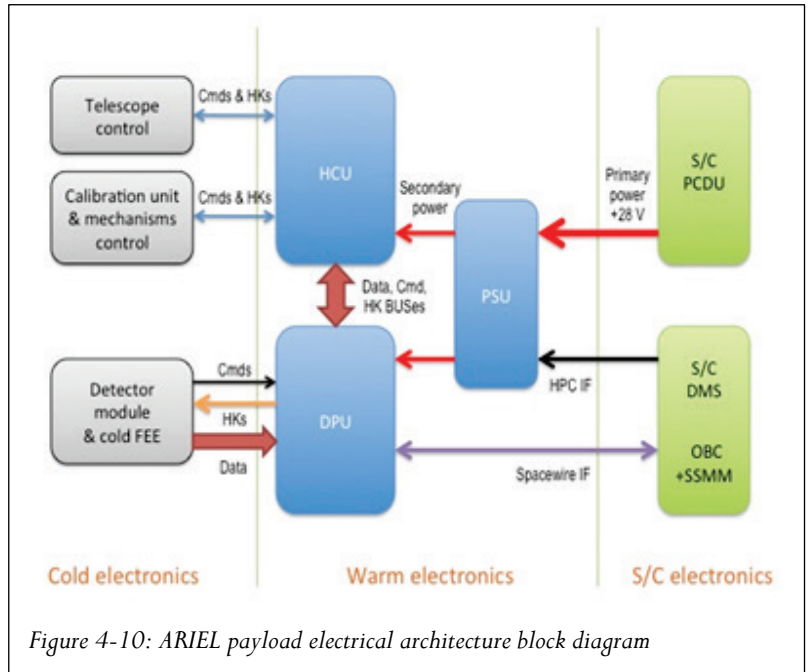
Figure 4-10: ARIEL payload electrical architecture block diagram

subsystems and ICU boards by means of DC/DC converters.

A single common TM/TC interface is foreseen at ICU level to minimize and simplify the number of interfaces to the S/C. The ICU electronics will rely on a cold-strapped redundant architecture with trade-off solutions removing or reducing any electronics single-point failures.

4.5.2 Detector Readout Schemes

The focal plane assembly includes the detector module coupled to proximity electronics that is mainly a ROIC and a cold front-end electronics (cFEE) for data digitalization, control signals, biasing, commands and housekeepings. On the warm side, the data will be pre-processed in the warm FEE. During the assessment phase will be evaluated if this will be included in the ICU assembly or external.
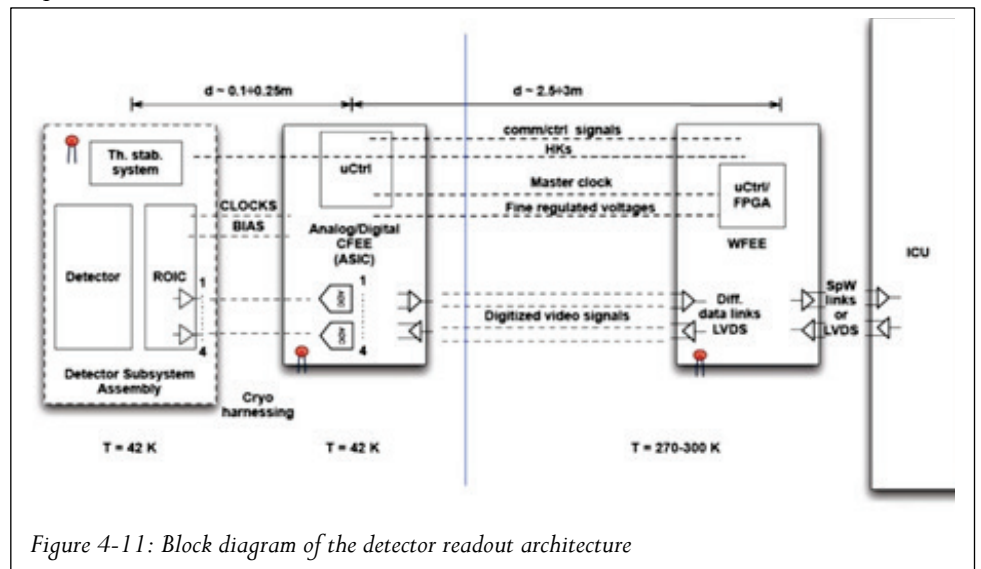
Figure 4-11: Block diagram of the detector readout architecture

4.5.3 Payload Power Budget

The overall power budget (including appropriate uncertainty figures) for the spacecraft is shown in Table 5-1 – this includes the estimated worst-case values for the power of the payload electronics modules.

4.5.4 Payload Data Rate

Table 4-5 gives a bottom up calculation of the expected data rate from the ARIEL payload. We have assumed that we transmit samples every 3 sec from the spectrometer and photometer channels with no significant on board processing except to co-add samples "up the ramp". We assume a glitch rate per pixel low enough that deglitching can occur on the ground with no significant loss of effective observing time. For the FGS we assume that we will telemeter the derived parameters from the centroiding to the ground at the same rate that they are supplied to the S/C AOCS system. Further we will telemeter

images of the PSF region of interest and 1/sec for the purposes of monitoring any change in the optical system. Neither of these add significantly to the overall data rate.

As a consequence of these initial assumptions the overall payload data rate will be ~ 11 Gbit/day. If we assume an X-band transponder operating at 10 Mbit/sec from L2 as per the ESA M4 Call Annex documentation (equivalent to 35 Gbit/hr) this means we will need a little over 2 hours downlink time per week. Allowing for some margin – i.e. the transponder works only at 5 Mbits/sec – we need a maximum of 4 hours downlink per week which can easily be accommodated within two 3-hour contact periods to include acquisition, ranging and telecommand upload. Some data compression could be designed into the ARIEL payload electronics which would reduce the data rate to within a single contact period if this were required for cost reasons.

	Pixels Spect.	Pixels Spat.	Chan Total	Bits per sample	Prim. Rate (Hz)	Int. time per ramp (sec)	No. Bits / ramp	Total Bits / sec	GBits Per day
Science Channels									
FGS photometer mode	32	32	1024	16	1			16384	1.32
FGS AOCS mode	16	1	16	21	10			3360	0.27
AIRS-1	512	16	8192	16	10	3	21	57344	4.61
AIRS-2	512	16	8192	16	10	3	21	57344	4.61
		Total	16400			**Total Sci (bits/sec)**		134432	
					Total sci/day (Gbits)				10.82
Houskeeping Channels									
Instrument									
Temps			16	16	2			512	
Electronics etc			32	12	2			768	
Telescope									
M2 actuators			8	16	0.5			64	
Heaters			8	16	0.5			64	
Temps			32	16	2			1024	
					Total HK bits/sec)			2432.00	0.20
Grand total									11.0

Table 4-5: Assumed data rates for the ARIEL Payload

4.5.5 Telescope Control Electronics

The telescope control electronics (TCE) is responsible for the thermal monitoring and control of the telescope and payload module contamination control heaters. It also controls the M2 refocusing

mechanism under control from the ground. This may either be a card(s) within the main Instrument Control Unit (ICU) or may be a stand-alone unit, this is to be studied further during the assessment phase.

4.6 CALIBRATION SCHEME

4.6.1 Ground Verification, Calibration and Performance testing

The ground testing of the ARIEL payload will be designed to ensure that it meets specification. It is not intended to provide an absolute calibration of the payload. The test plan will follow the methodology given below:

Unit Level

- **Detectors:** Standalone testing using suitable GSE readout electronics. Testing with instrument readout electronics prior to integration into the FGS and AIRS (TBD).
- **Warm electronics**: standalone testing before delivery to payload using instrument simulator
- **COM:** Optical testing as fitted onto the OB
- **FGS and AIRS:** Optical testing at unit level by the unit providers. The scope of this is TBD.
- **All Instrument units:** Qualification and acceptance vibration and thermal testing expected prior to delivery.
- **ATU**: Assembled, aligned and environmentally verified before delivery for payload testing.
- The OB with the COM fitted will be integrated with ATU and the alignment verified using GSE before integration of the instrument units.

Payload Level EM / FM Performance Testing
A full list of tests along with a verification matrix will be drawn up once a full set of payload requirements are in place. We give here some example tests. Except where indicated they would be run with the instrument in a flight-like environment at operational temperatures.

- **EGSE integration testing**: Tests using instrument electronics and an instrument simulator.
- **Payload functional tests:** testing both warm (at ambient) and cold. Expected detectors can be operated in a warm state and the functional testing will include detector operation.
- **Test facility functional test**: especially critical as a cold test facility is required.
- **Detector characteristics**: Determination of dead and bad pixels, latency, persistence, droops, other non-linearity, dark current and its stability. Effects of temperature on responsivity and noise
- **Optical characteristics**: Flatfield and intra-pixel response. Focus at operating temperature; co-focality of FGS and AIRS. Payload throughput.

Internal alignment confirmation. PSF and variation with temperature. Opto-mechanical stability (possible gravity release test). Wavelength calibration. Simulated pointing offsets and jitter via test facility source.

- **Operations:** Run tests of on-board data processing by taking data using standard observational modes and processing data both on-board and "on the ground".

4.6.2 In-flight Calibration

The measurements to be made by ARIEL require that the stability of the system is either maintained, or monitored to allow removal of drifts in the system performance to around 1 part in 10000. We present here a summary of the effects that the calibration scheme will need to deal with and a basic overview of our calibration approach. The effects can be gathered in 3 classes in order to distinguish between how they are monitored and controlled:

- Astrophysical effects: Associated with the observing "scene" and require measurement and monitoring schemes. The most obvious of these is the stellar activity which is monitored directly during the observation using the FGS.
- Spacecraft effects: Associated with any changes in the pointing, temperatures and, possibly, mechanical stability of the spacecraft. Although they will be "designed out" we will monitor for residual effects using housekeeping parameters such as temperature and the PSF. The PSF will be monitored using the FGS.
- The instrument effects: Mainly linked to the detection process and the associated detection chain. Major issues are likely to be associated with the detector performance which will be monitored by periodic calibrations using the internal calibrator, known calibration standard stars, off axis detectors and the target stars.

During the mission there will be a combination of long term housekeeping monitoring (temperatures, voltages etc), dedicated long term measurements (use of off axis detectors, dark detectors etc), short term measurements using internal calibration sources and medium and long term measurements on stellar calibration sources for both stability and absolute flux measurements.

4.7 PAYLOAD CONSTRAINTS ON SYSTEM

4.7.1 Pointing Stability

Pointing stability of the telescope contributes to the photometric stability budget, and it is quantified in terms of a performance reproducibility error (PRE) and relative performance error (RPE), defined in the ESA ECSS-E-ST060-1C document. Other pointing aspects are not relevant as the measurement is effectively differential between the in-transit and the out-of-transit time-series. The pointing drifts manifest themselves in the observed data product via two mechanisms: 1) the drift of the spectrum along the spectral direction, and 2) the drift of the spectrum along the spatial direction. Jitter introduces noise on the time series which is correlated over all focal planes, and it depends from the power spectrum of the telescope pointing, is proportional to the source intensity (therefore is more relevant for the brightest targets), and couples with the focal plane via two mechanisms: the intra-pixel response and the knowledge on the flat field (inter-pixel). It also depends from the PSF shape, where a broader PSF gives rise to a smaller photometric error. From realistic simulations (Figure 4-12), a PRE of ~100masc-rms over a temporal band spanning from 10s to the duration of a transit would be adequate when the PSF is sampled by at least two detector pixel per FWHM, even for the most challenging (from a pointing jitter point of view) of a
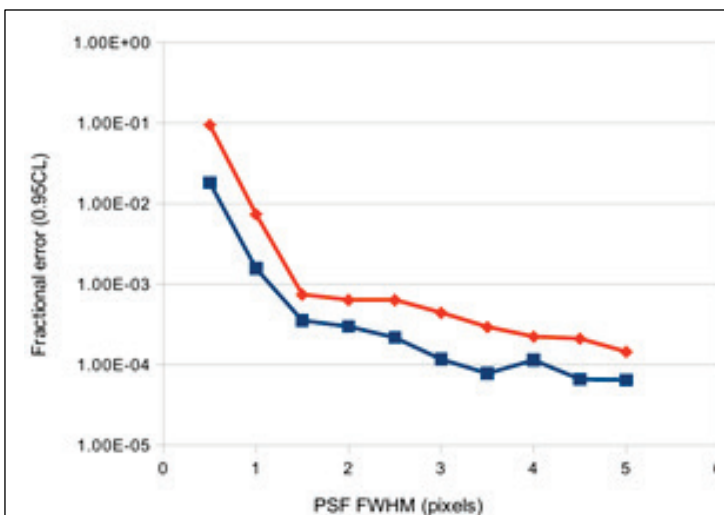
Figure 4-12 : Photometric error induced by pointing jitter in one frame. See Figure 4-13 for implications on the overall photometric budget. For the blue line, a PRE of 40 marcsec is used, for the red line 100marcsec is used (over a band spanning from 10s to the duration of a transit). RPE is set to 100masc rms up to 10s. When the PSF FWHM is sampled by less than two detector pixels, the photometric noise budget is dominated by intra-pixel response. Above this, uncertainties in the flat field (conservatively assumed here to be 0.5%) dominates.

bright target such as the star 55 Cnc, as shown also in Figure 4-13 in §4.8.

4.7.2 Cleanliness and Contamination Control

The cleanliness and contamination control requirements for ARIEL are TBC but likely to be comparable with similar visible and IR space instrumentation of which the Consortium have experience. The JWST MIRI contamination requirements at delivery of the instrument are taken here as an example of what will be required. These are for a surface cleanliness (on optical surfaces) of 300 (particulate) and A (molecular). The allowable degradation of cleanliness through flight is governed by the loss of throughput, and the appearance of spectral features caused by contamination deposition on the optical surfaces. Using an allocation of a 10% relative loss of throughput throughout the mission leads to an end of life allocated cleanliness level of 350D on optical surfaces. This degradation has been calculated, to first order, to be acceptable for the science requirements of capability to stack observations if assumed that the degradation is at an approximately constant rate, it can then be removed from the data by the planned in flight calibration. Although working to these levels of cleanliness presents challenges and care is necessary in all aspects of the design and AIV, they are achievable through existing means. As an example, the verified molecular cleanliness levels of JWST MIRI were <A/10 (<1 x 10-8 g/cm2) at delivery with a particulate contamination of better than level 300 on all optical surfaces.

4.8 PREDICTING PAYLOAD PERFORMANCE

The ARIEL baseline instrument is designed to achieve the required photometric stability and optical throughput to achieve the science goals. The overall instrument performance is estimated implementing detailed simulations of the proposed instrument baseline discussed in §4.2 and §4.3.

End-to-end simulations are conducted using the simulator discussed by Pascale et al. (2014). This is a highly configurable software tool which provides an advanced parametric implementation of the instrument design to simulate its time-domain performance. Validation was conducted by comparison with the ESA radiometric model discussed by Puig et al. (2014). The astronomical object (transiting or eclipsing planet and parent

star) is simulated and the detection of the modulated light curve takes into consideration all the major systematics and source of uncertainties expected, with their time-domain properties (whether these are Gaussian, time-correlated or spatial correlated processes). Optical aberrations and transmission, pointing stability and its coupling to focal plane non-idealities such as detector inter- and intra-pixel responses, and filling factors are accounted for, using realistic modelling derived from published work. Photon noise, dark current, detector readout noise, the effects of coupling of the PSF with the focal plane array, etc. are all accounted in the simulations which result in detector timelines used by an advanced data reduction pipeline (Waldman et al. 2014) to reconstruct the planet transmission and emission spectra. The pipeline also provides an estimate of the uncertainties on the final spectra. The reconstructed spectra are then used in the retrieval process to provide an estimate of how effective is the measurement to constrain pressure and temperature atmospheric profiles, and chemical abundances, as discussed by Barstow et al. (2014).

Results from these advanced simulations are used throughout this proposal, and in §2.5 in particular where Figure 2-8 shows reconstructed spectra arising from systems with different chemical compositions and physical conditions.

An analysis of the photometric budget for the Ariel spectrometer is shown in Figure 4-13 for two examples. 55 Cnc is a G star with Mag K = 4, hosting a hot super-Earth; GJ 1214 is an M start with Mag K = 9 hosting a warm super-Earth. These two stars are chosen to provide examples of what might be the brightest and faintest targets Ariel is likely to observe. Faint targets impose challenges on detector noise while bright targets challenges are related to pointing stability and detector saturation. Figure 4-13 shows the expected components of the photometric budget arising from the parent star, detector noise and thermal stability, zodiacal light, instrument emission, and pointing jitter. For both presented cases the detection is photon noise limited. Pointing jitter (here it is assumed PRE and RPE of 100 masc-rms as in §4.7.1) is more relevant for bright targets, detector performance is more relevant for faint targets, but with the baseline design all noise components are below limits imposed by the parent star.
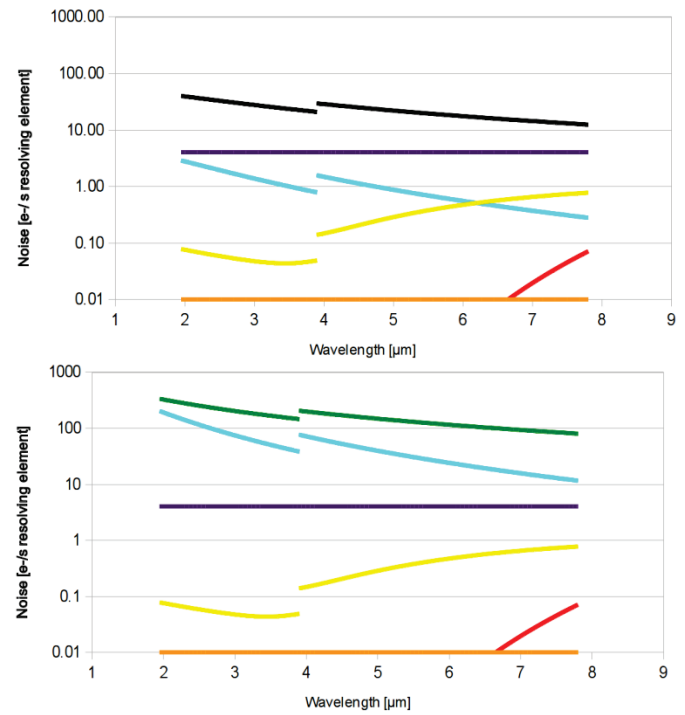
Figure 4-13: Predicted photometric noise for a bright (55 Cnc, green line, lower panel) and faint (GJ 1214, black line, upper panel) star targets. The noise is scaled too one second of integration and is estimated in a spectral resolving element, after binning adjacent detector pixels. Both cases are limited by the star photon noise. Other components of the predicted noise budget here shown are: pointing jitter (cyan), detector noise (violet), zodiacal light photon noise (yellow), photon noise from instrument emission (red), and detector noise induced by a 1mk-rms fluctuation in the detector temperature control (orange).

4.9 PAYLOAD TECHNOLOGY READINESS ASSESSMENT AND DEVELOPMENT PLANS

4.9.1 Baseline Payload Design TRL Levels

The current assessment of the TRL for the various key technologies within the proposed baseline design (and identified options) are summarised in Table 4-6 below.

4.9.2 Model philosophy

Expected Deliverables within the Payload Consortium

At payload level we assume a proto-flight approach where the integrated payload is environmentally tested to qualification levels for acceptance durations. In addition to the deliverable models to spacecraft we intend to develop an Engineering model of the Payload module for de-risking purposes. This will provide optical and electrical representivity and provide a pull-through of the AIV processes that will then be used for the flight model. The model philosophy for the deliverable units within the consortium is as given in Table 4-7 where the build standard is also indicated.

Expected Deliverables to the Spacecraft

The payload deliverables to the spacecraft AIV processes are planned to be as listed below:

Structural Thermal Model: A dedicated payload STM will be used for system level structural and thermal testing and basic metrology. We note that the payload as delivered to S/C will be internally self-aligned so the external alignment requirements to the S/C will only be to ensure knowledge of the alignment between the star trackers and the FGS is within specification.

Avionics Model: The AVM will be used for system level verification of electrical and command and data handling interfaces. We propose to deliver the three Engineering Model warm payload units with cold payload simulators as required.

ProtoFlight Model: The pFM is the fully functional and verified model of the cold and warm payload units intended for flight operations.

Technology	Current TRL	Expected TRL mid-2016	Current heritage / Development Plans
Baseline Design			
SiC Telescope and Structure for ~1m mirror with 3 μm diffraction limit with Silver coating	6	~7-9	SiC telescope for Gaia, Herschel. Smaller telescope and relaxed image quality compared to Euclid.
M2 Refocusing mechanism to operate at ~60-70K.	5	5-6	Based on Gaia & Euclid plus ESA TRP developments – TBC if needed
European MCT detectors for FGS (0.55 – 1.0μm)	~4-5	5	Under development through ESA TRP (AO6073) at Sofradir & Selex.
Cold FEE for European MCT detectors	4-5	>5	Development programs ongoing at SRON, Selex and elsewhere
US MCT detectors for Spectrometer (2 – 8μm) with low dark current	5	>5	Ref NEOCam detectors from Teledyne (McMurtry et al, 2013) with ~10.5 μm cutoff
SWIR Dichroics for FGS channel separation	5	>5	Similar specification to that in use on JWST NIRCam.
MWIR Dichroic for Spectrometer channel separation at ~4μm	6	>5	Similar specification and technology to EarthCARE BBR dichroic
CFRP Optical Bench Structure at cryogenic temperatures	5	6-7	
Data Processing Units and on-board payload electronics	9	9	No special data processing necessary on-board to meet data rate requirements
Fine Guidance System	5	>5	Similar to existing FGS designs and capabilities of SW.
Alternative Options			
European MCT detectors for Spectrometer (2 – 8μm) with low dark current	3-4	5	Sofradir development program (Geoffray et al, 2014) plus ESA TRP activities at Selex and others
US MCT detectors for FGS (0.55 – 1.0μm) with SideCAR ASIC	9	9	Similar to NIRCam / NIRSpec but smaller and relaxed requirements.

Table 4-6: TRL evaluation for Baseline ARIEL Payload

Unit	Breadboard / STM	EM	pFM
Telescope (ATU)	STM: Form, Fit. Possibly with M1 as optical testbed	pFM build standard. To be used for EM testing	Refurbished EM
Optics Bench (OB)	STM: Form, Fit. Basic metrology tools fitted	Form, Fit, Function.	pFM dedicated build / Refurb EM (TBC)
Common Optics	STM: Form, Fit. Basic alignment jigs fitted	Form, Fit, Function.	pFM dedicated build
Spectrometer (AIRS)	STM: Form, Fit. Basic alignment jigs fitted.	Form, Fit, Function. Engineering grade detectors.	pFM dedicated build

Unit	Breadboard / STM	EM	pFM
Fine Guidance OM (FGS)	STM: Form, Fit. Basic alignment jigs fitted	Form, Fit, Function. Engineering grade detectors.	pFM dedicated build
Thermal HW (ATH)	STM: Form, Fit, Function. Radiator used for thermal testing	pFM build standard.	Refurbished EM
Instrument Control Unit (ICU)	BB: Function	Form, Fit, Function. Industrial grade parts.	pFM dedicated build
FGS Electronics (FGSE)	BB: Function	Form, Fit, Function. Industrial grade parts.	pFM dedicated build
Telescope Control Unit (TCU)	BB: TBD	Form, Fit, Function. Industrial grade parts.	pFM dedicated build
Cryoharness	STM: Form, Fit, Function. GSE build standard	pFM build standard. To be used for EM testing	Refurbished EM

Table 4-7: Payload Unit Model Philosophy

5 PROPOSED MISSION AND SPACECRAFT CONFIGURATION

5.1 ORBIT

An L2 large amplitude Lissajous orbit is proposed for ARIEL. The relatively tight thermal stability constraints on the passively cooled payload, and the need to be able to access all the sky to benefit from the targets discovered by TESS drives this decision.

We investigated LEO Sun synchronous orbits, which will have the benefit of allowing a larger mass and therefore larger mirror. Nevertheless, it has many drawbacks in terms of system complexity and observing modes. First the whole telescope would need to be actively cooled, secondly it would give a limited field of regard of about $\pm$ 34 deg around the ecliptic, meaning that only ~20 % of the sky would be observable. In 2025, we do need to benefit from the targets harvested by all sky surveys. We discarded also other Low Earth Orbits, because the thermal constraints, combined with the successions of Earth eclipses make the case even worse than for the Sun Synchronous Orbits.

We also considered and modelled High Eccentricity Orbits (HEO) with typically 6-7 days period or the 13.7 days orbit of the NASA TESS satellite in resonance with the moon. It is certainly much better than the LEO orbit, but ARIEL observations would be constrained by the position of the Earth, the sun and the moon in the field of view and the thermal destabilisation of the satellite when it will be rapidly heated at perigee. A typical orbit would allow 6 days of observations, followed by 1 day of data download, housekeeping when passing at perigee. This is a reduced operating efficiency and field of regard compared to the baseline proposed L2 orbit. An additional drawback of an HEO is that it adds additional constraints compared to a L2 solution; it would still need a high delta-V to reach the HEO, the injected mass would hence be similar to L2.

As a consequence of the studies carried out in preparation of this proposal the L2 large amplitude Lissajous orbit is considered to be the optimal solution.

5.2 LAUNCHER

We have identified two launcher possibilities for ARIEL : Vega or Soyuz.

In order to fit within the current VEGA launcher mass performances and capability known as off today and stated within the Annex to the M4 AO (see SRE-F/2014.035) and the VEGA User Manual, we would have to de-scope ARIEL to a smaller mirror (~75 cm effective diameter) and to compensate this smaller collecting area with a longer mission life span to reach the science objectives.

In addition, the latest ministerial meeting in December 2014 adopted the development of a new capability for VEGA, called VEGA-C with enhanced mass performances that will be available for 2020 (ie well before the M4 mission launch date). ARIEL in our current baseline version has been optimised for a VEGA-C launch (as described in §5.4. This decision was made on the grounds of the estimated relative expense of the VEGA-C launch compared to the Soyuz alternative.

ARIEL as proposed has a dry mass of 780 kg (including 20 % margin) as shown in Table 5-3 and a

required orbit around L2. In order to reach a large amplitude Lissajous orbit at Sun-Earth L2, we have several possibilities. One of them is to make an optimal use of the Lisa Pathfinder stage and to inject ARIEL initially on a 250/3000 km orbit inclined by 5 degrees around Earth using the VEGA-C. Then, the LPF engine is ignited in order to put the spacecraft on a trajectory to the targeted orbit at L2.

During Phase A, a trade-off could be done by industry making a comparison between the system complexity of the use of on-board propulsion along with a VEGA-C launch to this injection orbit against the additional cost of a dedicated Soyuz launch (which could of course be mitigated by a shared launch).

As an alternative option we consider a Soyuz launch. In that case, ARIEL would be directly inserted on a trajectory to the large amplitude orbit at L2 by Soyuz. After a number of correction manoeuvres for launcher dispersion and fine-targeting during transfer, the spacecraft will be freely inserted into the final L2 orbit, i.e. no specific insertion manoeuvres are required. The transfer to L2 lasts about 30 days and the on-board propellant needed in this case is vastly reduced. A comparison of the relative costs for the Soyuz launch option is shown in §7.

The launch is possible (for either option) at almost any day of the year with minor restrictions to avoid eclipses during transfer and in the operational orbit. The in and out-of plane orbital periods are both close to 180 days. The frequency of station-keeping manoeuvres is ~30 days to correct for the instability inherent in the motion about L2.

5.3 MISSION CONCEPT

5.3.1 Observing Modes

There is expected to be a single observing mode (spectrometer, NIR-Phot & FGS observations in parallel of a single target) for the prime science activities for ARIEL. Additional modes (such as tracking modes for observation of solar system objects) can be studied as secondary science cases during the phase A study. See §3.2.3 for further details.

5.3.2 Pointing Constraints & Sky Coverage

In order to limit the size and mass of the V-grooves baffles needed to maintain cryogenic temperatures and stabilities for the payload, the pointing of ARIEL is assumed to be constrained to a solar aspect angle of approximately 25°. With an L2 Lissajous orbit this leads to the ability to access any point on the sky for at least 3-4 months of the year, and for the celestial poles the coverage is continuous. This is illustrated in Figure 5-1.
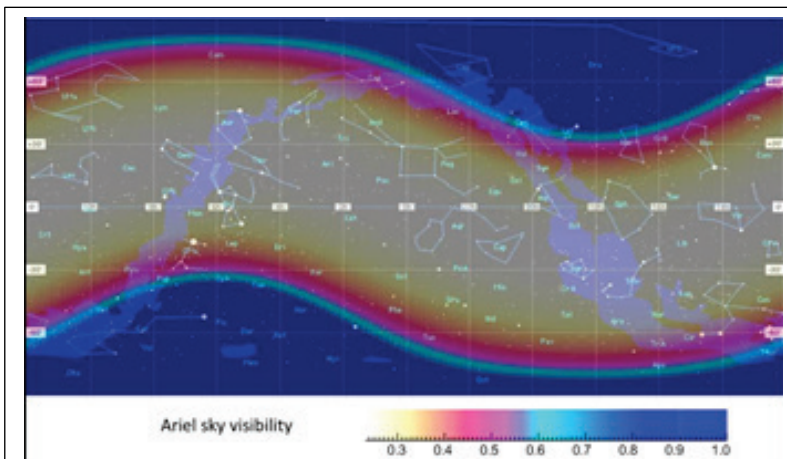
Figure 5-1: ARIEL Sky Visibility, units are fraction of each year that any region is observable

5.4 SPACECRAFT DESIGN CONCEPT

The spacecraft is classically composed of a payload module (PLM) and a service module (SVM). The PLM is mounted on top of the SVM, using the so-called horizontal accommodation, i.e. with the telescope line of sight perpendicular to the launcher axis. The PLM optical bench is attached to the SVM via three isostatic bipods, and the V-groove thermal insulation system is installed between the two modules.

The whole PLM is kept within the shadow provided by the SVM and its deployed solar array for all pointing attitudes prescribed by the science mission, to allow for an efficient passive cooling of the payload optics and detectors to cryogenic levels.

The SVM is built around the LISA Pathfinder Propulsion module (LPF-PM), allowing to benefit from a significant reuse. Basically, the LPF-PM central tube, propulsion subsystem and associated bracketery, harness and thermal control are kept unchanged; the modifications introduced for ARIEL are:

- The upper part (accommodating the separation system on LISA PF mission) is replaced by the structural pieces and top-floor needed to support the PLM bipods and MLI /V-Groove assembly;
- The SVM and warm payload electronics are accommodated in two equipment bays attached to

the LISA-PM central tube, located symmetrically in quadrature with the propellant tanks pairs;

- The bottom part is complemented by the solar array and communication antennas supporting hardware.

The spacecraft electrical & functional architecture is very classical for L2 observatory missions, derived from e.g. Euclid or EChO concepts.

5.5 CRITICAL RESOURCE BUDGETS

Mass: The mass budget for the ARIEL satellite is compiled in Table 5-3 below. The mass budget for the SVM is based on the LPF-MP reuse and on avionics studies conducted for the EChO M3 Assessment study, plus other evolutions as noted in the remarks column. The payload mass budget is based on the preliminary design work presented in §0 of this proposal; much of this is based on heritage designs from EChO, JWST, Herschel and other ESA missions. The nominal dry mass of the ARIEL satellite is predicted to be 780 kg (including 20% system margin). The transfer scenario to L2 means that a large propellant mass of 1152 kg is carried, giving a total mass at launch of 1992 kg (including propellant, launch adapter and all margins). This is within the capabilities of the Vega-C launch vehicle into a 250 x 3000 km elliptical orbit, and of the LPF-MP fuel tanking of 1200kg.
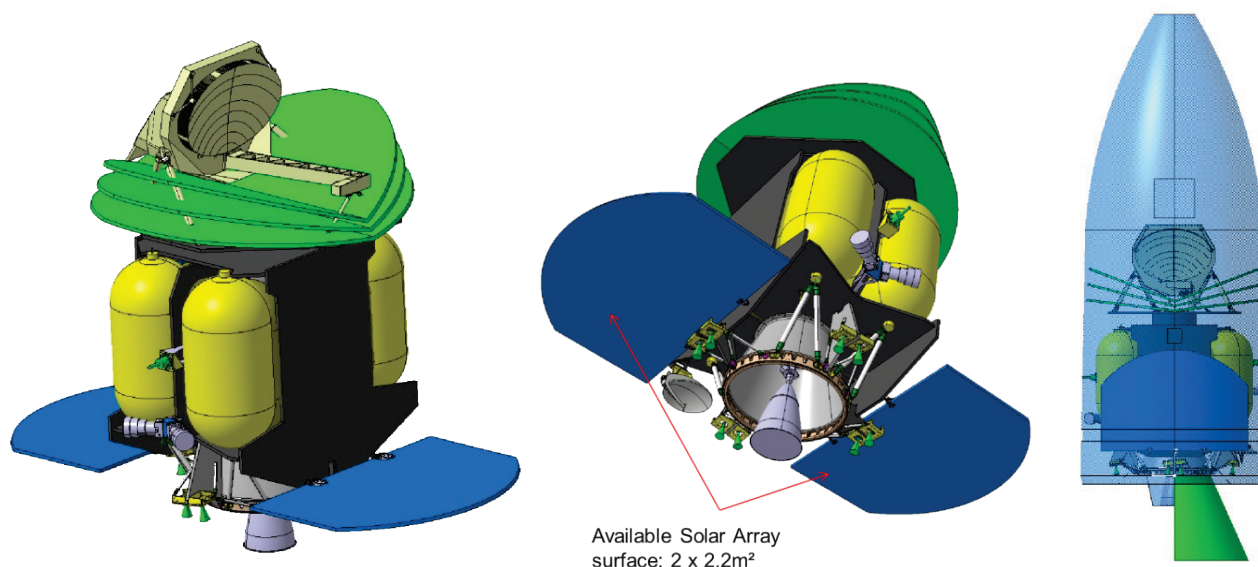
Figure 5-2 : Spacecraft Configurations. Left & Centre - deployed in orbit; Right - Shown within VEGA LV fairing envelope. Note that previous iteration (same overall envelope) of PLM design shown in these figures.
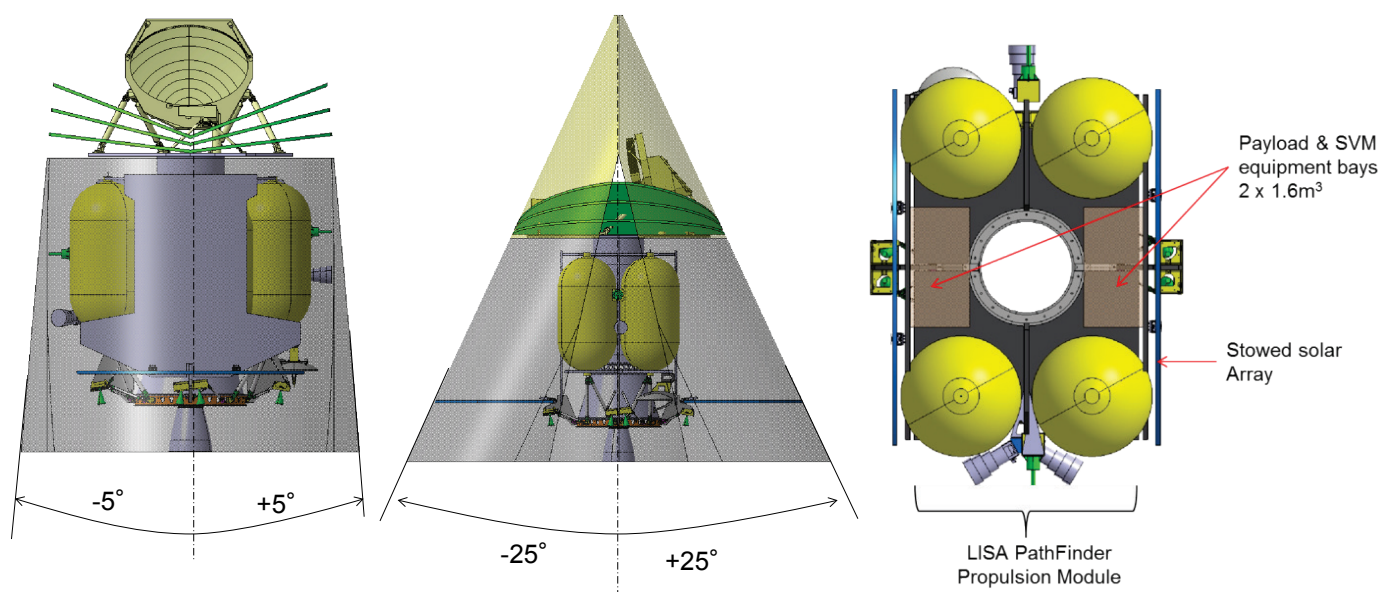
Figure 5-3: Left & Centre: Shadowing provided by the SVM for the PLM cryogenic passive cooling. Right: SVM concept based on the re-use of a LISA Pathfinder propulsion module

Power: The power budget for the ARIEL satellite is compiled in Table 5-1 below. Two operational cases are examined to give a worst-case sizing. These are the science operational case (at EOL) together with communication down-link period (assumed to be twice weekly for 3 hours each time) and the case during cool-down (BOL) where the telescope and instrument temperatures are controlled to avoid contamination. In each case a 20% contingency is taken from the current best estimate to give the nominal power shown here. This budget shows a required power of 492 W for the decontamination mode, although this would be at BOL. For the sizing of the solar arrays system the driver is actually the science & communications downlink mode at EOL, for which a rounded value of 500W power need is considered for the solar array sizing (details on solar array sizing are given as comments in the mass budget in Table 5-3).

Data: The payload proposed will produce data at a rate of approximately 11 Gb per day as described in §4.5.4. With the baseline assumption of a X-band downlink via a ~40cm High Gain Antenna to the New Norcia ground station, giving a 5Mbps transfer rate at 80% duty cycle (to account for contact acquisition & ranging, S/C telemetry, tele-command upload etc), this requires two 3-hour long communications sessions per week. The on-board data storage system would be sized to allow for 1 week of data to be stored on board in case a communications window is missed. The data rates of ARIEL are approximately an order of magnitude lower than Gaia, and two orders of magnitude lower than Euclid.

	Item	Decontam Mode (W)	Obs. & Comms. Mode (W)
PLM	Payload Module Thermal Control	100	0
Service Module (SVM)	Payload Warm Units		
	Instrument Control Unit (inc TCU)	0	45
	FGS Electronics	0	20
	LPF Propulsion Module	5	5
	SVM Thermal Control Systems	70	50
	AOCS		
	Sensors and Electronics	12	12
	Reaction Wheels & Isolators	30	10
	Data Handling		
	On Board Computer	15	15
	Remote Interface Unit	15	15
	Mass Memory	10	10
	Electrical and Power		
	PCDU	35	35
	Communications		
	Transponder	55	55
	SSPA	0	40
	SVM Harness Losses (2%)	8	8
Nominal Power per Mode		410	415
System Margin (20%)		82	83
Total ARIEL Power Requirement (W)		492	498

Table 5-1: Proposed ARIEL Design Power Budget

developments from existing hardware. The key aspects of the design, and areas where the technology proposed for ARIEL is an evolution of existing designs are highlighted in Table 5-2 below. All other aspects of the spacecraft design are evaluated as being at TRL 7 or above at the current time.

5.6 SPACECRAFT TECHNOLOGY READINESS LEVELS (TRL) ASSESSMENT

All of the major spacecraft subsystems in the proposed design are either heritage designs or

Technology	Current TRL	Expected TRL mid–2016	Current heritage / Development Plans
L2 Transfer Propulsion subsystem	9	9	Re-use of LISA pathfinder module
Cryogenic struts and V-Grooves for Passive cooling of PLM	6-7	7+	Based on Planck heritage
Cryogenic Harnesses	6-7	7+	Herschel, Gaia, Euclid design experience

Table 5-2: Spacecraft TRL Assessment

	Item	CBE Mass (kg)	Margin	Nominal Mass (kg)	Comments
Payload Module (PLM)	Cold Instrument Assembly	37.2		44.6	
	Spectrometer Optics Unit	6	20	7.2	ARIEL design proposal
	FGS / NIR-Phot Optics Unit	4	20	4.8	ARIEL design proposal based on EChO experience
	Common Optics & Cal Module	2	20	2.4	Two dichroics and mounts plus calibration module
	Radiators	10.2	20	12.2	Scaling of EChO radiator from 0.65m2 to 0.4m2 for ARIEL
	Payload Optical Bench	15	20	18.0	Pro-rata scaling of optical bench mass from EChO telescope size
	Telescope Assembly	84.3		100.8	
	M1 Mirror	27.8	20	33.4	SiC mirror
	M1 Mirror ISMs	1.8	20	2.2	Titanium /Invar KMs for M1 from baffle structure
	M2 Mirror	1.5	20	1.8	SiC mirror
	M2 Refocus Mechanism	3.8	10	4.2	Based on Gaia M2 mechanism re-use
	M3 Mirror	0.2	20	0.2	
	M3 Support structure	1.5	20	1.8	
	Baffle & Structure	47.7	20	57.2	Baffle provides radiator area, straylight control & M2 support structure
	Payload Cryo-harnesses	6.5	20	7.8	Based on approximate wire count from SVM to PLM and scaling from Euclid cryo-harness design
	Thermal Shield Assembly	30		36.0	
	Top floor MLI & connections	3	20	3.6	Reduction from EChO design by ratio of SVM size
	V-Groove Assy & PLM Struts	27	20	32.4	Scaled from EChO by linear factor on diameter of V-Grooves needed.
Service Module (SVM)	Payload Warm Units	17.5		21.0	
	Instrument Control Unit (inc TCU)	10.5	20	12.6	Based on EChO Study plus addition mass for 2 cards for telescope control
	FGS Electronics	7	20	8.4	Based on EChO FCU design
	Structure & Propulsion	264		284.7	
	Propulsion Module	214	5	224.7	Based on LISA Pathfinder design
	Secondary Structure	50	20	60.0	Approximate estimate based on SVM similarity
	SVM Thermal Control Systems	12	20	14.4	Approximate estimate based on SVM similarity
	AOCS	33		34.7	Note: No cold gas system needed in baseline
	Sensors and Electronics	8	5	8.4	STR-OH/EU, Sun Sensor, Gyros
	Reaction Wheels & Isolators	25	5	26.3	4 RW (Ref MyrEvo) + isolators (Airbus DS)
	Data Handling	15		18.0	
	On Board Computer	4	20	4.8	Next generation avionics. AS250 = 5 kg
	Remote Interface Unit	7	20	8.4	Next generation avionics. AS250 = 12 kg
	Mass Memory	4	20	4.8	Next generation avionics. Ref 5 kg for a downscale of Sentinel-2 MMFU (3 modules for 2400 Gbit EOL)
	Electrical and Power	21		25.2	
	Solar Generator	6	20	7.2	SA = 4,2 m² (66% packing factor) = half EChO. Power consumption = 500 W. Solar cells Azurspace 3G30, max off-pointing 20°, SA temp = 100°C => 181 W/m²
	Battery	4	20	4.8	Min nameplate energy = 625 W.h. Based on ABSL HC168650.NL cells (on-going development)
	PCDU	11	20	13.2	Next generation PCDU. Ref CRISA product = 15 kg
	Communications	21.5		24.4	
	Transponder	7	10	7.7	2 Rx/Tx bande X
	SSPA	5	20	6.0	2 next generation SSPA (Ref EChO = 8 kg)
	High Gain Antenna	2	20	2.4	Slight reduction vs EChO (2,5 kg)
	Low Gain Antennas & Bracket	5	5	5.3	EChO
	RFDU	2.5	20	3.0	EChO
	SVM Harnesses	32	20	38.4	Based on 8% of SVM mass
Nominal Dry Mass		574.0	13.2%	649.9	
System Margin			20	130.0	
Total ARIEL Dry Mass				779.9	
Propellant & Adapter	Total Propellant			1151.9	LISA Pathfinder stage capacity = 1200 kg
	AOCS Propellant Budget			20	Allocation for wheels off-loading + station keeping + safe mode (Ref EChO)
	L2 Transfer Propellant Budget			1131.9	DeltaV = 2723 m/s inc 5% margin, ISP = 319s, 2% ergol residuals
	Launch Adapter			60	Vega UM standard 937mm adapter
Total Mass at Launch				**1991.8**	c.f. Vega-C capacity of 2000kg for 250km x 3000km orbit

Table 5-3: Proposed ARIEL Design Mass Budget

6   MANAGEMENT SCHEME

The ARIEL mission is proposed to be a fully European mission, led by ESA, with the payload provided by a consortium of nationally funded institutes. This follows the classical approach to delivery of ESA M-class missions. The division of responsibilities between the payload consortium and ESA is clear and well defined; this is detailed in the following sections.

6.1   CONSORTIUM PROVIDED ELEMENTS

The multi-national payload consortium will be responsible for the provision of the payload module and the associated warm electronics modules that are accommodated within the S/C service module. The interface between the consortium provided PLM and the ESA / Prime provided spacecraft would be at the cold end of the PLM support structure as defined in §4.1. An interface control document documenting the vital mechanical and thermal aspects of this interface would be developed and agreed between the consortium and ESA as a priority in the assessment study phase.

The consortium will also provide the Instrument Operations and Science Data Centre as described below. This would be responsible for all instrument software, data processing and calibration and for long-term observation planning.

The key aspects of the split of the payload hardware and software provision are already agreed within the consortium. Details of the proposing responsible

nations for specific parts of the payload are shown in Figure 6-1 below. Other consortium partners contribute into some of these specific activities, the identifications here are only those that are current proposed lead the activity. Responsibilities and the division of work between the consortium partners will likely evolve through the assessment phase, however this demonstrates that all key areas are covered by the existing consortium team.

The potential interests and experience within the consortium of proposing institutes are given in the following lists. The work plan shown below selects only a subset of these interests in order to limit the national contributions for all consortium partners to the levels which the relevant national agencies have indicated are available for the M4 program.

- Austria: FGS Warm electronics SW, Science Ground Segment contribution.
- Belgium: Telescope AIV and characterisation at cryo, possible stray-light baffle, possible FGS detector module and characterisation, Science Grounds Segment contribution (calibration and observational strategies).
- France: Telescope design and manufacture, IR detector development & characterisation, Science Ground Segment contribution..
- Germany: Warm electronics, Detector procurement and characterisation (TBC), Science Ground Segment contribution.
- Ireland: Common optical elements, Science Ground Segment contribution.
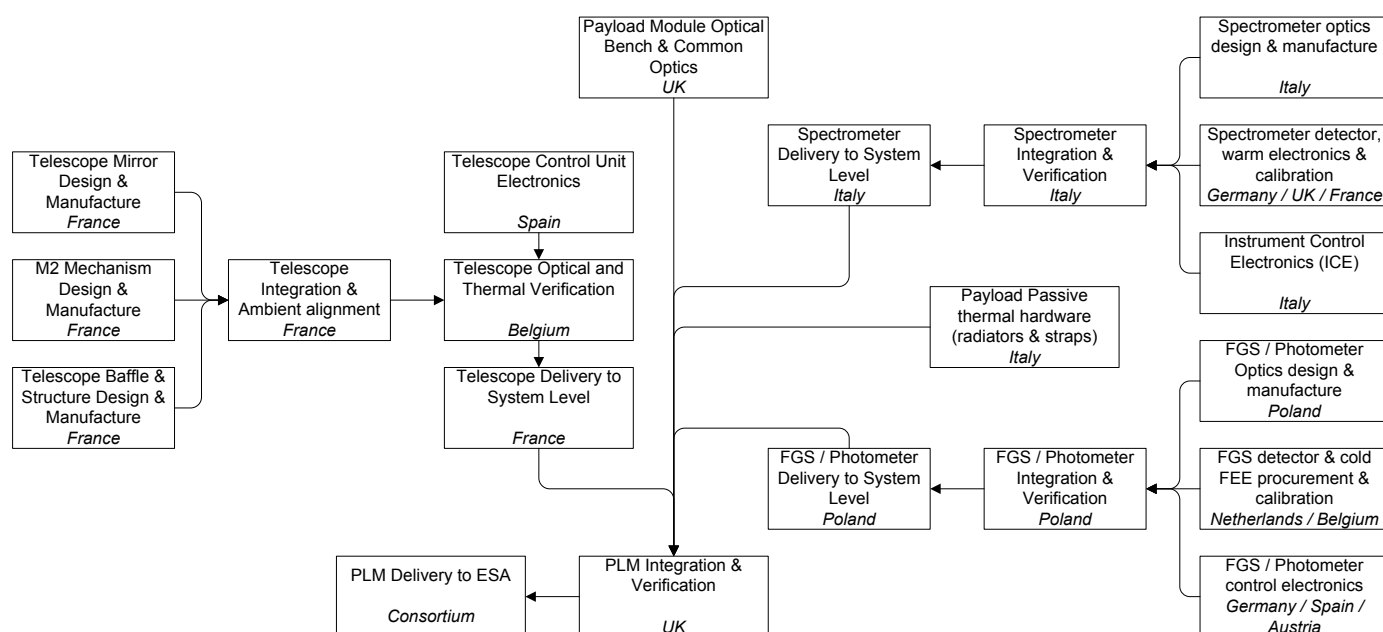
Figure 6-1: Consortium Responsibilities, Deliveries and Payload AIV Flow

- Italy: Spectrometer optics module, Electronics and on-board software (ICU & SW), Thermal system and hardware, Science Ground Segment contribution.

- Netherlands: Detector cold front end electronics for European detectors, Detector characterisation, support to AIV activities, Science Ground Segment contribution (TBC).

- Poland: Fine Guidance System: optics module (excluding detector), possible participation in electronics and software.

- Portugal: Contribution to optics module opto-mechanical design or OGSE, Science Ground Segment contribution.

- Spain: Contribution to spectrometer opto-mechanical design, Warm electronics for ICU or Telescope Control Unit, Science Ground Segment contribution to analysis and planning.

- UK: Consortium management & systems leadership, payload module AIV and calibration, Payload Module Optical Bench, Calibration system, IR detector system characterisation, Science Ground Segment contribution.

The management team of the ARIEL consortium consists of the Co-PIs, Co-Is and National Project Managers from each of the main contributing countries plus the central leadership of the consortium (PI, PM, Instrument Scientists). This is shown in Figure 6-2. The Co-PIs lead the national groups responsible for the major components of the payload, France, Italy & UK (telescope, spectrometer, overall PLM integration and calibration). All other contributing countries are led by a Co-I. All are assisted by a National Project Manager (NPM).
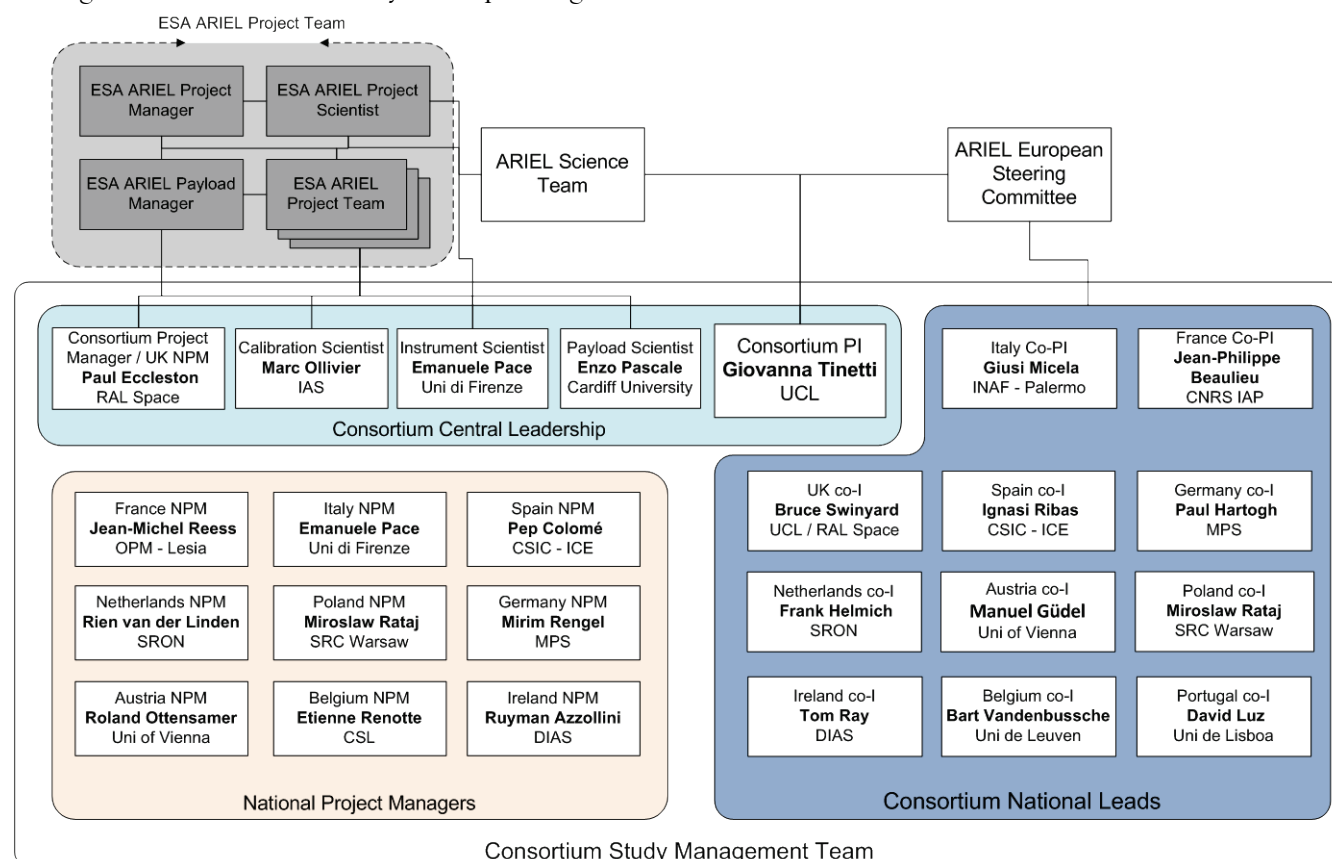
Figure 6-2: Proposed Consortium Management Team

6.2 ESA PROVIDED ELEMENTS

It is proposed that ESA would procure and manage the spacecraft contract from an industrial prime contractor. This contract would be for the development of the SVM and the support structure for the payload up to (and including) the struts and V-Groove system and the cryo-harnesses associated with the SVM to PLM thermal transition region. The prime contract would also include full-up S/C level AIT activities, with payload consortium support provided during this activity.

In the proposed management scheme ESA would also procure the launch vehicle for the mission. See §5.2 above for details.

The ARIEL mission ground segment is proposed to follow a similar model to other current ESA science missions, with the payload consortium providing the science ground segment and ESA providing the operations centres through the MOC & SOC. Further details on the proposed scheme are given in section 6.4.

6.3 DEVELOPMENT SCHEDULE

The ARIEL project would follow the classical ESA development schedule. The nominal schedule is based on the reference information given in the Annex to the call for M4 mission proposals and takes a conservative (low-risk) approach to the mission development. The mission would run through an Assessment Study (Phase A) which is assumed to take approximately two years with the Payload consortium and industrial studies into the spacecraft working in parallel during this time. The Assessment study concludes with a Preliminary Requirements Review (PRR) prior to the down-selection of the M4 mission to go forwards into Definition phase.

The Definition phase (Phase B1) is assumed to be 18 months and conclude with the System Requirements Review (SRR) and then mission adoption. This is then the point at which the industrial procurement by ESA of the spacecraft prime is assumed to take place. A 5 year development time from mission adoption to readiness for FM spacecraft AIV is assumed; the Payload Consortium assume a 6.5 year development time from mission selection to pFM payload delivery to S/C level. With an assumed 12-month S/C FM AIV flow, 6-month Launch Campaign and 9-month top-level schedule margin (to be held by ESA), this leads to a launch readiness in May 2025.

6.4 GROUND SEGMENT PROVISION

The ARIEL largely follows the standard model which

ESA have implemented for recent past and near future missions. It is proposed that ESA would take responsibility for the Mission Operations and Science Operations activities, while the consortium would provide the Instrument Operations and Science Data Centre (IOSDC). This operations model has been used in scoping the operations costs to both ESA and the Consortium in §7.

6.4.1 Ground Segment Architecture

The ground segment has three components:

- The Mission Operation Centre (MOC) would be situated at ESOC in Germany; responsible for communications with the spacecraft and its safe operation.
- The SOC would be situated at ESAC in Spain; responsible for mission planning, running the data processing software and archiving and also for all interactions with the community.
- The IOSDC would be distributed across consortium institutes; responsible for all the instrument related software, the instrument calibration, the instrument health and safe operation and for the long term observation planning.

Figure 6-4 shows the overall ground segment architecture and interfaces. While much of this is standard for ESA missions a particular feature of the ARIEL mission is the need to continuously schedule fixed time observations (the transit times for all targets are known in advance). This adds complexity to the scheduling, this has been studied in detail previously [Garcia-Piquer et al (2014), Morales et al (2014)]. Because of the expertise already resident within the consortium, the proposal is that the IOSDC will generate the long term schedule, this can be iterated during the assessment phase study.

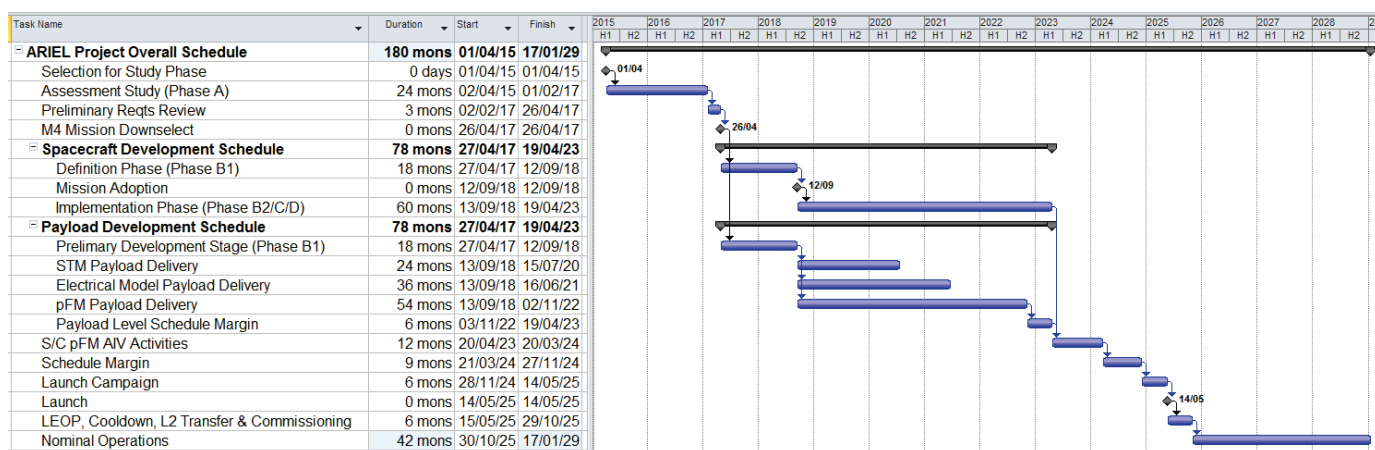| Task Name	Duration	Start	Finish
ARIEL Project Overall Schedule	**180 mons**	**01/04/15**	**17/01/29**
Selection for Study Phase	0 days	01/04/15	01/04/15
Assessment Study (Phase A)	24 mons	01/04/15	01/02/17
Preliminary Reqts Review	3 mons	02/02/17	26/04/17
M4 Mission Downselect	0 mons	26/04/17	26/04/17
Spacecraft Development Schedule	**78 mons**	**27/04/17**	**19/04/23**
Definition Phase (Phase B1)	18 mons	27/04/17	12/09/18
Mission Adoption	0 mons	12/09/18	12/09/18
Implementation Phase (Phase B2/C/D)	60 mons	13/09/18	19/04/23
Payload Development Schedule	**78 mons**	**27/04/17**	**19/04/23**
Prelimary Development Stage (Phase B1)	18 mons	27/04/17	12/09/18
STM Payload Delivery	24 mons	13/09/18	15/07/20
Electrical Model Payload Delivery	36 mons	13/09/18	16/06/21
pFM Payload Delivery	54 mons	13/09/18	02/11/22
Payload Level Schedule Margin	6 mons	03/11/22	19/04/23
S/C pFM AIV Activities	12 mons	20/04/23	20/03/24
Schedule Margin	9 mons	21/03/24	27/11/24
Launch Campaign	6 mons	28/11/24	14/05/25
Launch	0 mons	14/05/25	14/05/25
LEOP, Cooldown, L2 Transfer & Commissioning	6 mons	15/05/25	29/10/25
Nominal Operations	42 mons	30/10/25	17/01/29

Figure 6-3: ARIEL Development Schedule
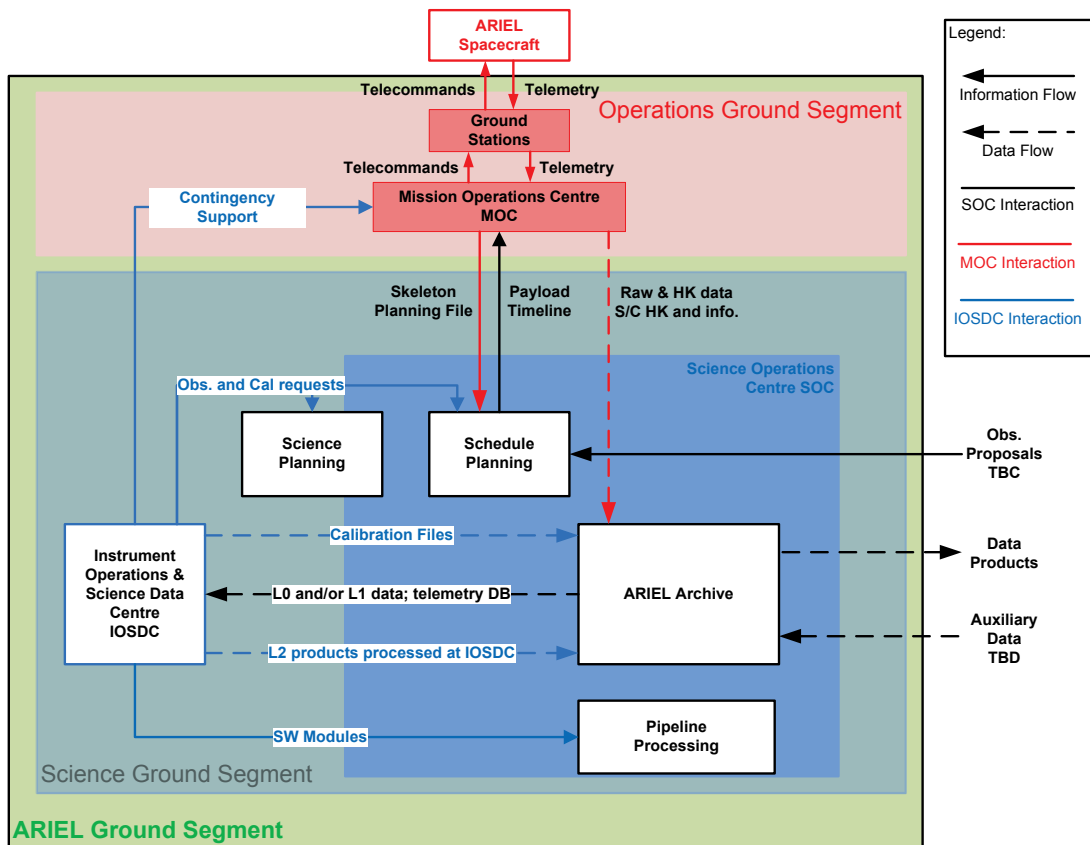
Figure 6-4: Overview of the ARIEL Ground Segment

6.5 DATA RELEASE AND EXPLOITATION POLICY

ARIEL is a survey mission with the primary objective to observe a diverse sample of known, transiting exoplanets as described in §2 and §3. The choice of targets will be made before launch and inputs will be solicited from the Community with the participation of the ESA Advisory structure. A fraction of the mission lifetime (~10-15%) will be devoted to an open time programme to which the Community will be able to subscribe through announcements of opportunity (AO). A first AO is envisaged 1.5 years before launch, with at least one additional call to be made during the mission. Proposals will be evaluated by a Time Allocation Committee made up of scientists with membership based on scientific excellence.

The data policy for the ARIEL programme is to provide rapid access to high quality exoplanet spectra for the Community. Datasets up to and including averaged exoplanet spectra for individual targets observed in the survey will be released a fixed number of months after the required signal-to-noise ratio (SNR) has been achieved. At the beginning of the mission the proprietary period, defined as the time elapsed between the date on which the last observation required to meet the SNR requirement is taken, and the date on which the data products are released, will be 6 months. This interval will reduce as the mission progresses, and a more complete understanding of the instrument characteristics, calibration needs and data processing/correction for systematics is gained by the IOSDC. In Year 1 of the mission data products will be released after 6 months; in Year 2 the period will be reduced to 3 months, falling to 1 month by Year 3 of the mission. The proprietary period for open time observations will be 1 year during the first 2 years of the mission, reducing to 6 months from Year 3.

6.6 PUBLIC RELATIONS AND OUTREACH

A mission to characterize the atmospheres of diverse worlds beyond our Solar System provides an excellent opportunity to harness curiosity, interest and familiarity in many diverse ways. The discovery of more than 2000 exoplanets in the last 20 years is possibly one of the most exciting developments of modern astronomy. The discoveries resonate with the Public who have already shown very strong curiosity and interest in the exploration of the diverse worlds in our own Solar System. Closer to home, the concept of a planetary atmosphere is one that is familiar to all, with the implications of the Earth's atmosphere so familiar that they are often taken for

granted. The atmosphere provides the air we breathe; its presence is felt through the winds that drive it, and most have witnessed a blue sky during the day which turns to orange/red at sunset and sunrise - both direct fingerprints of the Earth's atmosphere on the light arriving from the Sun.

ARIEL communication and outreach activities will reach out to a wide audience that includes the Public at large as well as focused groups such as school students, amateur astronomers, politicians and artists. The plan will be developed and executed by ESA and the Payload Consortium, with guidance from the ARIEL Science Team.

The Payload Consortium will work closely with space outreach and educational networks, including Europlanet RI (EU-funded), and its successor networks, Hands-on Universe, networks that have formed as a result of the 2009 International Year of Astronomy, ESA's own European Space Education Resource Offices, as well as national and more local networks. An open approach will be adopted; the payload consortium teams will welcome media professionals into their institutions, laboratories and workshops during all phases of the mission development and operation. Broadcasters will be invited to follow the mission with a view to producing bespoke programs and documentaries that cover scientific and engineering aspects of ARIEL from cradle to grave. These activities will build on the strong record that many ARIEL Payload Consortium scientists have in public outreach, which include TV and radio interviews with many European broadcasters.

Online media outlets such as YouTube and Twitter will be used to post interviews with ARIEL scientists and engineers. This will build on the rapid dissemination of mission news and updates possible through existing ESA channels. It will allow interested parties to follow many different aspects of the mission and to stay informed about mission progress, and performance during flight. Short, "Day in the life of…"-type films and vodcasts following ARIEL scientists and engineers will be made to illustrate the wide range of tasks that technical professionals engage in over the course of a space mission, not just for general interest but also targeting school and university students to highlight the very wide ranges of challenges on offer from careers in science and engineering.

The excitement generated by the ARIEL mission and its discoveries will provide a topical platform on which to develop educational materials, with many of the core concepts behind the ARIEL science objectives and technologies covered in school syllabi at different levels. Topics such as the study of exoplanets and their formation, and exoplanet discovery techniques, will join spectroscopic signatures of atoms and molecules, and "the conditions necessary for life to form" that are already common on school syllabi. Discussion of spacecraft engineering and operation, through topics such as power generation and orbital mechanics, will allow case studies to be made to give context to a wide range of technical areas and disciplines, in parallel helping to maintain the high profile of both ARIEL and ESA in general, within schools. Material will be developed for school students Europe-wide, and will be supported by CPD courses to inform school teachers of the science and engineering challenges of ARIEL.

Schools will be actively engaged in the selection of the ARIEL core sample. A competition will be run across ESA member states to choose a School's Target Exoplanet. Supporting material detailing potential ARIEL candidate targets will be developed to enable students to make a scientifically-informed vote. Students will be able to follow observations of the chosen planet via a dedicated website, and participate in the data analysis and interpretation.

An excellent way to engage and motivate the public is to provide access to data. The public will be invited to participate in the science exploitation of the ARIEL mission through access to data sets, taking advantage of the networks developed by very successful citizen science programs such as the Zooniverse/Planet Hunters team using Kepler data [Zooniverse website, 2013], and Solar Stormwatch [Solar Stormwatch website, 2013].

Amateur astronomers play a crucial role in leveraging the outreach efforts of professional scientists, providing both a link with the broader general public and key scientific input. ARIEL scientists will work to engage the amateur astronomer community - giving lectures, making available presentation material that can be used widely, and encouraging the community to undertake a programme of observations to support ARIEL in particular, and the science of exoplanets, in general.

The fascinating details of new worlds that will be revealed by ARIEL will need visual support to capture the imagination of the public. ARIEL scientists will work together with ESA to produce

images, animations, and 3-D simulations suitable for a wide range of online and broadcast media formats. A fine art program will be set up, to realise images that have high impact and at the same time are fully consistent with our best knowledge about these planets and the findings of ARIEL. This continues and expands the tradition of the "Space Art" movement that was initiated in Europe a century ago (most notably by L. Rudaux, [IAAA website, 2013]).

7 COSTING PROPOSAL

7.1 COST TO ESA ESTIMATES

The preliminary estimates of the costs to ESA for the ARIEL mission described in this proposal are shown in Table 7-1 below where all costs are in M€ at 2015 costs. The baseline mission concept of use of Vega-C with LPF based propulsion unit and the alternative concept of Soyuz launch (which would then use a more conventional S/C SVM bus design) are both shown to demonstrate that both fall within overall cost envelope for M4. We estimate some of the cost components through a benchmark to numbers used for the previous M-class mission selections (such as operations costs and ESA project team costs). This costing makes the following assumptions and takes the following inputs:

- Spacecraft prime contract estimate comes from detailed communications with Airbus Fr during the preparation of this proposal. The cost is consistent with other comparable missions; the spacecraft design does not pose significant challenges and is based on well-known technologies. Therefore the mission should be feasible within the proposed cost envelope.

- Costs for launchers are as provided by ESA at the M4 proposers briefing meeting at ESTEC on 26th Sept 2014.

- The mission operation costs for M1/M2/M3 are in the range of 14.8 to 16.4% of CaC. With ARIEL having a relatively short mission life (3.5 years) compared to these other missions we assume 15% of the ESA CaC cap for operations costs. An additional €5M for ESA ground segment costs in case of Vega-C launch is assumed to account for additional mission planning and early orbit operations needed for the additional burns to reach L2.

- We adopt the same fractions of the prime contract cost for the ESA project team as for M1/M2: 12.8% for the ESA M4 project team, 1.1% for ESA ESTEC overheads and 4.5% for technical support leading to ESA project team costs assumed to be 18.4% of prime contract value.

The top level evaluation of costs demonstrates that the proposed ARIEL mission is compatible with the ESA M4 cost envelope. Extensive steps have been taken by the proposing team to ensure that the mission will stay within the M4 limits, and further iteration will be expected in the assessment phase with ESA to ensure that this remains the case. The payload, spacecraft and mission design are all scalable and can be optimised to maximise the scientific return within the ESA M4 cost constraints. The cost estimate also takes heritage from the extensive studies completed as part of the EChO Assessment Study and is therefore believed to be a robust and accurate estimate of the cost of the ARIEL mission as proposed.

The proposed spacecraft and mission profile are consistent with the key guidelines set out in the technical annex to the M4 call for proposals. The dry mass of ARIEL is ~780kg (including margin), the payload mass is <200kg, the baseline technologies are all at TRL 5 (or have a plan to reach this within two years and have back-ups available at higher TRL), the mission lifetime is 3.5 years and the mission is

Line Item	Baseline (Vega-C + LPF Unit)	Alternative (Soyuz)
Spacecraft Prime Contract (including built in LPF propulsion unit for Vega-C launch option)	235	220
Launch Services	55	80
ESA Ground Segment (MOC & SOC) & S/C Operations Costs	73	68
ESA Project Team (18.4% of Prime contract value)	43	40
ESA Basic Cost at Completion	406	408
Margin to €450M M4 Cost Cap	**44**	**42**
Margin to €450M M4 Cost Cap	**9.7%**	**9.3%**

Table 7-1 : Estimates of ARIEL ESA CaC

compatible with both Vega and Soyuz launches. This all builds confidence that the mission can be executed within the constraints of the limitations of the M4 program.

7.2 COST TO CONSORTIUM ESTIMATES

The cost of the payload contributions from the consortium funded by the national agencies have been evaluated by analogy with previous space mission hardware (ISO, Planck, Herscel, JWST, Gaia, Euclid) and with the extensive costings conducted by the EChO consortium at the end of the M3 assessment phase. The instrument design proposed for ARIEL is substantially smaller, less complex and more compact than that proposed for EChO (single spectrometer module and detector instead of four modules, smaller wavelength range, no active cooling). The M4 mission constraints and the ARIEL science case allow a smaller telescope to be proposed than for EChO; this enables the consortium to take on the responsibility for the provision of the telescope assembly while remaining within the budget envelopes defined by the relevant national agencies for the participation in M4.

The preliminary cost estimate to national agencies for the ARIEL payload consortium is €110M including a suitable margin (dependant on the level of heritage on each item, generally in range of $10 - 20\%$) on all costs up to launch. Further funding for the Science Ground Segment operation costs (development is costed in the pre-launch costs) is in addition to this value. For comparison, the projected cost of the EChO M3 proposed payload contribution to the same point was significantly more at ~€160M.

8 ANNEX 1: BIBLIOGRAPHY AND REFERENCES

8.1 CHAPTER 2: SCIENCE CASE & CHAPTER 3: SCIENTIFIC REQUIREMENTS

Adams E.R., Seager, S., ApJ **673**, 1160 (2008)

Agúndez, M., et al., A&A, 548, A73 (2012)

Apai, D., et al., ApJ **768** 121 (2013)

Ballerini, P., et al., A&A, 539, 140 (2012)

Bakos G. A.,et al., PASP, 974 (2002)

Barman, T. S., ApJ **661**, L191 (2007).

Barstow, J.K., et al., MNRAS, **430**, 1188 (2013).

Barstow, J.K., et al., MNRAS **434**, 2616 (2013a)

Barstow, J.K., et al.: Exoplanet atmospheres with ARIEL: spectral retrievals using ARIELSim. Exp. Astron. accepted (2014).

Basri, G., Walkowicz L.M., Batalha N., et al., AJ, **141**, 20 (2011).

Batalha, N., et al ApJS **204**, 24 (2013)

Batalha, N., Proc. NAS, 111,12647 (2014)

Bean, J. L., Miller-Ricci Kempton, E., Homeier, D., Nature **468**, 669 (2010).

Beaulieu, J.-P., Kipping, D.M., Batista, V., et al. MNRAS **409**, 963 (2010).

Beaulieu J.-P., Tinetti, G., Kipping, D.M., et al. ApJ **731**, 16 (2011).

Beichman, C., et al. Kepler white paper (2014)

Berta, Z. et al. ApJ **747** 35 (2012)

Birkby, J.L., et al. MNRAS **436**, L35 (2013).

Bodenheimer, P., et al., ApJ, **548**, 466, (2001).

Bonnefoy, M., et al. A&A, 555, 107 (2013)

Borucki, W.J., et al., Science, **325**, 709 (2009).

Broeg et al., EPJWC, 47, 03005 (2013)

Brown, T.M., ApJ, **553**, 1006 (2001).

Burrows, A., Hubeny, I., Budaj, J., Hubbard, W.B., ApJ **661**, 502 (2007).

Broomhall, A.-M., et al. (2009), MNRAS, 396:L100-L104.

Cassan, A., et al (2012) Nature **481**, 167 (2012).

Charbonneau, D., Brown T.M., Noyes R.W., Gilliland R.L., ApJ **568**, 377 (2002).

Charbonneau, D., Allen L.E., Megeath S.T. et al, ApJ **626**, 529 (2005).

Charbonneau, D., et al. ApJ **686**,1341 (2008).

Chatterjee, S., Ford, E., Matsumura, S., Rasio, F.A., , ApJ **686**, 580 (2008).

Chazelas, B., et al. SPIE, 8444,10 (2012)

Crouzet, N., McCullough, P.R., Burke, C., Long, D., ApJ **761**, 7 (2012).

Crouzet, N., et al.: Water vapor in the spectrum of the extrasolar planet HD 189733b: 2. The eclipse, ApJ accepted, arXiv:1409.4000 (2014).

D'Angelo, G., et al. Vol. 2011, pp. 319–346. U. of Arizona Press (2011)

Danielski, C., et al. ApJ 785, 35 (2014).

Danielski C., et al.: Gaussian Process for star and planet characterisation, ApJ, submitted, (2014).

Deming, D., Seager, D., Richardson L.J. et al. Nature **434**, 740 (2005).

Deming, D., et al. ApJ **774**, 95, (2013).

Demory, B. O., et al. 2013, ApJ **776,** L25 (2013)

De Wit, J., Gillion, M., Demory, B.O., Seager, S., A&A **548**:128 (2012).

Dumusque, X., et al., ApJ **789**, 154 (2014).

Eccleston, P., et al. Exp. Astron., accepted (2014).

Elkins-Tanton, Astrophysics and Space Science, **332**, 359 (2011).

Encrenaz, T., et al. Exp. Astron., accepted (2014).

Ehrenreich, D., et al, A&A in press, arXiv:1405.1056 (2014)

Forget, F., Leconte, J., Phil. Trans. Royal Society **372**, #20130084 (2014).

Fortney, J., et al., ApJ, 659, 166 (2007)

Fraine, J., et al., Nature, **513**, 526 (2014).

Fukui, A., et al., ApJ **770** 95 (2013)

Garcia-Piquer, A., et al., 'EChO Long Term Mission Planning Tool', Exp. Astron., accepted.

Grasset, O., Schneider, J., & Sotin, C. ApJ **693**, 722 (2009).

Guillot, T., Gladman, B.: Disks, Planetesimals, and planets, ASP conference proceedings, Vol. 219. In: (2000)

Grillmair, C. J., Burrows, A., Charbonneau, D., et al., Nature **456**, 767 (2008).

Guillot, T., Showman, A.P., A&A **385**, 156 (2002).

Gustafsson B., et al., A&A **486**, 951 (2008).

Habets, and Heintze, (1981), A&AS, 46,193-237.

Herrero, E. et al.: Correcting ARIEL data for stellar activity, by direct scaling of activity signals. Exp. Astron., accepted (2014).

Ikoma M., Hori, Y., ApJ **753**, 6 (2012)

Irwin, P., et al., JQSRT, 109,1118 (2008)

Kley, W., Nelson, R.P.: ARAA 50, 211 (2012)

Knutson, H.A., Charbonneau, D., Allen, L.E. Nature **447**, 183 (2007).

Knutson, H.A. et al., ApJ **735**, 23 (2011).

Knutson, H.A. et al., Nature **505**, 66 (2014).

Kreidberg, L., et al. Nature **505**, 69 (2014).

Kreidberg, L., et al. ApJ (2014b).

Konopacky, Q., et al. Science, 339, 1398 (2013)

Leconte, J., Forget, F., Lammer, H.: The diversity of terrestrial planet atmospheres. Exp. Astron., accepted (2014).

Lee, J.-M., Fletcher, L. N. and Irwin, P. MNRAS **420**, 170 (2012).

Léger, A., et al. Icarus **213**, 1 (2011).

Léger, A., Selsis, F., Sotin, C. et al. Icarus **169**, 499 (2004).

Levison, H.F., Morbidelli, A., Tsiganis, K., Nesvorny, D., Gomes, R.: Astron. J. 142, 152 (2011)

Lindegren, L., et al., IAU Symp., 248, 217 (2007)

Line, M.R., Yung, Y. ApJ **779**, 6 (2013)

Linsky, J. L. et al., ApJ **717**, 1291 (2010).

Lissauer J. et al., 2011Natur.470...53L

Lodders & Fegley, 'Chemistry of Low Mass Substellar Objects', Springer (2006)

Madhusudhan, N., Seager, S., ApJ **707**, 24 (2009).

Majeau, C., Agol, E. and Cowan, N. B., ApJ **747**, id L20 (2012).

Matter, A., Guillot, T., Morbidelli, A.: Planet. Space Sci. 57, 816–821 (2009)

McCullough, P., et al., ApJ **791**, 55 (2014).

Micela, G., et al., The contribution of the major planet search surveys to ARIEL target selection, Exp. Astron., accepted.

Micela, G. et al.: Correcting for stellar activity. Exp. Astron., accepted (2014).

Morales, J.C., et al.: Scheduling the ARIEL survey with known exoplanets, Exp. Astron., accepted (2014).

Morello, G., et al., ApJ **786**, 22 (2013).

Moses, J., Visscher, C., Fortney, J., et al. ApJ **737**, 15 (2011).

Nutzman, P. & Charbonneau, D., 2008, PASP 120, 317

Palle, P. L., et al. (1995) ApJ, 441,952-959.

Pascale, E., et al.: ARIELSim: The Exoplanet Characterisation Observatory software simulator. Exp. Astron., arXiv:1406.3984 (2014).

Perryman, M. A. C. and ESA, editors 2007, ESA –SP 2000

Pickles, A. J. (1998), PASP, 110,863-878.

Pollacco, D.L., Skillen, I., Collier Cameron, A., et al., 2006, P ASP , 118, 1407

Puig, L., et al. Exp. Astron., accepted (2014).

Rauer, H., et al. Exp. Astron., 38, 249 (2014)

Rauscher, E., Menou, K., Cho, J.Y.-K., Seager, S., & Hansen, B.M.S. ApJ **662**, L115 (2007).

Raymond S. N., Quinn T., Lunine J. I.; Icarus 183, 265-282 (2006)

Ribas, I., Lovis, C & EChO Study Science Team, EChO targets: the Mission Reference Sample and Beyond, EChO-SRE-SA-PhaseA-001 (2013)

Ricker et al., SPIE, 9143,20 (2014)

Rowe, J., et al., ApJ **689**,1345 (2008).

Scandariato, G., et al.: ARIEL spectra and stellar activity II. The case of dM stars. Exp. Astron. accepted (2014).

Seager, S., Sasselov, D.D., ApJ **537**, 916 (2000).

Sharp, C. M., Burrows, A. ApJS, **168**, 140 (2007).

Sing, D. K., et al. MNRAS **416**, 1443 (2011).

Snellen, I., et al., Nature **465**, 1049 (2010).

Sozzetti, A., 2010, Highlights of Astronomy, 15, 716

Sozzetti, A., 2013, EPJWZ, 47, 03006 (2013)

Sozzetti, A., et al. The Gaia Survey Contribution to ARIEL Target Selection & Characterization. Exp. Astron. Accepted (2014).

Stevenson, K. B., et al. Nature **464**, 1161 (2010).

Stevenson, K. B., et al. ApJ (2014).

Swain, M. R. et al., Nature **463**, 637 (2010).

Swain, M. R., Vasisht, G., Tinetti, G., Nature **452**, 329 (2008).

Swain, M. R., et al. ApJ **690**, L114 (2009).

Taylor, F.W., et al.: Jupiter. 2014, The planet, satellites and magnetosphere. In: Bagenal, F., Dowling, T.E.,

Tinetti, G., Encrenaz E., Coustenis A., Astron Astrophys Rev. **21**, 63 (2013).

Tinetti, G., M.C. Liang, et al. ApJ, **654**, L99 (2007a).

Tinetti, G., et al. Nature **448** 169 (2007b).

Tinetti, G., Deroo, P., Swain, M., et al. ApJ **712**, L139 (2010).

Todorov, K. O. et al., Updated Spitzer Emission Spectroscopy of Bright Transiting Hot Jupiter HD189733b, ApJ Accepted, arXiv:1410.1400 (2014).

Tsiganis, K., Gomes, R., Morbidelli, A., Levison, H. F., Nature **435**, 459 (2005).

Turrini, D., Nelson, R., Barbieri, M.: The role of planetary formation and evolution in shaping the composition of exoplanetary atmospheres, Exp. Astron., accepted. arXiv:1401.5119 (2014).

Turrini, D., Svetsov, V.: Life 4, 4–34 (2014). doi:10.3390/life4010004

Valencia, D., O'Connel, R. J., Sasselov, D., Icarus **181**, 545 (2006).

Valencia, D., Sasselov, D.D., O'Connell, R.J., ApJ **665**, 1413 (2007).

Valencia, D., Guillot T., Parmentier V., Freeman R., ApJ **775**, 10 (2013).

Varley, R. et al. Generation of a target list of observable exoplanets for ARIEL, Exp. Astron., Accepted, arXiv:1403.0357.

Venot, O., Hébrard, E., Agundez, M., et al., A&A **546**, A43 (2012).

Venot, O., et al.: Chemical modelling of exoplanet atmospheres, Exp. Astron., Accepted (2014).

Vidal-Madjiar, A. et al., Nature, **422**, 143 (2003).

Waldmann, I.P., ApJ **747**, 12 (2012).

Waldmann, I.P., Pascale, E.: Data analysis pipeline for ARIEL end-to-end simulations, Exp. Astron., Accepted, arXiv:1402.4408 (2014).

Waldmann, I.P., et al.: Tau-REx I: A next generation retrieval code for exoplanetary atmospheres, ApJ, arXiv:1409.2312 (2014).

Weidenschilling, S. J., Marzari, F., Nature **384**, 619 (1996).

Wordsworth, R.D., Forget, F., Selsis, F., et al., A&A **522**, A22 (2010).

Yurchenko, S.N., Tennyson, J., Bailey, J., Hollis, M.D.J., Tinetti, G., Proc. Nat. Acad. Sci. **111**, 9379 (2014).

8.2 CHAPTER 6: MANAGEMENT SCHEME

Garcia-Piquer, A., et al., 'EChO Long Term Mission Planning Tool', Exp. Astron.(2014)

Morales, J.C., et al.: Scheduling the ARIEL survey with known exoplanets, Exp. Astron., accepted (2014).

IAAA website: accessed September, 2013 http://iaaa.org/gallery/rudaux/

LCOGT website: accessed September, 2013 http://lcogt.net/

SolarStorm Watch website: accessed September, 2013 http://www.solarstormwatch.com/

Zooniverse website: accessed September, 2013 https://www.zooniverse.org/project/planethunters

9 ANNEX 2: LIST OF ACRONYMS

AIRS	ARIEL IR Spectrometer		EM	Engineering Model
AIT / AIV	Assembly, Integration and Test / Verification		EOL	End Of Life
AO	Announcement of Opportunity		EPRAT	ExoPlanet Roadmap Advisory Team
AOCS	Attitude and Orbit Control System		ERC	European Research Council
AR	Anti-Reflection		ESA	European Space Agency
ARIEL	Atmospheric Remote-Sensing Infrared Exoplant Large-Survey		ESAC	European Space Astronomy Centre
ASIC	Application-Specific Integrated Circuit		ESOC	European Space Operations Centre
ATH	ARIEL Thermal Hardware		ETLOS	EChO Target List Observation Simulator
ATU	ARIEL Telescope Unit		FEE	Front End Electronics
AU	Astronomical Units		FGE	FGS Electronics
AVM	Avionics Model		FGS	Fine Guidance Sensor / System
BB	BreadBoard		(p)FM	(proto-)Flight Model
BBR	BroadBand Radiometer		FoV	Field of View
BOL	Beginning Of Life		FPA	Focal Plane Array
CaC	Cost at Completion		FWHM	Full Width Half Maximum
CAD	Computer-Aided Design		GMM	Geometrical Mathematical Model
CDMS	Command and Data Management System		GPI	Gemini Planet Imager
cFEE	Cold Front End Electronics		GSE	Ground Support Equipment
CFRP	Carbon Fibre Reinforced Plastic		HARPS	High Accuracy Radial-velocity Planet Searcher
CHEOPS	Characterizing Exoplanets Satellite		HCU	Housekeeping and Calibration Source Unit
CoRoT	Convection, Rotation & planetary Transits		HEO	Highly Eccentric Orbit
CPD	Continuing Professional Development		HGA	High Gain Antenna
CTE	Coefficient of Thermal Expansion		HK	Housekeeping
DPU	Data Processing Unit		H-R	Hertzsprung – Russell
EChO	Exoplanet Characterisation Observatory		I/O	Input / Output
ECSS	European Cooperation for Space Standardization		ICU	Instrument Control Unit
EGSE	Electronics Ground Support Equipment		IOSDC	Instrument Operations and Science Data Centre
(E)-ELT	(European) Extremely Large Telescope		IR	InfraRed
			ISM	Iso-Static Mounts
			ISO	Infrared Space Observatory
			JUICE	JUpiter ICy moons Explorer
			JWST	James Webb Space Telescope

KM	Kinematic Mounts		S/C	Spacecraft
L2	Second Lagrangian Point		SA	Solar Array
LEO	Low Earth Orbit		SCExAO	Subaru Coronagraphic Extreme Adaptive Optics
LISA	Laser Interferometer Space Antenna		SED	Spectral Energy Distribution
LPF-PM	LISA PathFinder Propulsion Module		SNR	Signal-to-Noise Ratio
LV	Launch Vehicle		SOC	Science Operations Centre
LWIR	Long Wave InfrarRed		SPHERE	Spectro-Polarimetric High-contrast Exoplanet REsearch (On VLT)
LWS	Long Wave Spectrometer			
MCT	Mercury Cadmium Telluride		SPIRE	Spectral and Photometric Imaging Receiver
MIR(I)	Mid-InfaRed (Instrument)			
MLI	Multi-Layer Insulation		SRR	System Requirements Review
MOC	Mission Operations Centre		SSPA	Solid State Power Amplifier
MWIR	MidWave InfraRed		STM	Structural and Thermal Model
NEMESIS	Non-linear optimal Estimator for MultivariateE Spectral analysis		SVM	SerVice Module
			SW	Software
NEOCam	Near Earth Object Camera		SWIR	Short-Wave InfraRed
NGTS	Next-Generation Transit Survey		TBC	To Be Confirmed
NIR	Near InfraRed		TBD	To be Determined / Decided
NPM	National Project Manager		TCE	Telescope Control Electronics
OAP	Off Axis Parabola		TCS	Temperature Control Stage
OB	Optical Bench		TCU	Telescope Control Unit
PCDU	Power Control and Distribution Unit		TDV	Transit Depth Variation
PI	Principal Investigator		TESS	Transiting Exoplanet Survey Satellite
PLM	Payload Module		TIF	Thermal InterFace
PM	Project Manager		TM/TC	TeleMetry / TeleCommand
PRE	Performance Reproducibility Error		TMM	Thermal Mass Model
PRR	Preliminary Requirements Review		TRL	Technology Readiness Level
PSF	Point Spread Function		TRP	Technology Research Programme
PSU	Power Supply Unit		UM	User Manual
QE	Quantum Efficiency		VG	V-Groove
R	Resolving power		VIS	Visible Light
RFDU	Radio Frequency Distribution Unit		VLT	Very Large Telescope
ROIC	Read-Out Integrated Circuits		WFE	WaveFront Error
RPE	Relative Performance Error		WFEE	Warm Front End Electronics
RTU	Remote Terminal Unit			
RV	Radial Velocity			

10 ANNEX 3: LIST OF CO-PI'S, CO-I'S AND CONSORTIUM PARTICIPANTS

10.1 CO-PI'S AND CO-I'S

Giovanna Tinetti, University College London, UK; Jean-Philippe Beaulieu, Institut d'Astrophysique de Paris, France; Giusi Micela, INAF – Osservatorio Astronomico di Palermo, Italy; Bart Vandenbussche, Univerity of Leuven, Belgium; Manuel Guedel, University of Vienna, Austria; Paul Hartogh, Max Planck Sonnnensystem, Germany; David Luz, Universidade de Lisboa, Portugal; Tom Ray, Dublin Institute for Advanced Studies, Ireland; Ignasi Ribas, CSIC – ICE, Spain; Mirek Rataj, Space Research Centre, Polish Academy of Science, Poland; Frank Helmich, SRON Netherlands Institute for Space Research, Netherlands; Bruce Swinyard, RAL Space / University College London, UK.

10.2 INSTITUTE CONTACT POINTS

Denis Grodent, Université de Liège, Belgium; Etienne Renotte, CSL, Belgium; Paulina Wolkenberg, Space Research Centre, Polish Academy of Science, Poland; Mike Barlow, UCL, UK; Neil Bowles, University of Oxford, UK; Graziella Branduardi-Raymont, MSSL, UK; Vincent Coudé du Foresto, LESIA-Astro, France; Pierre Drossart, LESIA-Planeto, France; Christopher Jarchow, MPS-Planeto, Germany; Franz Kerschbaum, University of Vienna, Austria; Pierre-Olivier Lagage, CEA – Saclay, France; Mercedes Lopez-Morales, CSIC – ICE, Spain; Giuseppe Malaguti, INAF – IAPS – Bologna, Italy; Marc Ollivier, IAS Paris, France; Emanuele Pace, Università di Firenze, Italy; Enric Pallé, IAC, Spain; Enzo Pascale, Cardiff University, UK; Giuseppe Piccioni, INAF - IAPS – Roma, Italy; Alessandro Sozzetti, INAF – Osservatorio Astrofisico di Torino, Italy; Bart Vandenbussche, Leuven University, Belgium; Ian Bryson, UK ATC, UK; Gonzalo Ramos Zapata, INTA, Spain; Maria Rosa Zapatero Osorio, CAB, Spain.

10.3 CONSORTIUM TECHNICAL TEAM COORDINATORS

Consortium Project Manager – Paul Eccleston, RAL Space, UK. **Payload Scientist** - Enzo Pascale, Cardiff University, UK. **Calibration Scientist –** Marc Ollivier, IAS Paris, France. **Instrument Scientist –** Emanuele Pace, Università di Firenze, Italy. **Systems Engineering Working Group –** Ana Balado, INTA, Spain; Ian Bryson, UK ATC, UK; Vincent Coudé du Foresto, LESIA-Astro, France; Anna Di Giorgio, Italy; Kevin Middleton, RAL Space, UK; Frederic Pinsard, CEA – Saclay, France; Gianluca Morgante, INAF – IASF Bologna, Italy; Emanuele Pace, Università di Firenze, Italy; Pep Colomé, ICE – CSIC, Spain; Bruce Swinyard, RAL Space / UCL UK; Tom Hunt, MSSL, UCL, UK. Alberto Adriani, IAPS-IAPS, Italy; Neil Bowles, University of Oxford, UK; Roland Ottensamer, University of Vienna, Austria; Gonzalo Ramos Zapata, INTA – LINES, Spain; Jean-Michel Reess, LESIA-Planeto, France. **National Project Managers –** Ruymán Azzollini, DIAS, Ireland; Mirim Rengel, MPS, Germany; Josep Columé, CSIC-ICE, Spain; Roland Ottensamer, University of Vienna, Austria; Emanuele Pace, Università di Firenze, Italy; Mirek Rataj, Space Research Centre, Polish Academy of Science, Poland; Jean-Michel Reess, LESIA-Astro, France; Rien van der Linden, SRON Netherlands Institute for Space Science, Netherlands.

10.4 CONSORTIUM SCIENCE TEAM COORDINATORS

Science Team Co-leads – Giovanna Tinetti, UCL, UK and Pierre Drossart, LESIA-Planeto, France. **Science Team Working Group Leads –** Joanna Barstow, Oxford University, UK; James Cho, QMUL, UK; Charles Cockell, ROE, UK; Athena Coustenis, LESIA, France; Leen Decin, University of Leuven, Belgium; Therese Encrenaz, LESIA, France; Francois Forget, LMD, France; Marina Galland, Imperial College, UK; Paul Hartogh, MPS Germany; Jeremy Leconte, LMD, France; Pierre Maxted, Keele University, UK; Giusi Micela, INAF, Palermo, Italy; Ingo Mueller-Wodarg, Imperial College, UK; Chris North, Cardiff, UK; Isabella Pagano, OACt, Italy; Guseppe Piccioni, INAF/IAPS, Italy; David Pinfield, UH, UK; Remco de Kok, SRON, Netherlands; Ignasi Ribas, CSIC-ICE, Spain; Franck Selsis, Université de Bordeaux, France; Ignas Snellen, Leiden University; Lars Stixrude, UCL, UK; Jonathan Tennyson, UCL, UK; Diego Turrini, INAF-IAPS, Italy; Olivia Venot, University of Leuven, Belgium; Paulina Wolkenberg, Space Research Centre, Polish Academy of Science, Poland; Mariarosa Zapatero-Osorio, CAB, Spain.

10.5 CONSORTIUM CONTRIBUTING SCIENTISTS & ENGINEERS

Austria – W. Magnes, IWF Graz; E. Dorfi, University of Vienna; M. Güdel, University of Vienna; F. Kerschbaum, University of Vienna; A. Luntzer, University of Vienna; E. Pilat-Lohinger, University of Vienna; T. Rank-Lüftinger, University of Vienna;

Belgium – B. Bonfond, Université de Liège; J.-C. Gerard, Université de Liège; M. Gillon, Université de Liège; J. Gustin, Université de Liège; B. Hubert, Université de Liège; A. Radioti, Université de Liège; L. Soret, Université de Liège; A. Stiepen, Université de Liège; O. Venot, University of Leuven; Pieter Deroo, Xenics

France – E. Pantin, CEA; C. Alard, IAP; V. Batista, IAP; A. Cassan, IAP; J.-P. Maillard, IAP; J.-B. Marquette, IAP; F. Mogavero, IAP; J.-C. Morales, IAP; P. Tisserand, IAP; P. Bordé, IAS; C. Danielski, IAS; O. Demangeon, IAS; P. Gaulme, IAS; P. Lognonné, IPGP; C. Michaut, IPGP; S. Jacquemoud, IPGP; M. Turbet, LMD; Martin Giard, IRAP; P. Fouqué, IRAP; P. Bernadi, LESIA; B. Bézard, LESIA; Y. Hello, LESIA ; P. Kervella, LESIA; E. Lellouch, LESIA; N. Nguyen Tuong, LESIA; B. Sicardy, LESIA; S. Vinatier, LESIA; T. Widemann, LESIA; D. Cordier, Obs. Besancon; M. Agundez, Obs. Bordeaux; M. Dobrijévic, Obs. Bordeaux; V. Eymet, Obs. Bordeaux; I. Gomez-Leal, Obs. Bordeaux; E. Hébrard, Obs. Bordeaux; F. Hersant, Obs. Bordeaux; A.-S. Maurin, Obs. Bordeaux; P. Tanga, Obs. Cote d'Azur; F. Vakili, Obs. Cote d'Azur; L. Abe, Obs. Nice; V. Parmentier, Obs. Nice; R. Petrov, Obs. Nice; F.-X. Schmider, Obs. Nice;

Germany – M. de Val-Borro, MPS; N. Krupp, MPS; U. Mall, MPS; A. Medvedev, MPS; M. Rengel, MPS; N. Iro, Hamburg University;

Italy – M. Focardi, INAF-Arcetri; M. Pancrazi, INAF-Arcetri; A. Adriani, INAF-IAPS; F. Altieri, INAF-IAPS; A. Aronica, INAF-IAPS; G. Bellucci, INAF-IAPS; F. Bernardini, INAF-IAPS; F. Capitanio, INAF-IAPS; C. Carli, INAF-IAPS; M. Ciarniello, INAF-IAPS; MC. De Sanctis, INAF-IAPS; AM. Di Giorgio, INAF-IAPS; M. Di Mauro, INAF-IAPS; M. Farina, INAF-IAPS; G. Filacchione, INAF-IAPS; S. Giuppi, INAF-IAPS; D. Grassi, INAF-IAPS; A. Migliorini, INAF-IAPS; F. Oliva, INAF-IAPS; P. Palumbo, INAF-IAPS; G. Piccioni, INAF-IAPS; A. Raponi, INAF-IAPS; G. Rinaldi, INAF-IAPS; G. Sindoni, INAF-IAPS; S. Stefani, INAF-IAPS; D. Turrini, INAF-IAPS; G. Malaguti, INAF-IASFBo; G. Morgante, INAF-IASFBo; L. Terenzi, INAF-IASFBo; F. Villa, INAF-IASFBo; K. Biazzo, INAF-OACt; G. Leto, INAF-OACt; I. Pagano, INAF-OACt; G. Scandariato, INAF-OACt; L. Affer, INAF-OAPa; A. Ciaravella, INAF-OAPa; A. Maggio, INAF-OAPa; J. Maldonado Prado, INAF-OAPa; G. Micela, INAF-OAPa; L. Prisinzano, INAF-OAPa; S. Sciortino, INAF-OAPa; S. Benatti, INAF-OAPd; R. Claudi, INAF-OAPd; V. D'Orazi, INAF-OAPd; S. Erculiani, INAF-OAPd; R. Gratton, INAF-OAPd; D. Mesa, INAF-OAPd; F. Fiore, INAF-OARoma; A. Bonomo, INAF-OATo; M. Damasso, INAF-OATo; P. Giacobbe, INAF-OATo; A. Riva, INAF-OATo; A. Sozzetti, INAF-OATo; M. Cestelli Guidi, INFN-LNF ; A. Marcelli, INFN-LNF ; R. Bonito, Univ. Di Palermo; E. Pace, Univ. Firenze; V. Nascimbeni, Univ. Padova; G. Piotto, Univ. Padova;;

The Netherlands – C. Keller, Leiden University; M. Kenworthy, Leiden University; I. Snellen, Leiden University; R. de Kok, SRON / Leiden University; R. Waters, SRON / University of Amsterdam; C Dominik, University of Amsterdam;

Poland – H. Rickman, SRC-PAS; M. Banaszkiewicz, SRC-PAS; M. Błacka, SRC-PAS; A. Wawrzaszk, SRC-PAS; T. Winiowski, SRC-PAS; M. Rataj, SRC-PAS; P. Sitek , SRC-PAS ; R. Graczyk, SRC-PAS; M. Stolarski, SRC-PAS; P. Wawer, SRC-PAS; R. Pietrzak, SRC-PAS; W. Winek, SRC-PAS;

Portugal – M. Montalto, CAUP; V. Adybekian, CAUP ; I. Boisse, CAUP ; E. Delgado-Mena, CAUP ; P. Figueira, CAUP ; M. Monteiro, CAUP; N. Santos, CAUP ; S. Sousa, CAUP; T. Kehoe, I3N; H. Morais, I3N ; M. Abreu, CAAUL; D. Berry, CAAUL; A. Cabral, CAAUL; S. Chamberlain, CAAUL; R. Herdero, CAAUL; P. Machado, CAAUL; J. Peralta, CAAUL.

Spain – D. Barrado, CAB-INTA; H. Bouy, CAB-INTA; N. Huelamo, CAB-INTA; J. Martín Torres, CAB-INTA; M. Morales-Calderón, CAB-INTA; A. Moro Martín, CAB-INTA; A. Moya Bedon, CAB-INTA; J. Sanz Forcada, CAB-INTA; E. García Melendo, FOED/ICE; P. Amado, IAA; A. Claret, IAA; M. Fernández, IAA; M. Lopez-Puertas, IAA; M.A. Lopez-Valverde, IAA; C. Allende Prieto, IAC; C.A. Alvarez Iglesias, IAC; J.A. Belmonte Avilés, IAC; H.J. Deeg, IAC; M. Espinoza Contreras, IAC; M. Esposito, IAC; B. Femenía Castella, IAC; R.J. García López, IAC; J. Gonzalez Hernandez, IAC; B. González Merino, IAC; G. Israelian, IAC; B. Laken, IAC; J. Licandro Goldaracena, IAC; N. Lodieu, IAC; P. Miles-Paez, IAC; P. Montañés Rodríguez, IAC; F. Murgas Alcaino, IAC; E. Palle, IAC; H. Parviainen, IAC; K.Y. Peña Ramírez, IAC; R. Rebolo López, IAC; V.J. Sánchez Béjar, IAC; E. Sanromá Ramos, IAC; B.W. Tingley, IAC; M.L. Valdivieso, IAC; J. C. Morales, ICE; J. Colomé, ICE; E. Garcia-Melendo, ICE; L. Gesa, ICE; J. Guardia, ICE; E. Herrero, ICE; F. Rodler, ICE; C. Eiroa, UAM; J. Maldonado, UAM; E. Villaver, UAM; F.J. Alonso Floriano, UCM; D. Montes, UCM; H.M, Tabernero, UCM; R. Hueso, UPV; S. Perez-Hoyos, UPV; A. Sanchez Lavega, UPV;

UK –P. Ade, Cardiff; S. Doyle, Cardiff; S. Eales, Cardiff; W. Gear, Cardiff; H. Gomez, Cardiff; M. Griffin, Cardiff; P. Hargrave, Cardiff; A. Papageorgiou, Cardiff; G. Pisano, Cardiff; C. Tucker, Cardiff; A. Whitworth, Cardiff; M. Galand, IC; J. Haigh, IC; C. Theobald, MSSL; B. Winter, MSSL; A. Smith, MSSL; L. Fletcher, Oxford; P. Irwin, Oxford; M. Tecsa, Oxford; J. Temple, Oxford; P. Read, Oxford; C. Agnor, QMUL; I. Polichtchouk, QMUL; C. Watkins, QMUL; P. Eccleston, RAL Space; R. Irshad, RAL Space; T. Lim, RAL Space; D. Waltham, RHUL; N. Achilleos, UCL; A. Aylward, UCL; R. J. Barber, UCL; E. Barton, UCL;P. Doel, UCL; S. Fossey, UCL; P. Guio, UCL; M. Hollis, UCL; O. Lahav, UCL; C. Lithgow-Bertelloni, UCL; M. Matsuura, UCL; G. Morello, UCL; R. Prinja, UCL; M. Rocchetto, UCL; G. Savini, UCL; M. Tessenyi, UCL; A. Tsirias, UCL; S. Viti, UCL; R. Varley, UCL; I. Waldmann, UCL; S.N. Yurchenko, UCL; D. Pinfield, UH; N. Bezawada, UK ATC; I. Bryson, UK ATC; A. Glasse, UK ATC; W. Taylor, UK ATC; G. Wright, UK ATC; C. Hellier, Un. Keele; P. Maxted, Un. Keele; M. Burleigh, Un. Leicester; E. Kerins, Un. Manchester;

USA (collaborating scientists) – Y. Yung, Caltech; L. Brown, JPL; G. Orton, JPL; M. Swain, JPL; G. Vasisht, JPL; G. Bakos, Princeton; C. Griffith, UoA; T. Koskinen, UoA; P. Mauskopf, UoA R. Yelle, UoA;.R. Zellem, UoA;

10.6 ACKNOWLEDGEMENTS

The consortium would like to thank the following:

- Airbus France and Rodolphe Cledassou for their support and input on the mission and spacecraft design during the development of this proposal.
- Airbus UK for useful discussions and inputs.
- Our institutes for support during the preparation of the proposal.

11 ANNEX 4: NATIONAL LETTERS OF ENDORSEMENT

The following letters of endorsement have been sent by the relevant national funding agencies directly to ESA. They are copied here for completeness.

Prof. Alvaro Giménez Cañete
Director of Science and Robotic Exploration
ESA

18th December 2014

Dear Prof. Giménez,

Letter of Endorsement for the ARIEL M4 mission candidate

I understand that the proposal submitted to ESA in response to the call for a Medium sized mission candidate for launch in 2025 requires a Letter of Endorsement from the national funding agency in support of the proposed national activities. This is to cover the study phase and to indicate a willingness to seek funding should the mission be selected for further development.

I can confirm that we are aware that the ARIEL mission would be led by the UK through Professor Giovanna Tinetti of the University College London and will consider supporting it on this basis.

We have been informed of intended UK Co-Investigator status on this mission with potential involvement from the Universities of Oxford, UCL Mullard Space Science Laboratory and Cardiff and STFC Rutherford Appleton Laboratory.

The Cosmic Vision programme remains a high priority for the UK and we intend to build a planning figure into our budget going forward to enable participation in the M4 mission opportunity. As with previous UK funding for Cosmic Vision missions, any such budget will be subject to the usual internal agency procedures in consultation with the Science and Technology Facilities Council and on a Government wide Spending Review for support beyond 2016. I will keep you informed of any further developments.

Yours sincerely,

C. Castelli

Dr Chris Castelli   CC. Prof G Tinetti, UCL
Director Programmes

Polaris House, North Star Avenue, Swindon, Wiltshire, SN2 1SZ
An executive agency of the Department of Business, Innovation and Skills

Direction de la Prospective, de la Stratégie, des Programmes
de la Valorisation et des Relations Internationales
Programme Sciences de l'Univers, Microgravité et Exploration
Sent by Email : M4support@cosmos.esa.int

Prof. Alvaro Giménez Cañete
Director of the ESA Science and Robotic Exploration
Program
8-10 Rue Mario Nikis,
75338 Paris Cedex 15

Paris, January 10th, 2015
Réf : DSP/SME/2015-0000304

Subject**: Endorsement of French contribution responding to the M4 call**

Dear Alvaro,

The Centre National d 'Etudes Spatiales (CNES) is aware of the contribution of the French scientists in the **Ariel** proposal submitted in response to the call for the fourth medium size mission of Cosmic Vision :
In addition to scientific contributions, the French component of the consortium intends to provide :
- The telescope,
- The characterization of the detectors,
- A contribution to the science ground segment, in particular on the production of L2 products.

Should this proposal be selected by ESA and the French involvement corresponding to the final proposal successfully checked by CNES (before mid-February), CNES intends to support the activities of the French members of the consortium throughout the study phase.

Should this mission be selected as the Cosmic Vision 4th medium size mission, CNES will do its best efforts to secure the funding for the development and implementation of the proposed nationally provided elements. The level of support is being subject to the availability of funds within the CNES budget for Science.

Sincerely,

Sirmain

Christian Sirmain
Acting Head of Space Science,
Microgravity and Exploration Office

CENTRE NATIONAL
D'ÉTUDES SPATIALES

Siège
2, place Maurice Quentin
75039 Paris cedex 01
tél. : 33 (0)1 44 76 75 00

Direction des lanceurs
52, rue Jacques Hillairet
75612 Paris cedex
tél. : 33 (0)1 80 97 71 11

Centre spatial de Toulouse
18, avenue Edouard Belin
31401 Toulouse cedex 9
tél. : 33 (0)5 61 27 31 31

Centre spatial guyanais
BP 726
97387 Kourou cedex
tél. : 33 (0)5 94 33 51 11

www.cnes.fr   RCS Paris B 775 665 912 — Siret 775 665 912 000 82 — Code APE 731 Z — N° identification TVA FR 49 775 665 912

ESA Director of Science and Robotic Exploration
ESA HQ
8-10 Rue Mario Nikis
75738 Paris Cedex 15, France

Subject: ASI endorsement to the participation of the Italian Scientific Community
to the ESA Cosmic Vision proposal ARIEL – Call M4

Dear Dr. Giménez,

The Italian Space Agency hereby endorses the participation of the Italian
Scientific Community to the ESA Cosmic Vision Proposal ARIEL – Atmospheric
Remote-sensing Infrared Exoplanet Large survey, presented in response to the
call for missions under the aegis of the Cosmic Vision 2015-2025 plan.
The Italian Space Agency decided to endorse the Italian participation to a subset
of proposals, based on the excellence of the scientific content and the compliance
to the Italian technology interests.

Should the mission be selected, ASI will make its best effort to support its
development and exploitation. The level of the above mentioned support will be
subject to availability of funds within the overall ASI budget allocation for the
Exploration and Observation of the Universe related missions.

Yours sincerely,

Barbara Negri
Head of Exploration and
Observation of the Universe

Copy: E. Flamini, J. Sabbagh, G. Micela

Innovation and Industry Department   Warsaw, 15th January 2015

DIP-VI-522-1/3/15   **Dr. Alvaro Giménez**
DIP/174/15   **Director of Science and Robotic Exploration**
                                             European Space Agency

Dear Mr. Giménez,

The Polish Delegation to ESA is informed of dr. Miroslaw Rataj from Space Research Centre, Polish Academy of Science proposed involvement in the ARIEL project in view of the M4 mission as the leader of team. Dr. Miroslaw Rataj proposes to provide Opto-mechanical part of the Fine Guidance System, Warm Front End Electronic of FGS, Control Electronics of FGS, Mechanical Structure for the above units, as well as MGSE, EGSE, OGSE for the above units.

The Polish Delegation to ESA confirms that it is willing to support the above referred responsibilities.

Should this project be selected by ESA, the Polish Authorities are willing to consider its funding, the level of which being decided according to the Polish Space Authorities' internal review procedure.

ZASTĘPCA DYREKTORA

Otylia Trzaskalska - Stroińska

BELGIAN SCIENCE POLICY OFFICE

Louizalaan 231 avenue Louise
B-1050 BRUSSELS
Tel. +32 2 238 34 11 ▪ Fax +32 2 230 59 12
www.belspo.be

belspo

Dr. Alvaro Giménez Cañete
Director of Science and Robotic Exploration
ESA
8-10, rue Mario Nikis
F-75738 Paris Cedex 15

your reference	our reference		enclosure(s)
	E:\S\scienc\missions\m4\15_WV_M4_ARIEL_LoE.docx		

contact	e-mail	telephone	date
Werner VERSCHUEREN	verw@belspo.be	+32.2.23.83.589	12/1/2015

Subject : ESA Science Programme
Call for a medium-size mission opportunity (M4) issued on 19/8/2014
Mission proposal: **ARIEL**
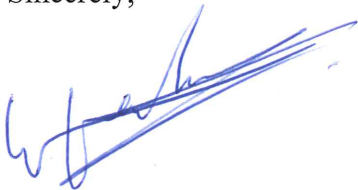Letter of Endorsement

Dear Director,

The Belgian Federal Science Policy Office (BELSPO) is aware of the mission proposal called **ARIEL** in response to the abovementioned call.

BELSPO is supportive of the proposed mission elements that fall under the responsibility of the Centre Spatial de Liège (CSL), the Katholieke Universiteit Leuven (KU Leuven) and the Université de Liège (ULg).
We confirm that we will fund the relevant activities of CSL during the mission study phase, while existing funding will be used by KU Leuven and ULg. In addition, we will undertake the necessary action to secure funding for the mission elements to be provided by Belgium during the definition and implementation phases of the project.

The funding will be implemented via the ESA-PRODEX Programme and is subject to the selection of this mission proposal by ESA, subject to successful contract negotiation, and subject to the availability of the necessary funds at Belgian level within the relevant years.

Yours Sincerely,

Dr. Werner Verschueren
Belgian ESA Delegation - Science Programme Committee

Cc. Dr. Etienne Renotte (CSL), Dr. Bart Vandenbussche (KUL), Dr. Denis Grodent (ULg)

.be

DLR Deutsches Zentrum
für Luft- und Raumfahrt
German Aerospace Center

DLR e. V.   Space Administration
Postfach 30 03 64, 53183 Bonn, Germany

Prof. Alvaro Giménez Cañete
European Space Agency

Headquarters

8-10 rue Mario Nikis

75738 Paris Cedex 15, France

Your reference
Your letter
Our reference

Your correspondent   Dr. Bachem

Telephone +49 228 447-   357
Telefax +49 228 447-
E-mail   eberhard.bachem@dlr.de

14 January 2015

ESA call for a medium-size mission opportunity (M4)

German Participation in the proposal Atmospheric Remote sensing Infrared Exoplanet Large survey (ARIEL)

Dear Prof. Gimenez,

Dr. P. Hartogh (Max-Planck-Institut für Sonnensystemforschung (MPS), Göttingen) intends to participate in the ARIEL-mission poposal submitted by Prof. G. Tinetti (University College London, Dept. of Physics and Astronomy).

The intended German contribution comprises the warm read out electronics and a contribution to the detector procurement.

We take note of the intended German contribution and will consider the support of the work in the study phase in case ARIEL will be selected.

It is understood that the support during the study phase is subject to the relevant DLR funding procedures.

Therefore, at present time this letter does not constitute any obligation to provide financial support.

Sincerely

i. V. Dr. Th. Galinski

i. A. Dr. E. Bachem

copy: Prof. G. Tinetti

DIN EN ISO 9001:2008
OHSAS 18001:1999
DIN EN ISO 14001:2005

Bonn-Oberkassel
Koenigswinterer Str. 522-524
53227 Bonn, Germany
Telephone +49 228 447-0
Internet www.DLR.de

SRON

Netherlands Institute for Space Research

Prof. Dr. A. Gimenez

SRON Utrecht

Sorbonnelaan 2, 3584 CA Utrecht, The Netherlands
T +31 (0)88 777 5600, F +31 (0)88 777 5601
www.sron.nl

Our reference: SON-15-0008

E-mail: L.B.F.M.Waters@sron.nl

Re: Letter of Support mission proposal ARIEL

Date: January 14, 2015

Dear Prof. Gimenez,

The ARIEL mission addresses key science of the ESA Cosmic Vision program and in particular it will address Theme 1: What are the conditions for life and planetary formation.
With ARIEL the goal of characterising a wide variety of exo-planetary atmospheres will become a reality.

SRON will support this proposal by supplying the cold read-out electronics for European detectors, support to Assembly, Integration and Verification and to the science ground segment as well as to the science to be conducted with the ARIEL data.

Yours sincerely,

Prof. Dr. L.B.F.M Waters
Scientific Director/General Director
NL SPC delegate

Dir. Alvaro Giménez
Science and Robotic Exploration
ESA

Mail: M4support@cosmos.esa.int

ALR-STN-0004-2015_rev0

Vienna, 9 January 2015

**ESA, M4 Mission Call
Letter of Endorsement, UV- IfA, ARIEL Science Instruments**

Dear Dir. Giménez,

The Aeronautics and Space Agency (ALR) endorses the proposed involvement of the University of Vienna, Institute for Astrophysics (UV-IfA) in the Science Instruments to be proposed by the consortium led by the University College London (UCL)/ UK for the M4 Mission candidate ARIEL (Atmospheric Remote sensing Infrared Exoplanet Large survey) of the ESA Science Programme.

We understand that UV-IfA would be involved in the phases A, B1, B2, C, D, E1and be responsible for:
- the on-board software of the Fine Guidance System (FGS) electronics: design, implementation, validation up to in-orbit commissioning,
- participation in the ground segment definition,
- significant contributions to the principal science work packages.

The maintenance of the software after commissioning will be covered by UV-IfA.

We have received a very preliminary description of the relevant activities up to an amount of:
- Phase A/B1:   105 k€ (2015- 2018)
- Phases B2/C/D/E1:   343 k€ (2018- 2026)

Total: 448 k€

Provided the selection by ESA of the ARIEL Mission within the ongoing "Call for M4 Mission", ALR will:

- *fund the activities of phases A, B1.*
- Provided the adoption by ESA of the ARIEL Mission in 2018, *do its best efforts to provide the funds required for the Phases B2/C/D/E1 within the financial envelope available.*

The funding of both above periods are naturally subject to a successful agreement on the activities after evaluation by ALR of detailed proposals to be submitted later by UV-IfA.

Best regards

Andre Peter
Space science
Aeronautics and Space agency

C/C:

Harald Posch, ALR, Head of Agency
Franz Kerschbaum, UV-IfA

Contact Point:
Prof. Giovanna Tinetti
University College London
Dept. of Physics and Astronomy
Gower Street,
London, WC1E 6BT
UK
Phone: +44 (0)7912 509617
Fax: +44 (0)207 6792328
e-mail: g.tinetti@ucl.ac.uk

The PI, all Co-PI's and Co-I's and key technical staff all confirm their availability (at least 20% FTE) to support the assessment phase study of ARIEL if this proposal is accepted.